Technische Universität München

Lehrstuhl für Technische Chemie II

Catalyzed Synthesis of Dimethyl Carbonate

Herui Dou

Vollständiger Abdruck der von der Fakultät für Chemie der Technischen Universität München zur Erlangung des akademischen Grades eines

Doktors der Naturwissenschaften (Dr. rer. nat.)

genehmigten Dissertation.

Vorsitzender: Univ.-Prof. Dr. K. Köhler

Prüfer der Dissertation:

    1.   Univ.-Prof. Dr. J. A. Lercher

    2.   Univ.-Prof. Dr. T. Nilges

Die Dissertation wurde am 23. 09. 2010 bei der Technischen Universität München eingereicht und durch die Fakultät für Chemie am 12. 11. 2010 angenommen.

Abstract:

The direct strongly equilibrium limited synthesis of dimethyl carbonate from CO_2 and methanol has been studied by combining a back-mixed reactor with a recycle loop in which a drying bed was integrated. The reaction zone is so thermally separated from the low temperature separation bed by which the produced water is selectively removed. An unprecedented DMC yield of 17 wt. % was achieved with ZrO_2 as catalyst and 3A zeolite as drying agent. The adsorption and diffusion kinetics of water and methanol in LTA and FAU zeolites were studied to fine tune the materials. The pore opening size of LTA subtly depends on the concentration of exchanged potassium. Based on the understanding of how to control the pore openings of LTA zeolites, a new generation of LTA type zeolite membrane was successfully developed, which led to enhanced separation factors (＞1000) between water and methanol.

Die Synthese von Dimethylcarbonat (DMC) aus Methanol und Kohlenstoffdioxid ist durch die Gleichgewichtslage auf weniger als 1% limitiert. Wird das Nebenprodukt Wasser durch externe Trocknung entfernt kann die Ausbeute unter Verwendung eines ZrO_2 Katalysators auf 17% gesteigert werden. Die Grenze des Umsatzes zu DMC ist durch die Effektivität der Entfernung des Wassers limitiert. In der vorliegenden Arbeit wurde das Reaktionsgemisch durch Umpumpen extern in einen zweiten Reaktor über Zeolith 3A getrocknet. Da die Restmenge von Wasser die maximale Ausbeute limitiert, wurden die Sorption von Wasser in Gegenwart von Methanol physikalisch-chemisch untersucht. Durch sorgfältige Wahl des ausgetauschten Kations wurde ein neues Material, basierend auf LTA entwickelt, das in der Lage ist sehr selektiv Wasser von Methanol zu trennen. In Form einer Membran verwendet konnten Trennfaktoren größer 1000 realisiert werden.

CATALYZED SYNTHESIS OF DIMETHYL CARBONATE

To my mother,

to Xiu

Acknowledgements

I would like to thank Prof. Dr. Johannes A. Lercher for giving me the opportunity to carry out my PhD work in TCII. His scientific insights and supports in my work and life are especially valuable for the implementation of this work. I am grateful to Xuebing Li and Thomas E. Müller for their supervisions.

Very special thanks are given to Hui Shi for the help with the corrections of my papers and helpful scientific discussions; Tobias Förster for his instructions to the NMR and FR setup, and helpful suggestions; Yanzhe Yu for his help in FR measurements; Dr. Jianqiang Wang for helpful scientific discussions and single crystal X-ray diffraction measurements; Florian Schüßler, Linus Schulz and Sarah Maier for the help of TPD measurements; Manuela Bezen, Richard Knapp, Baoxiang Peng, Ana Hrabar, Michael Salzinger, Sabine Scholz, Xianyong Sun, Lin Lin, Sonja Wyrzgol and Daniela Hartmann, for all sorts of help inside the lab.

"Towards Optimized Chemical Processes and New Materials by Combinatorial Science" work package which comes from EU is acknowledged for financial support. I would like to thank Frau Helen Lemmermöhle, Frau Katharina Thies and Stefanie Maier for their help.

Technical supports from Xaver Hecht, Andreas Marx, Martin Neukamm are highly appreciated, especially the SEM and AAS measurements by Martin Neukamm.

The encouragements from my family and friends are especially helpful to my PhD study. I would like to thank my wife, Jinxiu, for her love, supports and understanding.

<div align="right">

Herui

August 2010

</div>

Table of contents

Chapter 1

Introduction

1.1. General introduction

The chemical industry has been one of the major economic activities in the past century and will also be so in this century. However, the industry has been blamed for producing environmentally hazardous substances, which cause acid rain, a reduction of stratospheric ozone levels and so on.

In the past several decades, the public dialogues have increasingly addressed the environmental impact of the chemical substances, an issue fully recognized as a major concern. As a consequence, this awareness is pushing governments toward more severe laws for environment safeguards, which although beneficial, are becoming burdensome on industry budgets. To overcome the problem at the source, the chemical industry must develop cleaner chemical processes by the design of innovative and environmentally benign chemical reactions. *Green chemistry* offers the tools for this approach [1-3]. Therefore, many efforts have been focused on eliminating or decreasing environmentally hazardous substances.

Green organic syntheses must meet, if not all, at least some of the following requirements: avoid waste [4], be atom-efficient [5], avoid the use and production of toxic and dangerous chemicals, produce compounds that perform better as well as existing ones and are biodegradable, avoid auxiliary substances (e.g., solvents) or use eco-compatible solvents (water or dense CO_2), reduce energy requirements, use renewable materials, and use catalysts rather than stoichiometric reagents. [6]

Dimethyl carbonate (DMC) is a "green" chemical reagent in terms of its low toxicity (Table 1, [3]), non-corrosiveness and ready biodegradation. DMC is classified as a flammable liquid, smells like methanol, and does not have irritating or mutagenic effects either by contact or inhalation. Therefore, it can be handled safely without the special precautions required for the poisonous and mutagenic methyl halides and

2

dimethyl sulphate (DMS) and the extremely toxic phosgene. CH3–, CH3O–, and –CO– functional groups in the DMC molecule render its wide applications as methylating, methoxylating and carbonylating agent in replacement of some virulent carcinogens, such as phosgene, DMS and chloromethane [7-9].

Table 1 Comparison between the Toxicological and Ecotoxicological Properties of DMC, Phosgene, and DMS

property	DMC	phosgene	DMS
oral acute toxicity (rats)	LD_{50} 13.8 g/kg		LD_{50} 440 mg/kg
acute toxicity per contact (cavy)	LD_{50} > 2.5 g/kg		
acute toxicity per inhalation (rats)	LC_{50} 140 mg/L, (4 h)	LC_{50} 16 mg/m3; (75 min)	LC_{50} 1.5 mg/L (4 h)
mutagenic properties	none		mutagenic
irritating properties (rabbits, eyes, skin)	none	corrosive	
biodegradability (OECD 301 C)	> 90% (28 days)	rapid hydrolysis	rapid hydrolysis
acute toxicity (fish) (OECD 203)	NOEC*1000 mg/L		LC50 10-100 mg/L
acute toxicity on aerobial bacteria of wastewaters (OECD 209)	EC_{50}> 1000 mg/L		

NOEC Concentration which does not produce any effect.

DMC applications will be sorted according to its use as a chemical intermediate (carbonylating or methylating reagent), solvent and fuel additives and monomer for the synthesis of polycarbonate resins [10-12]. By far the most prominent example of DMC industrial exploitation as a chemical intermediate is currently represented by the production of aromatic polycarbonates: a total world-wide capacity of about 170 kt per year aromatic polycarbonates via DMC has been installed by General Electric Plastics, while further 130 kt per year are scheduled [13].

DMC is also used as material for carbamates and isocyanate productions. The reaction between DMC and primary or secondary amines bring to carbamates. The production of carbamates from DMC represents the first step of a non-phosgene route

to isocyanates involving liquid or gas-phase thermolysis of the carbamate precursor, a process of potential outstanding industrial interest that is being pursued by several companies [14, 15].

DMC is a versatile reagent for methylation reactions at C, N, O and S centers, behaving as a good substitute for DMS or methyl halides which are toxic and corrosive. For the mono-methylation of activated methylene groups in substrates such as arylacetonitriles, useful intermediates for anti-inflammatory drugs, DMC is better than other methylating agents for selectivity to mono-methylated derivatives [16-18].

DMC represents a reliable alternative to acetate esters and ketones as solvents in most applications, from paints to adhesives, taking advantage of its good solvency power [19]. Moreover, in recent years, DMC has been taken in consideration as oxygenate to reduce vehicle emissions associated to environmental and health risks. The reasons are the outstanding oxygen content in the DMC molecule (53.3 wt.%) combined to its good blending properties [20]. DMC was shown to have a photochemical ozone creation potential (POCP) negligible when compared to conventional fuels and its use in fuels would be environmentally safe [21]. As a matter of fact, DMC has been reported to have the lowest POCP of all the oxygenated volatile organic compounds (VOCs) [22].

1.2. DMC production

The phosgenation of methanol was the most important method to produce DMC till the 1980s [23-25]. The reaction is carried out contacting phosgene with methanol, (Equation 1) through the formation of methylchloroformate as intermediate, whereas the reaction can be accelerated using an acid scavenger such as a tertiary amine or an inorganic base, e.g. NaOH [26, 27].

(1) Phosgenation of methanol

$$2\ CH_3OH\ +\ Cl\!-\!\overset{\overset{\displaystyle O}{\|}}{C}\!-\!Cl\ \longrightarrow\ H_3CO\!-\!\overset{\overset{\displaystyle O}{\|}}{C}\!-\!OCH_3\ +\ 2HCl \qquad (1)$$
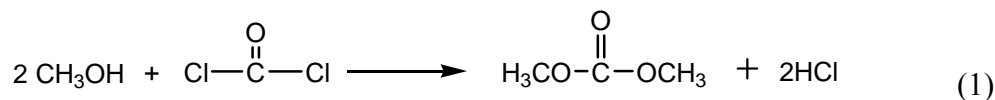
The methods oxidative carbonylation of methanol to produce DMC, which are based on the catalytic reaction of methanol with carbon monoxide and oxygen (Equation 2), have been the subject of intensive studies [28- 31].

(2) Oxidative carbonylation of methanol

$$2\ CH_3OH\ +\ CO\ +\ 0.5\ O_2\ \longrightarrow\ H_3CO\!-\!\overset{\overset{\displaystyle O}{\|}}{C}\!-\!OCH_3\ +\ H_2O \qquad (2)$$
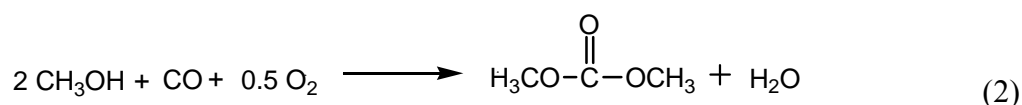
Since the 1970s, EniChem set-up a project aimed at the development of a non-phosgene synthesis of DMC for large volume usage. As a result, a new industrial process was established, based on methanol oxidative carbonylation in the presence of copper chlorides as catalysts [32]. The reaction was carried out by feeding at the same time methanol, carbon monoxide and oxygen to the suspension of the catalyst in a mixture of water, produced DMC. And produced DMC is separated by distillation after the catalysts separation [33].The first industrial plant, based on the developed technology went on stream since 1983 [34，35], up to now the world-wide total capacity installed is over 70 kt per year. Cobalt (II) complexes [36] and nitrogen oxides [37] were also studied as catalyst for DMC synthesis by Oxidative carbonylation of methanol.

An alternative to the oxy-carbonylation processes is the transesterification of ethylene carbonate (EC) with methanol. In this process, DMC is co-generated with ethylene glycol (equation 3) [38,39].

(3) Transesterification of ethylene carbonate with methanol.

$$2\ CH_3OH\ +\ \begin{array}{c}H_2C\!-\!O\\ |\qquad\ \ \diagdown\\ \ \ \ \ \ \ \ \ C\!=\!O\\ |\qquad\ \ \diagup\\ H_2C\!-\!O\end{array}\ \rightleftharpoons\ H_3CO\!-\!\overset{\overset{\displaystyle O}{\|}}{C}\!-\!OCH_3\ +\ \begin{array}{c}CH_2OH\\ |\\ CH_2OH\end{array} \qquad (3)$$
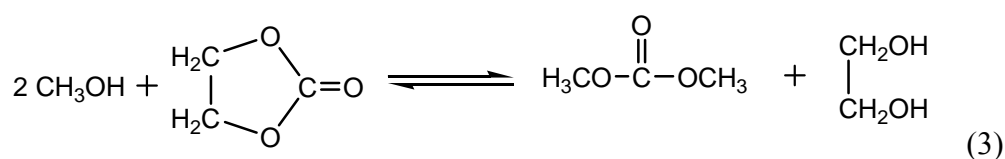
This reaction takes place in the presence of a catalyst at about 100–150 °C at moderate pressure, for example by working in an homogeneous phase in the presence of tin, zirconium or titanium complexes [40]. Both homogeneous and heterogeneous basic or acid catalysts can also be used for the reaction. Furthermore, the DMC synthesis by transesterification can also start from urea and methanol (equation 3) [41,42].

(4) Transesterification of urea with methanol

$$2\ CH_3OH\ +\ CO(NH_2)_2\ \rightleftharpoons\ H_3CO-\overset{\overset{\displaystyle O}{\|}}{C}-OCH_3\ +\ 2NH_3 \qquad (4)$$
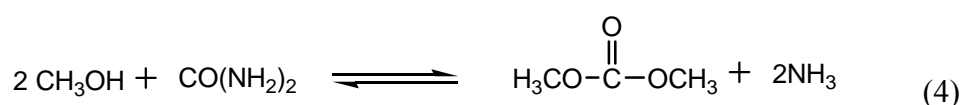
The phosgenation of methanol has to be replaced eventually because of the inevitable use of extremely toxic phosgene. Oxidative carbonylation of methanol was once considered as the most potential approach. The low methanol conversion and DMC selectivity and the corrosive catalysts applied, however, limit its industrial application. The process of transesterification of ethylene carbonate and methanol is also not profitable due to the usage of commercial EC. Unfortunately, the transesterification reaction of EC with methanol is an equilibrium reaction and the formation of DMC is not thermodynamically favored.

Although the direct synthesis of DMC starting from urea and methanol (equation 4) would be very attractive, its thermodynamics is not favorable also [43].In fact, by this process the synthesis of a carbonate starting from an alcohol and carbon dioxide would also be achieved, since in principle the evolved ammonia can be recycled to the synthesis of urea. Derect DMC synthesis from methanol ad CO_2 (equation 5), has also been proposed recently. Because of using CO_2, the well-known 'greenhouse' gas, as starting material, the latter has been studied as a very promising process to fix the CO_2 for useful chemical production.

(5) Direct DMC synthesis from CO_2 and methanol

$$2\ CH_3OH\ +\ CO_2\ \rightleftharpoons\ H_3CO-\overset{\overset{\textstyle O}{\|}}{C}-OCH_3\ +\ H_2O \tag{5}$$
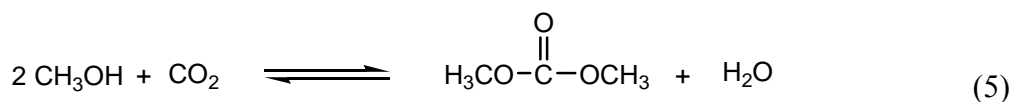
ZrO_2 as well as CeO_2-ZrO_2 have been reported as the catalysts for DMC direct synthesis from methanol and CO_2, where the basic sites on ZrO_2 serve to activate methanol and CO_2, while acidic sites supply methyl groups from methanol in the last step of the reaction mechanism [44 , 45]. Nevertheless, this reaction is an equilibrium-limited reaction and only a very small amount of DMC could be produced [44,46- 51]. Not surprisingly, many efforts have sought to shift the reaction towards DMC formation, e.g. increasing reactant concentration and removing co-produced water.

According to Jiang et al., the formation of DMC seemed to be almost proportional to the concentration of methanol in the range of 0-10 mol L^{-1} [48]. Higher partial pressure of CO_2 is also beneficial for higher DMC yields because of higher dissolved amount of CO_2. For instance, when the reaction was carried out at CO_2 pressure of 12 MPa, Hou et al. claimed that methanol conversion as high as 7 % could be obtained [52]. Methanol conversion of nearly 50% after 72 h under 30 MPa was achieved in Choi et al.'s work when 3A zeolite functioned as desiccant at room temperature [53]. Note that the large excess of applied CO_2, compared to methanol (100 mmol), discourage its industrial application because the investment of construction and the cost of routine maintenance of the extremely high pressure reaction unit [54]. For the second strategy, using water scavengers is a good approach to remove the extremely low concentration of water in methanol. Although 2,2-dimethoxypropane (DMP) and dicyclohexylcarbodiimide (DCC) can be used as water scavengers for this purpose, the main barricade against practical application is the high expense for the regeneration of the spent stoichiometric scavengers [55, 56]. By contrast, the high availability and easy recovery of inorganic adsorbents, e.g. zeolites [52, 53], make them most promising candidates as water scavengers for direct DMC synthesis.

1.3. Structure of LTA zeolites

Zeolites are porous materials consisting of aluminum and silicon tetrahedra connected via oxygen atom bridges with the negative charge on tetra-coordinated Al atoms compensated by different cations. Approximately 40 natural zeolites and more than 150 zeolites have been found and synthesized. [57,58] Typically, zeolites can be classified into five categories: 8-, 10-, 12-membered oxygen ring, dual pore and mesoporous systems. [59] The characteristics of some typical zeolites are listed in Table 2 [60].

Table 2 Characteristics of some typical porous materials

Zeolite	Number of rings	Pore size (Å)	Pore/channel structure
8-membered oxygen ring			
Erionite	8	3.6×5.1	Intersecting
10-membered oxygen ring			
ZSM-5	10	5.1×5.6	Intersecting
		5.1×5.6	
ZSM-11	10	5.3×5.4	Intersecting
Dual pore system			
Ferrierite	10, 8	4.2×5.4	One dimensional
		3.5×4.8	10:8 intersecting
Mordenite	12	6.5×7.0	One dimensional
	8	2.6×5.7	12:8 intersecting
12-membered oxygen ring			
ZSM-12	12	5.5×5.9	One dimensional
Faujasite	12	7.4	intersecting
		7.4×6.5	12:12 intersecting
Mesoporous system			
VPI-5	18	12.1	One dimensional
MCM41-S	-	16-100	One dimensional

Zeolites have excellent adsorption and molecular sieving properties, making them good candidates for catalysis, adsorption, and selective membrane separation and

ion-exchange agents [61,62]. The size of the channels and cages in different zeolites covers a wide range, and accordingly, the type of molecules that can penetrate and get absorbed varies widely for different types of zeolites. Among them, small-pore zeolites have gained especially increasing interest in application fields such as selective gas adsorption/separation and membrane technology because of their high selectivity of adsorption and transportation for small size molecules.

Linde Type A (LTA, zeolite A) is a typical small-pore zeolite which was widely used and studied since it was synthesized and reported [63,64]. Currently, it has the biggest production scale among all small-pore zeolites, which is not only used as the additives for detergents, but also for adsorptions and membranes [65‐68]. In addition, all LTA zeolites can be used as dehydration agents for separation processes [69‐71] and water scavengers for shifting chemical equilibriums [72‐75]. Normally, zeolite A is synthesized in the Na-form, which has a chemical formula of $Na_{12}Al_{12}Si_{12}O_{48}$. Its structure is better described as space group Fm3c (a =24.6 Å) with eight formula units of the composition given above. Common designations are also 4A for the Na-LTA zeolite which has a pore opening of 4.1 Ångstroms. When Na cations are partly exchanged by Ca^{2+}, the pore opening size increase to 5 Ångstroms after which the 5A zeolite is named, which can accommodate bigger molecules smaller than 5 Å. And 3A zeolite is named for the K-form of zeolite, when Na cations are partly exchanged by K^+ [76,77].

All LTA zeolites share the same topological structure and the only difference lies in their compensating cations. However, they showed big differences when used as adsorption agents, especially for water in low alcohols. Many scientists realized this fact and did a lot of work to evaluate the effect of different cations on their adsorption performances of LTA zeolites [78‐80], but no convincing and universal explanation was given. Weitkamp et al. interpreted in a quite straightforward way that zeolites can only absorb molecules whose kinetic diameter or minimum cross sectional diameter are smaller than the pore openings of zeolites [62]. This is in most cases reasonable

and true, but a notable exception must be mentioned here that 3A zeolites do absorb large amounts of methanol at certain conditions, whose kinetic diameter is 3.6 Ångstroms, being already larger than the acknowledged pore opening dimension of 3A zeolite.
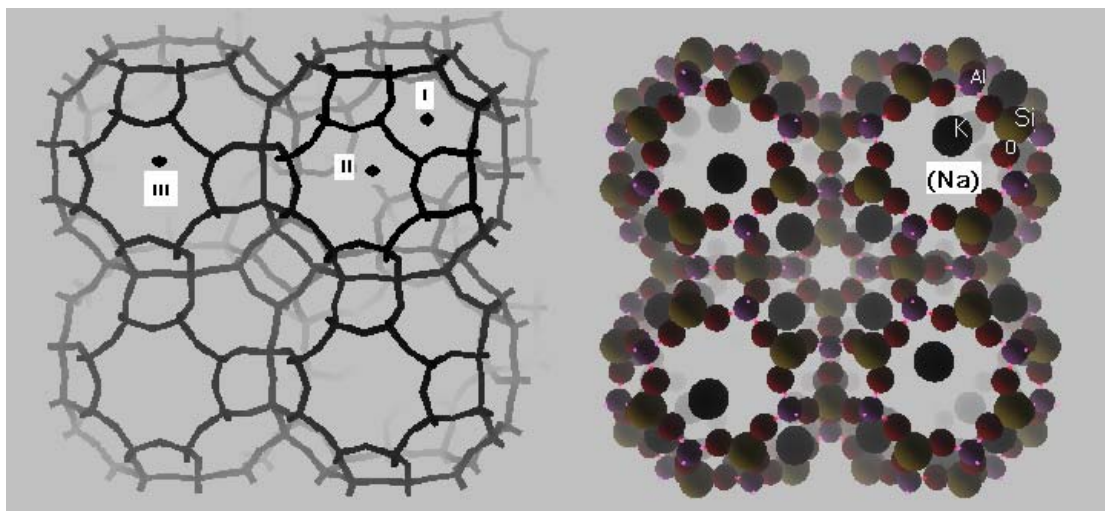
Figure 1 Stereo view of LTA unit cell with cations placed statistically in three kinds of sites (left), and site II which located in the 8-rings (right).

Figure 1 shows a graphical representation of the LTA unit cell with statistical locations sites in it. For hydrated sodium type or fully K^+ exchanged zeolite A, the statistical location sites of cations are almost identical and are shown in the left picture of Figure 1. Among these 12 sodium cations in the unit cell ($Na_{12}Al_{12}Si_{12}O_{48}$) eight are displaced by 0.2Å into the α-cage from the center of six-membered rings (site I). Three Na^+ are locate in the plane of 8-membered rings 1.2 Å from the center (site II). The twelfth Na^+ is located in the center of the α-cage and is coordinated with water molecules (site III). For fully K^+ exchanged A, the statistical location sites are almost the same and the differences are related to minor variations of the distances from sites I to the center of six-membered rings, and from sites II, which are occupied by K^+ cations near the center of the eight-membered rings [81-83].

1.4. Diffusions in zeolites

For the adsorptions and reactions occurring in the porous materials, most of the active sites (vacancies) usually are in the interior channels of the porous materials and molecules have to diffuse into the channels or inner cages. During the diffusion processes, the hindrance in different degrees possibly occurs based on the relative kinetic diameters of the molecules to that of the channels of the catalytic materials. The hindrance effects may become marked if the diameters of the reactant and product molecules are comparable to the pores or channels of these porous materials.
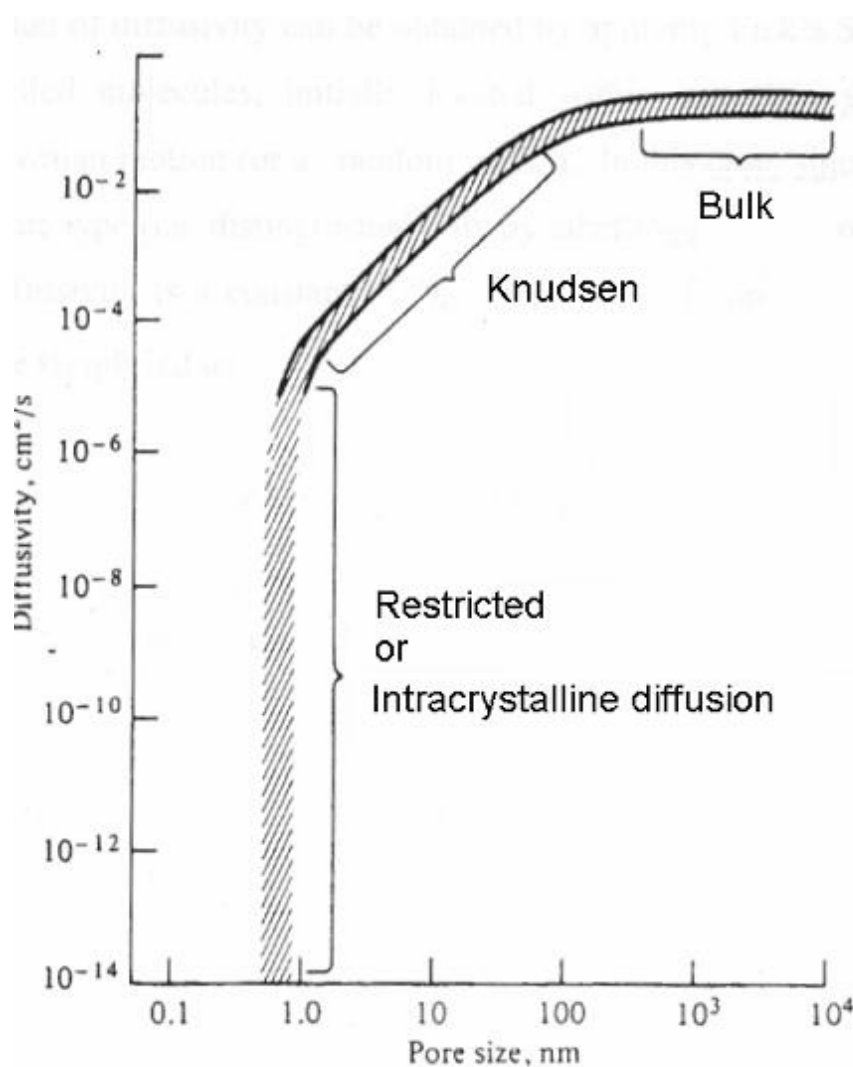
Figure 2 The dependence of the diffusivity on the relative pore diameter

A variety of studies have addressed the measurements of the diffusivities of different molecules in porous materials. Typically, diffusion of molecules in the porous materials can be divided into three different regimes [84]. (i) Bulk diffusion; (ii) Knudsen diffusion and (iii) Restricted or Intracrystalline diffusion. When the average free distance of molecules is much smaller than the pore diameter of the porous materials, collision between molecules is dominant and the diffusion behaves as bulk diffusion. If the average free distance of diffusion molecules is larger than the diameter of pores, collision between molecules and the wall of the channels is dominant and the diffusion behaves as Knudsen diffusion. When the diameter of diffusion molecules is comparable to that of the channels of the porous materials, diffusion converts from Knudsen diffusion to restricted or intracrystalline diffusion. The diffusion regimes are shown in Figure 2.

Some experimental studies have been carried out on adsorption of water and alcohols in 4A zeolite, and most of them revealed that Langmuir isotherm model fit their data adequately [66, 85 - 87]. However, due to the complexity of such experiments, only limited data are available, and research effort of water and methanol on 3A and 5A zeolites is still lacking. Because of the apparent lack of relevant adsorption kinetic measurements, many scientists performed a lot of simulations for modeling the adsorption and diffusion behaviors of different molecules in LTA zeolites [88 - 91]. Such work provides a useful insight into diffusion/adsorption behaviour of appropriately sized molecules within zeolite systems. But the efficiency of the computational implementations has not yet allowed productive simulation of most zeolite-adsorbate systems. Also, it is not surprising that discrepancies still exist between the experimental and simulation results, or results from different simulation studies.

Although many scientists prefer to apply Nuclear magnetic resonance (NMR) and infrared absorption (IR) to study the sorption kinetics of zeolites [92,93], Direct Measurements of Mass Transport (DMMT) approach still represents a useful method

for sorption kinetic studies when the diffusivities are small enough and zeolite crystallizes in the range of 1-10 μm [77]. According to what R. M. Barrer emphasized thirty years ago, "it must also be borne in mind that it is these directly measured sorption kinetics which are technically important because they determine the rates in practical applications".

1.5. Methanol dehydration and membrane separation

The methanol production capacities throughout the world have increased from 18.5 $\times 10^6$ tons/year in 1985 to 26.8 $\times 10^6$ tons/year in 1995, and are expected to reach 50.5 $\times 10^6$ tons/year by the year of 2010 [94-96]. Methanol has already established itself as a leading chemical feedstock. It is one of the three basic primary chemicals, after ammonia and ethylene. About 70% of the present methanol production is used as a feedstock for chemical syntheses like the synthesis of formaldehyde, methyl tertiary butyl ether (MTBE), acetic acid, methyl methacrylate and dimethyl terephthalate. In addition, methanol is used as antifreeze, inhibitor and solvent. Moreover, methanol can be catalytically converted into olefins (MTO technology), the demand of which is extremely high especially for the production of polyolefins. Methanol can also be converted into gasoline (MTG process). With oil reserves diminishing, it may play a significant role as a synthetic fuel for the future.

Presently, the majority of methanol is made from natural gas, but also some methanol is made from coals. Both are converted into synthesis gas, via catalytic steam reforming in the case of natural gas, and through gasification in the case of coals. Further steps of the methanol plant are usually based on the ICI technology, including three steps of syngas compression, methanol synthesis and distillation of crude methanol. Crude methanol leaving the reactor contains water and other impurities, which are generally separated in several stages. First, all components boil at lower temperature, and impurities with low boiling points are removed in the light end from the distillation column. Second, heavier impurities are removed in a second

distillation column. At last, pure methanol is distilled overhead in one or more distillation columns to remove excess water. Purification or distillation is essential for methanol production though it is highly energy-demanding. In modern methanol production process, energy relationships have been integrated among different sections in various ways to minimize the overall energy input per unit of purified product methanol [97- 102]. However, the inevitable energy loss during distillations is still as high as 800-900 MJ per ton of methanol [103].

Vapor permeation (VP) and pervaporation (PV) of membranes have gained widespread acceptance in the chemical industry as an effective process for separation of some mixtures that are difficult to separate by distillation, extraction or sorption [104- 107]. Membranes used for VP and PV are operated continuously without regeneration, with low energy input and they are modular-designed, which are flexible. These advantages make membrane processes or hybrid processes involving membranes economically attractive to many industrial applications. It has been applied to the dehydration of organic liquids (ethanol, iso-propanol or ethylene glycol etc.) [108].

Practical applications of polymeric membranes have been carried out for dehydration of alcohols. However, no successful application has been reported for the separation of methanol and water [108]. Inorganic membranes are generally superior to polymeric membranes in terms of thermal, mechanical, and chemical stability, and zeolite membranes have received the most attention among inorganic membranes [109- 116]. Researchers have noticed that zeolite NaA membranes are nearly ideally suited for removing residual water in organics because they are highly hydrophilic and their pore opening (4.1Å) are smaller than most organic molecules but larger than water. However, the molecular sizes, polarities and chemical properties of water and methanol are all similar. More critically, the kinetic diameter of methanol is only 3.6 Å, smaller than the pore openings of zeolite NaA, allowing it to pass through the membranes, hindering the separation efficiency of methanol and water. Some scientists reported some membrane dehydration experimental results for methanol, but

with very low separation factor [117], or very thick membrane with higher separation factor but very small fluxes [118,119].

1.6. Scope and structure of this thesis

Techniques were performed for the yield improvement of direct synthesis of dimethyl carbonate (DMC) from CO_2 and methanol. Strategies include catalyst design, reaction unit optimization, synthesis and modification of zeolite. Then isothermal adsorption and diffusion kinetics of water and methanol in LTA and FAU zeolites were studied. Based on the understanding of how to regulate the pore openings of LTA zeolites, a new generation of potassium exchanged LTA zeolite membranes were successfully developed, which was used for water/methanol separation.

Strategies for DMC yield improvements and thermodynamic calculations were described in **Chapter 2**. Then isothermal adsorption and diffusion kinetics of water and methanol in LTA and FAU zeolites were studied in **Chapter 3**. Both diffusion kinetics and DMC direct synthesis for higher potassium exchanged LTA zeolites were studied in **Chapter 4.** LTA zeolite membranes synthesis and water/methanol separation studies were proposed in **Chapter 5**. Finally, the results of this thesis were summarized in **Chapter 6**.

References

[1] P. Tundo, P. Anastas, D. Black, J.Breen, T. Collins,; S. Memoli, J. Miyamoto, M. Polyakoff, W. Tumas, Pure Appl. Chem. 72 (2000) 1207-1228.

[2] Green Chemistry, Theory and Practice, P. Anastas, T. Warner, J. C., Eds.; Oxford University Press: Oxford, 1998.

[3] P. Tundo, M. Selva, Acc. Chem. Res. 35 (2002) 706-716.

[4] R. A. Sheldon, Atom efficiency and catalysis in organic synthesis. Pure Appl. chem. 72 (2000) 1233-1246.

[5] B. M. Trost, Science 254 (1991) 1471-1477.

[6]Anastas, P. T. T. Williamson, In Green Chemistry: Designing Chemistry for the Environment; Anastas, P. T., Williamson, T., Eds.; ACS Symposium Series 626; American Chemical Society: Washington, DC, 1996; pp 1-17.

[7] D. Delledonne, F. Rivetti, U. Romano, Appl. Catal., A 221 (2001) 241-251.

[8] Y. Ono, Catal. Today 35 (1997) 15–25.

[9] Y. Ono, T. Baba, Catal. Today 38 (1997) 321–337.

[10] P. Jessop, T. Ikariya, R. Noyori, Chem. Rev. 99 (1999) 475–494.

[11] S. Neil Isaaca, B. O. Sullivan, C. Verhaelen, Tetrahedron 55 (1999) 11949–11956.

[12] M. A. Pacheco, C. L. Marshall, Energy Fuels 11(1997) 2-29.

[13] Chem. Week March 24 (1999) 41.

[14] F. Mizia, F. Rivetti, U. Romano, US Patent 5,315,034 (1994).

[15] M. Aresta, E. Quaranta, Tetrahedron 47 (1991) 9489.

[16] M. Selva, C.A. Marquez, P. Tundo, J. Chem. Soc., Perkin Trans. 1 (1994) 1323.

[17] P.C. Loosen, P. Tundo, M. Selva, European Patent 525,506 (1992).

[18] A. Bomben, C.A. Marques, M. Selva, P. Tundo, Tetrahedron 51 (1995) 11573.

[19] F. Rivetti, in: P.T. Anastas, P. Tundo (Eds.), Green Chemistry: Challenging Pespectives, Oxford University Press, Oxford, 2001, p. 201.

[20] M.A. Pacheco, C.L. Marshall, Energy Fuel 11 (1997) 2.

[21] M. Bilde, T.E. Mogelberg, J. Sehested, O.J. Nielsen, T.J. Wallington, M.D. Hurley, S.M. Japar, M. Dill, V.L. Orkin, T.J. Buckley, R.E. Huie, M.J. Kurylo, Phys. Chem. A 101 (1997) 3514.

[22] M.E. Jenkin, G.D. Hayman, Atmos. Environ. 33 (1999)1275.

[23] H.-J. Buysch, H. Krimm, S. Bohm, (1982), US Patent 4335051.

[24] Y. Ono, Appl. Catal., A 155 (1997) 133–166.

[25] S. Uchiumi, K. Ataka, T. Matsuzaki, J. Organomet. Chem. 576 (1999) 279–289.

[26] H. Babad, A.G. Zeiler, Chem. Rev. 73 (1973) 75.

[27] H.J. Buysch, in: Ullmann's Encyclopaedia of Industrial Chemistry, VCH Publishers, Weinheim, Vol. A5, p. 197.

[28] I. J. Drake, K. L. Fujdala, A. T. Bell, T. D. Tilley, J. Catal. 230 (2005) 14–27.

[29] D. Delledonne, F. Rivetti, U. Romano, J. Org. Chem. 448 (1995) C15-C19

[30] Y. Sato, M. Kagotani, T.Yamamoto, Y. Souma, Appl. Catal., A 185 (1999) 219-226.

[31] K. Tomishige, T. Sakaihori, S. Sakai, K. Fujimot, Appl. Catal., A 181 (1999) 95-102.

[32] U. Romano, R. Tesei, M. Massi Mauri, P. Rebora, Ind. Eng. Chem. Prod. Res. Dev. 19 (1980) 396.

[33] U. Romano, R. Tesei, G. Cipriani, L. Micucci, US Patent 4,218,391 (1980).

[34] U. Romano, M. Massi Mauri, F. Rivetti, Ing. Chim. Italy 21 (1985) 6.

[35] U. Romano, Chim. Ind. (Milan) 75 (1993) 306.

[36] D. Delledonne, F. Rivetti, U. Romano, European Patent 463,678 (1991).

[37] H. Miyazaki, Y. Shiomi, S. Fujitsu, K. Masunaga, H.Yanagisawa, US Patent 4,384,133 (1983).

[38] H. Cui, T. Wang, F. Wang, J. Supercrit. Fluids. 30 (2004) 63-69.

[39] A. Dibenedetto, M. Aresta, F. Nocito, C. Pastore, A. M. Venezia, E. Chirykalova, V. I. Kononenko, V.G. Shevchenko, I. A. Chupovaet, Catal. Today 115 (2006) 117-123.

[40] J. F. Knifton, US Patent 4,661,609 (1987).

[41] B. Yang, D. Wang, H. lin, J. Sun, X. Wang, Catal. Comm. 7 (2006) 472-477.

[42] M. Wang, N. Zhao, W. Wei, Y. Sun, Ind. Eng. Chem. Res. 44 (2005) 7596-7599.

[43] M.A. Pacheco, C.L. Marshall, Energy Fuel 11 (1997) 2.

[44] K. Tomishige, T. Sakaihori, Y. Ikeda, K. Fujimoto, Catal. Lett. 58(1999) 225-229.

[45] K. Tomishige, Y. Ikeda, T. Sakaihori, K. Fujimoto, J. Catal. 192 (2000) 355-362.

[46] J. Choi, T. Sakakura, T. Sako, J. Am. Chem. Soc. 121 (1999) 3793-3794.

[47] K. Tomishige, Y. Furusawa, Y. Ikeda, M. Asadullah, K. Fujimoto, Catal. Lett. 76 (2001) 71-74.

[48] C. J. Jiang, Y. Guo, C. G. Wang, C. Hu, Y. Wu, E. Wang, Appl. Catal., A 256 (2003) 203-212.

[49] X.. L. Wu, M. Xiao, Y. Z. Meng, Y. X. Lu, J. Mol. Catal. A 238 (2005) 158-162.

[50] X. L. Wu, Y.Z. Meng, M. Xiao, Y.X. Lu, J. Mol. Catal. A 249 (2006) 93-97.

[51] Y. Zhang, Ian J. Dranke, D. N. Briggs, A. T. Bell, J. Catal. 244 (2006) 219-229.

[52] Z. Hou, B. Han, Z. Liu, T. Jiang, G. Yang, Green Chem. 4 (2002) 467-471.

[53] J. Choi, L. He, H. Yasuda, T. Sakakura, Green Chem. 4 (2002) 230-234.

[54] T. Zhao, Y. Han, and Y. Sun, Nat Gas Chem. Ind. (Chin.) 23 (1998) 52-55.

[55] K. Tomishige, K. Kunimori, Appl. Catal., A 237 (2002) 103-109.

[56] M. Aresta, A. Dibenedetto, E. Fracchiolla, P. Giannoccaro, C. Pastore, I. Pápai, G. Schbert, J. Org. Chem. 70 (2005) 6177-6186.

[57] Meier, W. M. and Olson, D. M., Atlas of Zeolite Structure Types, 3th ed., Butterworth-Heinemann, London (1992).

[58] Vaughan, D. E. W., "Natural Zeolites: Occurrence, Properties and Use", Sand, L. B. and Mumpton, F. A. Eds., London Pergamon, 1978.

[59] Chen, N. Y., Garwood, W. E. and Dwyer, F. G. Shape selective Catalysis in Industrial Application , 2nd ed., revised and expanded, Marcel Dekker, New York, 1996.

[60] Shourong Zheng, Surface modification of HZSM-5 zeolites, PhD thesis. Technischen Universität München.

[61] D. W. Breck, Zeolite molecular sieves, Structure Chemistry and Use. New York, John Wiley, 1974.

[62] J. Weitkamp, L. Puppe, Catalysis and Zeolites fundamentals and applications, Springer, 1999.

[63] D. W. Breck, W. G. Eversole, R. M. Milton. J. Am. Chem. Soc. 78 (1956) 5963–5972

[64] R. M. Milton. (1959) US Pat 4534947

[65] V. P. Lakeev, Razrabotka Gazovykh Mestorozhdenii, Transport Gaza, 1974, 1, Pt2, 120-136.

[66] K.-I. Okamoto, H. Kita, K. Horii, K. T. Kondo, Ind. Eng. Chem. Res. 40 (2001) 163-175.

[67] T. C. Bowen, R. D. Noble, J. L. Falconer, J. Membr. Sci. 245 (2004)1–33.

[68] Y. Li, W. Yang, J. Membr. Sci. 316 (2008) 3–17.

[69] Salem M. Ben-Shebi, Chem. Eng. J. 74 (1999) 197-204.

[70] Kokai Tokkyo Koho, (1982) JP 57101757

[71] X. Liu, H. Yao, Gaoxiao Huaxue Gongcheng Xuebao, 6(2) (1992) 153-159.

[72] D. E. Chasan, L. L. Pytlewski, R. O. Hutchins, N, M, Karayannis and C. Owens, Inorg. Nucl. Chem. Lett. 11(1) (1975) 41-45.

[73] M. Goyal, R. Nagahata, J. Sugiyama, M. Asai, M. Ueda, K. Takeuchi, Polymer, 40 (1999) 3237–3241

[74] Q. Wang and R. Huang, Tetra. Lett. 41 (2000) 3153–3155

[75] C. E. Outlaw, C. F. Fillers, B. T. Smith, K. H. Maness, D. J. Olsen, WO 2000029366

[76] R.X. Fischer, W.H. Baur. Microporous and other Framework Materials with Zeolite-Type Structures, Springer, 2006.

[77] R. M Barrer, Zeolites and Clay minerals as sorbents and Molecular Sieves, Frs. Chemistry Department, Imperial College, London. 1978.

[78] I. E. Neimark, M. A. Piontkovskaya, A. I. Lukash, R. S. Tyutyunnik, Otd. Khim. Nauk. (1962) 49-58.

[79] R. Maachi, M. J. Boinon, J. M. Vergnaud, Journal de Chimie Physique et de Physico-Chimie Biologique 75(1) (1978) 116-120.

[80] N. Tessa, B. Tyburce, G. Joly, Journal de Chimie Physique et de Physico-Chimie Biologique, 88(5) (1991) 603-613.

[81] R. Y. Yanagida, A. A. Amaro, K. Seff, J. Phys. Chem. 77(6) (1973) 805-809.

[82] P. C. W. Leung, K. B. Kunz, K. Seff, J. Phys. Chem. l79 (20) (1975) 2157-2162.

[83] J. M. Adams, D. A. Haselden, J. Solid State Chem. 47 (1983) 123-131.

84. Jiaong Xiao and James Wei, Chem. Eng Sci. 47 (1992) 1123.

[85] T. Shigetomi, T. Nitta, T. Katayama, J. Chem. Eng. Jpn. 15(4) (1982) 249-254.

[86] C. Akosman, M. Kalender, Fresenius Environ. Bull. 16(5) (2007) 500-507.

[87] K. F. Loughlin, Adsorption, 15(4) (2009) 337-353.

[88] Gábor Rutkai, Éva Csányi, Tamás Kristóf, Microporous Mesoporous Mater. 114 (2008) 455–464.

[89] Éva Csányi, Tamás Kristóf, and György Lendvay, J. Phys. Chem. C113 (2009) 12225–12235

[90] J. Y. Wu, Q. L. Liu, Y. Xiong, A. M.Zhu, Y. Chen, J. Phys. Chem. B 113 (2009) 4267–4274.

[91] J. Kuhn, J. M. Castillo-Sanchez, J. Gascon, S. Calero, D. Dubbeldam, T. J. H. Vlugt, F. Kapteijn, J. Gross, J. Phys. Chem. C 113 (2009) 14290–14301.

[92] K. Cho, H. S. Cho, L. de Menorval, R. Ryoo, Chem. Mater. 21(23) (2009) 5664-5673.

[93] C. A Koh, J. A.Zollweg, K. E. Gubbins, Stud. Surf. Sci. Catal. 87 (1994) (Characterization of Porous Solids III), 61-70.

[94] K. J. Ptasinski, C. Hamelinck, P. J. A. M. Kerkhof, Energy Convers. Manage. 43

(2002) 1445–1457.

[95] G. Ertl, H. Knözinger, J. Weitkamp, Handbook of Heterogeneous Catalysis, Weinheim, Sellchaft mbH, 1997, P1856-1876.

[96] P. Galindo Cifre, O. Badr, Energy Convers. Manage. 48(2) (2002) 519-527.

[97] R. H. Scott, (1977) USP 4013521.

[98] A. Pinto, (1980) USP. 4210495.

[99] Y. Saito, O. Hashimoto, (1988) USP. 4744869.

[100] C. Rescalli, R. Ricci, A. Scazzosi, F. Cianci, (1989) USP. 4874474.

[101] R. L. Kao, Sarabijit. S. Randhava, Surjit. S. Randhava, (1992) USP. 5079267.

[102] Methanol production, comparing the LP and LCM process, SenterNovem, Available at:

//www.senternovem.nl/mmfiles/Project_experience_factsheet_MethanolUK_tcm24-2 39416.pdf; November 2009.

[103] D. F. Othmer, (1983) USP 4405343.

[104] H.L. Fleming, Chem. Eng. Prog. (1992) 46-52.

[105] R.Y.M. Huang (Ed.), Pervaporation Membrane Separation Processes, Elsevier, Amsterdam, 1991.

[106] S.I. Semenova, H. Ohya, K. Soontarapa, Desalination 110 (1997) 251-286.

[107] X. Feng, R. Y. M. Huang, Ind. Eng. Chem. Res. 36 (1997) 1048-1066.

[108] Y. Morigami, M. Kondo, J. Abe, H. Kita, K. Okamoto, Sep. Purif. Tech. 25 (2001) 251–260.

[109] J. Caro, M. Noack, P. Kölsch, R. Schäfer, Microporous Mesoporous Mater.38 (2000) 3-24.

[110] T. C. Bowen, R. D. Noble, J. L. Falconer, J. Membr. Sci. 245 (2004) 1–33.

[111] Y. Li, W. Yang, J. Membr. Sci. 316 (2008) 3–17.

[112] J. Caro, M. Noack, Microporous Mesoporous Mater. 115 (2008) 215-233.

[113] M. E. Davis, Nature 417 (2002) 813-821.

[114] S. A. I. Barri, G. J. Bratton, T. d. Naylor, (1997) US 5605631.

[115] J. C. Jansen, F. Kapteijn, S. A. Strous, (2007) US 7214719, B2.

[116] A. S. T. Chiang, G. Shu, J. Liu, R. Selvin, (2007) US 7253130, B2.

[117] Q. Liu, R.D. Noble, John. L. Falconer, H. H. Funke, J. Membr. Sci. 117 (1996) 163-174.

[118] K. Okamoto, H. Kita, M. Kondo, N. Miyake, Y. Matsuo, U.S. Patent. (1996) 5554286.

[119] K. Okamoto, H. Kita, K. Horii, K. T. Kondo, Ind. Eng. Chem. Res. 40 (2001) 163-175.

Chapter 2

Direct Dimethyl Carbonate Synthesis from Methanol and CO$_2$: Strategies for Yield Improvement

Abstract

Experiments and thermodynamic calculations showed that the direct synthesis of dimethyl carbonate from CO$_2$ and methanol is a highly equilibrium limited reaction at approximately 1-2 % DMC yield. Its equilibrium constant is only 8.5×10^{-6} at 433 K limiting the yield of dimethyl carbonate. Removing water using dehydrating agents can shift the reaction and increase the DMC yield significantly. Decoupling the reaction and the removal of water into different reaction zones increased the dimethylcarbonate yield to 17 % using zeolite 3A at 248 K as drying agent.
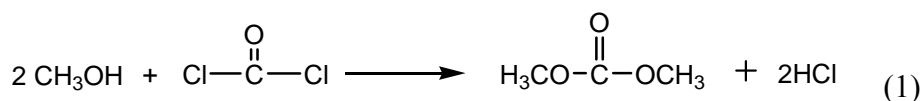
Key words: Dimethyl carbonate; Artificial CO$_2$ fixation; Equilibrium limitation; Equilibrium shift; 3A Zeolite; dehydrating agent.
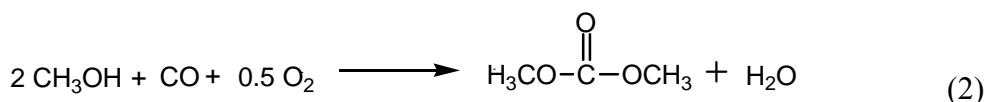
2.1. Introduction

Dimethyl carbonate (DMC) is a "green" chemical reagent in terms of its low toxicity, non-corrosiveness and ready biodegradation. CH3–, CH3O–, and –CO– functional groups in the DMC molecule render its wide applications as methylating, methoxylating and carbonylating agent in replacement of some virulent carcinogens, such as phosgene, dimethyl sulphate and chloromethane [1-3]. Moreover, DMC is also a good solvent, useful fuel additive and monomer for the synthesis of polycarbonate resins [4-6].

Currently, DMC is synthesized mainly via three commercial processes:

(1) Conversion of phosgene with methanol [7-9],

$$2\,CH_3OH \;+\; Cl-\!\overset{\overset{\textstyle O}{\|}}{C}\!-Cl \;\longrightarrow\; H_3CO-\!\overset{\overset{\textstyle O}{\|}}{C}\!-OCH_3 \;+\; 2HCl \qquad (1)$$

(2) Oxidative carbonylation of methanol [10-13],

$$2\,CH_3OH + CO + 0.5\,O_2 \;\longrightarrow\; H_3CO-\!\overset{\overset{\textstyle O}{\|}}{C}\!-OCH_3 \;+\; H_2O \qquad (2)$$

(3) Transesterification of ethylene carbonate with methanol [14-15].

$$2\,CH_3OH + \begin{matrix}H_2C-O\\ |\qquad\;\;\;\;\;C=O\\ H_2C-O\end{matrix} \;\rightleftharpoons\; H_3CO-\!\overset{\overset{\textstyle O}{\|}}{C}\!-OCH_3 \;+\; \begin{matrix}CH_2OH\\ |\\ CH_2OH\end{matrix} \qquad (3)$$
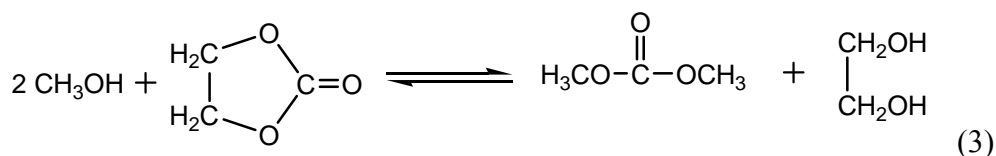
The first route (Equation 1) has to be replaced eventually, because of the inevitable use of the extremely toxic phosgene gas. Oxidative carbonylation (Equation 2) has been considered as the most potential approach. The low methanol conversion and DMC selectivity and the corrosive catalysts applied, however, limits its industrial

application. The process of transesterification of ethylene carbonate and methanol (Equation 3) is also commercially problematic due to the use of ethylene carbonate.

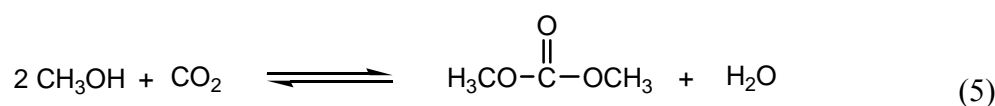(4) Transesterification of urea with methanol [16-17]

$$2\ CH_3OH + CO(NH_2)_2 \rightleftharpoons H_3CO-\overset{\overset{\displaystyle O}{\|}}{C}-OCH_3 + 2NH_3 \qquad (4)$$

(5) Direct DMC synthesis from CO$_2$ and methanol [18-26]

$$2\ CH_3OH + CO_2 \rightleftharpoons H_3CO-\overset{\overset{\displaystyle O}{\|}}{C}-OCH_3 + H_2O \qquad (5)$$
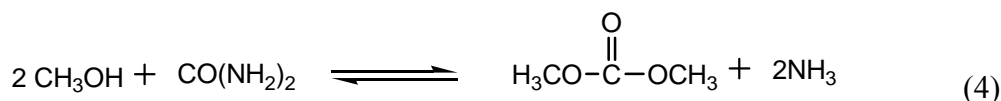
Others DMC synthesis routes such as the urea methanolysis (Equation 4) and direct synthesis from methanol/CO$_2$ (Equation 5) have been proposed recently. Because of the increasing availability of CO$_2$ and environmental concerns associated with it, the latter process may be a very promising approach.

ZrO$_2$ as well as CeO$_2$-ZrO$_2$ have been reported as catalysts for DMC direct synthesis from methanol and CO$_2$. The basic sites on ZrO$_2$ serve to activate methanol and CO$_2$, while the acidic sites supply methyl groups from methanol in the last step of the reaction mechanism [18, 19, 21 and 26]. Nevertheless, this reaction is an equilibrium-limited reaction and only a very small amount of DMC could be produced [18, 20-25].

Not surprisingly, many efforts were performed directed to shifting the reaction towards DMC formation, e.g., increasing the reactant concentration and removing the by produced water. According to Jiang et al., the formed DMC seemed to be almost proportional to the methanol in the range of 0-10 mol L^{-1} [22]. A higher partial pressure of CO$_2$ is also beneficial for higher DMC yields because a higher concentration of CO$_2$ is dissolved. For instance, when the reaction was carried out at CO$_2$ pressure of 12 MPa, Hou et al. claimed that methanol conversion as high as 7 % were obtained [28]. Methanol conversion of nearly 50 % after 72 h under 30 MPa was achieved in work of

Choi et al. when 3A zeolite was applied as desiccant at room temperature [29]. Note that the large excess of applied CO_2, compared to methanol would impede its practical industrial realization. The reason for this is that the investment of construction and the cost of routine maintenance of extremely high pressure reaction unit [30] are too big to be sustainable.

The second strategy, using water scavengers has shown to be a good approach to remove the extremely low concentration of water in methanol. Although 2,2-dimethoxypropane (DMP) and dicyclohexylcarbodiimide (DCC) can be used as water scavengers for this purpose, the main problem for this practical application is the high cost for the regeneration of the spent stoichiometric scavengers [26,27]. By contrast, the high availability and easy recovery of inorganic adsorbents, e.g., zeolites [28, 29], make them the most promising candidates to remove the water in the direct synthesis of DMC.

In this paper, a detailed calculation of thermodynamic parameters under reaction conditions is presented and used to predict the maximum DMC yields under selected reaction conditions. To enhance DMC yields, the strategy of utilizing 3A zeolite to adsorb the co-produced water is shown to be successful under moderately high pressures (max. several tens of bars). The finding that water-adsorption efficiency of 3A zeolite greatly increases at temperatures far below 273 K inspires us to design a new reaction unit with two temperature zones, high-temperature reaction zone and low-temperature water-removal zone. After the reactant composition and reaction conditions being optimized, the final concentration of DMC in methanol reaches sufficiently high levels for further DMC separation from methanol in industrial applications.
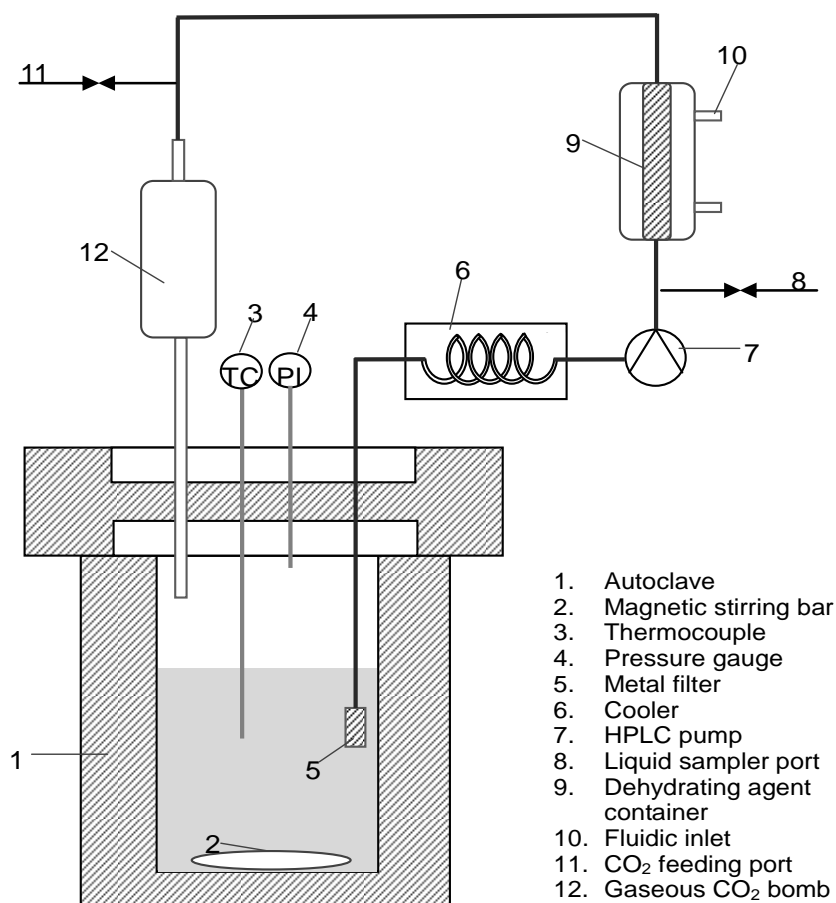
2.2. Experimental

2.2.1. *Preparation of catalysts*

The hydrous zirconia was obtained by hydrolysis of 400 ml of 0.34 M solution of zirconyl nitride ($ZrO(NO_3)_2 \cdot 8H_2O$, 99 %, Aldrich) with 600 ml of 2 mol l^{-1} solution of NH_3 (Aldrich) [32, 33]. Zirconyl nitride solution was added (5 ml min^{-1}) into the NH_3 solution under vigorous stirring. During the entire course of precipitation, the pH was maintained in the range of 11.6-10.6. After precipitation, the mixture was heated to 373 K and digested for 24 h. After aging, the samples were removed, vacuum filtered and extensively washed with bi-distilled water for 5 times. Then the cake was dried at 383 K overnight in a drying oven followed by calcination in synthesis air flow of 100 ml min^{-1} at 673 K for 4 h.

2.2.2. *DMC synthesis from methanol and CO₂*

The reaction was carried out in a stainless steel autoclave (autoclave-I) with an inner volume of 70 ml. The standard procedure is as follows: 23.8 g of methanol (Aldrich, >99.9%) and 0.5 g of catalyst were put into an autoclave. The reactor was purged by filling and releasing 10 bar of N_2 for 4 times. After the autoclave was heated to designated temperatures (413-453 K), liquid CO_2 (5.0 g, 114 mmol, Westfalen AG, 99.995%) was introduced into the autoclave at a flow rate of 10 ml min^{-1} using a syringe pump (Teledyne ISCO; Model 500). The pressure was monitored by a mechanical pressure gauge. Liquid samples were taken at intervals and analyzed by a gas chromatograph (FISONS GC8160) equipped with a RTX-5AM column. A blank test preliminarily excluded any extent of reaction without ZrO_2. DMC yields were calculated based on initial CO_2 amount according to Equation 6 (N_{DMC}: produced DMC in mmol, N^0_{CO2}: CO_2 amount used in mmol). H_2O concentrations were measured by Karl-Fisher water analyzer (SCHOTT TA10 plus).

$$Yield_{DMC}(mol\%) = \frac{N_{DMC}}{N^0_{CO2}} \times 100\% \qquad (6)$$

2.2.3. DMC synthesis from methanol and CO$_2$ with water removal

1. Autoclave
2. Magnetic stirring bar
3. Thermocouple
4. Pressure gauge
5. Metal filter
6. Cooler
7. HPLC pump
8. Liquid sampler port
9. Dehydrating agent container
10. Fluidic inlet
11. CO$_2$ feeding port
12. Gaseous CO$_2$ bomb

Figure 1 Schematic diagram of optimized reaction unit for DMC synthesis.

In order to shift the reaction by removing the produced H$_2$O and adding more CO$_2$, an optimized setup with a 70 ml autoclave (autoclave-II) has been designed (Figure 1). The standard reaction procedure is as follows: 39.6 g of methanol and 2.0 g of catalyst were first loaded into the autoclave. The dehydrating agent container was fully filled with 18 g 3A zeolite pellets (pellet size: 2-3 mm, Sigma Chemicals), and the temperature was adjusted and maintained by circulating the liquid from a refrigerator (FBC 740) through the jacket tube. Then, the reactor was purged with N$_2$ for 4 times, than heated to 433 K and CO$_2$ was fed (3.0-20 g). The reaction mixture was recirculated between reactor and zeolite trap by a HPLC pump at a speed of 2 ml min^{-1}. Before entering the HPLC pump head, the reaction mixture was cooled down to room temperature. The formed trace amounts of water were then selectively adsorbed by the

zeolite in the dehydrating agent container. After that, the reaction mixture was driven back into the autoclave. During the reactions, liquid samples were taken at intervals and analyzed by a GC and Karl-Fisher water analyzer. DMC yields were also calculated based on initial CO_2 amount used.

2.3. Results

2.3.1. *DMC synthesis without water removal*

Figure 2 shows the profiles of DMC yield versus residence time over ZrO_2 at 413, 433 and 453 K. By-products, e.g. dimethylether (DME) which may be expected from bimolecular dehydration of methanol, were always below the detection limit of GC-FID. This is not surprising considering the fact that DME is only easily formed on the strong acid sites [31], while there are only weak acid and base sites in ZrO_2 present. Therefore, the selectivity to DMC based on total carbon is essentially 100%. It can be seen that DMC yields finally reached a plateau in all cases, indicative of the establishment of chemical equilibrium. With respect to kinetics, it is clearly seen from the slope of the curves that the reaction rates are faster at higher temperatures at the early stage of the reaction. At lower temperatures, the established rate of equilibrium is slower and thus longer time is needed to attain the maximum yield for DMC. On the other hand in terms of thermodynamic calculations, lower reaction temperatures led to higher DMC yields at equilibrium.

This can be explained by the fact that the reaction is exothermic with $\Delta_r H^o$ of -15 kJ mol^{-1} [30]. However, it can be misled to analyze the data, if the reaction is terminated before reaching the DMC yield plateau. For example, the ranking of DMC yield after 2 h of reaction at different temperatures is reversed in comparison with that at equilibrium. This suggests that DMC formation was kinetically controlled at short experimental duration in a certain temperature range, while the reaction was thermodynamically controlled during longer experiments. This is similar to what had been observed for ZrO_2 and $H_3PW_{12}O_{40}/ZrO_2$ catalytic systems [18, 22].
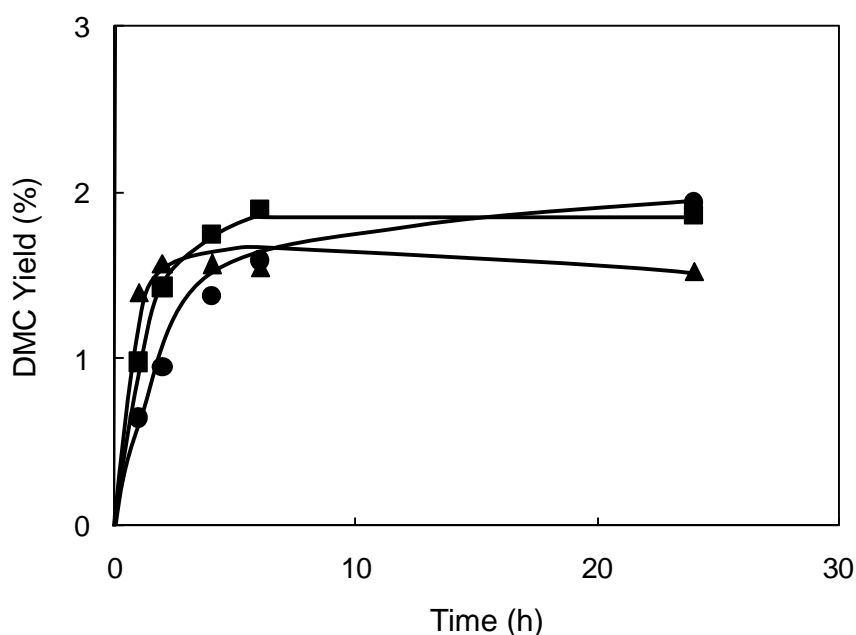
Figure 2 DMC yields versus reaction time at different temperatures, (●) 413 K; (■) 433 K; (▲) 453 K, over ZrO_2. Reaction conditions: autoclave-I (volume: 70 ml), ZrO_2: 0.5 g, methanol: 23.8 g (742 mmol), liquid CO_2: 5 g (114 mmol), temperature: 433 K.

Table 1 Liquid phase concentrations of chemical compounds involved in the DMC direct synthesis at different temperature when equilibrium is established.[*]

T (K)	P_{total} (bar)	C_{CO2} (mol l⁻¹)	C_{CH3OH} (mol l⁻¹)	C_{DMC} (mol l⁻¹)	C_{H2O} (ppm)	K_c' (×10⁻⁶)	Theoretical K (×10⁻⁶)
413	48	2.4	24.7	0.042	4170	8.8	9.5
433	57	2.4	24.7	0.041	3410	7.1	8.5
453	72	2.5	24.7	0.034	3710	6.1	7.5
433-2	57	2.4	24.7	0.038	3900	7.4	8.5

[*] Reaction conditions: autoclave-I (70 ml inner volume), ZrO_2: 0.5 g, methanol: 23.8 g, liquid CO_2: 5.0 g.

Table 1 lists the concentrations of all reactants and products in the liquid phase, when reaction equilibria were reached after 24 h at three different temperatures. Note that at higher temperatures somewhat less DMC was formed. The concentrations of CO_2 and methanol do not change, because of the low conversions achieved. The

concentration of water in the solution did not show a definite trend with the increasing temperature. The estimated water concentration from reaction, however, would be less than 1000 ppm. Therefore, we conclude here that most of the water in Table 1 did not only originate from the reaction, but also was introduced by the impurities of starting reactants or intake from the atmosphere during the experiment. The concentration of CO_2 dissolved in liquid mixture is obtained by subtracting amount of CO_2 in gas phase from the fed amount of CO_2 (5 g) and dividing it by liquid volume. Liquid CO_2 was fed into the reactor at a precisely- controlled rate using a high pressure ISCO syringe pump. CO_2 in the gas phase was estimated by applying ideal gas law and using its vapor pressure (total pressure minus the vapor pressure of methanol) at this temperature. It is found that more than 90% of CO_2 remains in the liquid phase (2.4 mol l^{-1}) at all three temperatures in line with the fact that CO_2 is well soluble in methanol. The possibility of catalyst deactivation (e.g., by H_2O) limiting the conversion was excluded by repeating the experiment with the spent catalyst at 433 K.

To compare the experimental and theoretical values of equilibrium constants, detailed calculations were conducted. The theoretical equilibrium constants K were calculated from the change of Gibbs free energies from reactant to products [34]. A different method uses the approximation that the ratio of activity coefficients is constant, and $K_c{'}$ was calculated according Equation 7. The (dimensionless) equilibrium constant is defined as the ratio of the activities, normalized to the standard state.

$$K_c{'} = \frac{(C_{H2O}/C^o)*(C_{DMC}/C^o)}{(C_{CO2}/C^o)*\left(C_{MeOH}/C^o\right)^2} \tag{7}$$

The density of the mixture was taken as the density of methanol at room temperature, 0.792 g ml^{-1}, and was supposed to change negligibly throughout the reaction because of the low conversion level. Table 1 showed that the equilibrium constant of this reaction is very low at 413 - 453 K and decreases with increasing reaction temperature. The theoretical and experimental values are of the same order of

magnitude with very small discrepancies documenting that the reaction of DMC synthesis from methanol and CO_2 is highly equilibrium-limited.

2.3.2. *DMC synthesis with water removal*

The results reported were obtained in the modified reaction unit (Figure 1) with recirculation of the reaction mixture between the reactor and the zeolite trap. In addition, a CO_2 storage tank (part 12 in Figure 1) was used to allow applying more CO_2 for reactions. The cooled trap packed with 3A zeolite as dehydrating agent (part 9 in Figure 1) is part of the circulation loop.
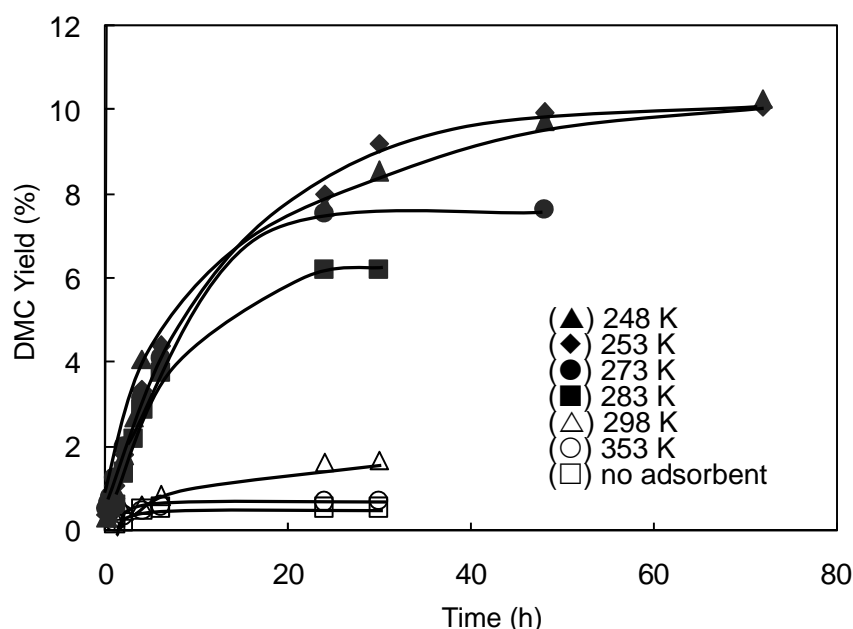
Figure 3 Dependence of DMC yield (%) on the temperature of water removal trap containing zeolite 3A. Reaction conditions: autoclave-II, temperature: 433 K, total pressure: 42 bar, ZrO_2: 2.0 g, liquid CO_2: 10 g, methanol: 39.6 g, 3A zeolite: 18.0 g, liquid phase mixture circulation rate: 2.0 ml/min.

When the 3A zeolite trap temperature was set to 353 K, the yields of DMC were very low (<1%), because the zeolite was not able to absorb a significant amount of water from the reaction mixture under these conditions (Figure 3). Reducing the 3A

zeolite trap temperature by 45 K to 298 K induce increased the DMC yield only moderately to 1.8 % at equilibrium after 30 h. It is interesting to note that DMC yield increased threefold, when the adsorbent temperature was lowered to 283 K. This indicates a sudden efficiency enhancement at lower temperatures for the 3A zeolite to adsorb water from the mixture containing methanol-CO_2-DMC-water.

At even lower temperatures, e.g., 248 and 253 K, higher DMC yields were obtained, but the time to establish the equilibrium extended to approximately 72 h. It implies that the water removal rate was significantly reduced by lowering the temperature. Understanding the water-adsorptions of the 3A material at 273 K and below require detailed characterizations of the state of water adsorbed in the zeolite, which is beyond this contribution and will addressed in further contributions.
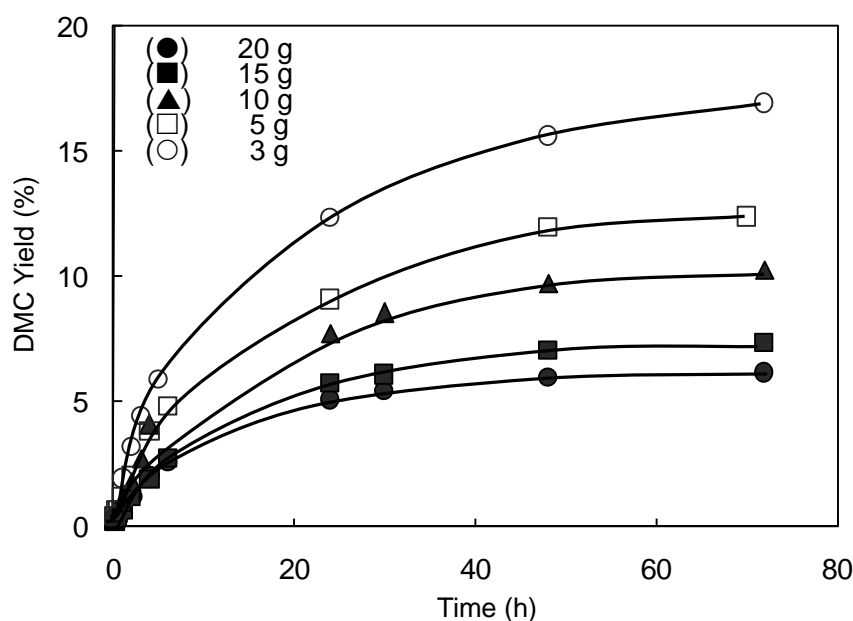
Figure 4 Effect of CO_2 feeding amount on the DMC yield (%). Reaction conditions: autoclave-II, temperature: 433 K, ZrO_2: 2.0 g, methanol: 39.6 g, 3A zeolite: 18.0 g maintained at 248 K, liquid phase mixture circulation rate: 2.0 ml/min.

Figure 4 shows the effect of the initially introduced amount of CO_2 on the DMC yield at the reaction-zone temperature of 433 K and a temperature of the water-

removal-zone of 248 K. This was the lowest temperature of 3A zeolite for maximizing its water-adsorption efficiency investigated. As shown in Figure 4, increasing the CO_2 loading amount resulted in lower CO_2 based DMC yields. We will explain these observations in details below.

Substituting C_{DMC} in equation 6 by Equation 8 (a transformation of Equation 7) produces the formula of DMC yield shown as Equation 9:

$$C_{DMC}\ (\text{mol}\,\text{l}^{-1}) = \frac{K'C_{CO_2} \cdot (C_{MeOH})^2}{C_{H_2O}C^o} \tag{8}$$

$$\text{Yield}_{DMC}\,(\text{mol}\%) = \frac{K'(C_{CO_2}V_{liquid})(C_{MeOH})^2}{C_{H_2O}C^o N^0_{CO_2}} \tag{9}$$

The initially fed CO_2, N^0_{CO2}, partly exists in gas-phase and is partly dissolved in liquid mixture, which would give Equation 10:

$$N^0_{CO2}\ (\text{mol}) = \frac{P_{CO2}V_{CO2}}{RT} + C_{CO2}V_{liquid} \tag{10}$$

Combining Equations 9 and 10, at a particular temperature, the partial pressure of CO_2 in the reactor (P_{CO2}), the concentration of dissolved CO_2 in the liquid (C_{CO2}) and the concentration of water in the liquid mixture (C_{H2O}) would all influence the maximum DMC yields at equilibria. When the introduced amount of CO_2 was changed at a certain temperature, for instance, comparing 10 to 3 g, the P_{CO2} was also tripled according to the experiment (shown in Figure 4 as legend). And it would indicate, from equation 10, that C_{CO2} in liquid phase would then be approximately tripled accordingly. As a result, C_{CO2}/N^0_{CO2} would remain almost constant even if a minor deviation is taken into account. Based on such analysis, the DMC yield would remain almost unchanged according to Equation 9 (equilibrium constant K', C_{MeOH}, V_{liquid} and V_{CO2} are the same for the data set in Figure 4), providing that the H_2O concentration was constant during different CO_2 loading. However, this is not the case. A higher amount of CO_2 fed into the reactor led to a lower DMC yield. As in Table 2, the H_2O

concentrations in liquid mixture were totally different, when the introduced amount of CO_2 changed. The higher the CO_2 amount, the more water was formed and the DMC yield was therefore lowered (C_{H2O} is in the denominator of Equation 9). As more CO_2 is introduced into the reactor, the equilibrium was shift towards the formation of more DMC, and thus higher concentrations of DMC in liquid mixture can be expected. This is in good accordance with the results that were shown in Table 2 and Figure 5.

Table 2 Dependence of DMC yields on loaded CO_2 amounts for DMC direct synthesis from methanol and CO_2 at 433 K with water removal by 3A zeolite.[*]

Loaded CO_2 (g)	P (bar)	DMC yield (mol%)	DMC conc. (wt %)	H_2O (ppm)	$K_c'(\times 10^{-6})$
20	66	6.1	6.0	1340	9.79
15	53	7.3	5.4	510	7.10
10	40	10.3	4.6	480	10.5
5	30	12.4	3.1	320	8.87
3	26	16.9	2.5	200	7.83

[*] Reaction conditions: ZrO_2: 2.0 g, methanol: 39.6 g, 3A zeolite (operated at 243 K): 18.0 g; liquid phase mixture was circulated at a speed of 2.0 ml min⁻¹.
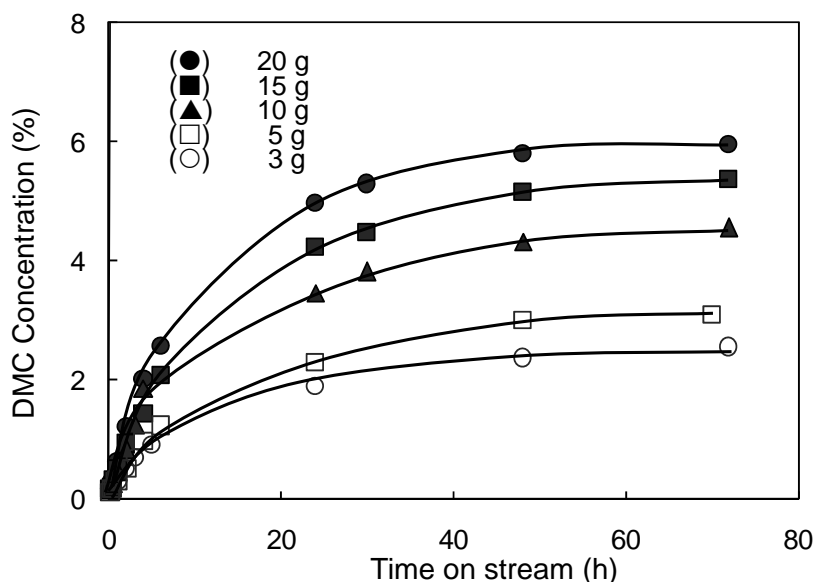

Figure 5 Effect of CO_2 feeding amount on the DMC concentrations (wt. %). Reaction conditions: autoclave-II, temperature: 433 K, ZrO_2: 2.0 g, methanol: 39.6 g, 3A zeolite: 18.0 g maintained at 248 K, liquid phase mixture circulation rate: 2.0 ml/min.

2.4. Discussion

The thermodynamic constraints of DMC direct synthesis from methanol and CO_2 had been reflected in recent publications [18-20, 30]. The maximal attainable extent of reaction for a designed chemical process is determined by the reaction equilibrium constant (K) under certain temperatures, i.e., by the changing of Gibbs free energy from reactants to products ($\Delta_r G°$). In this present work, thermodynamic calculations were performed using data acquired form the handbook, literature [30, 34-36] and internet NIST Chemistry Web Book.

As shown in Figure 6, the title reaction is a thermodynamically strongly limited reaction. Note that the activity coefficients of reactants and products which seriously limits the accuracy of the present calculations. For the present system the difference between the concentration ratio and the activity ratio is small. This is reflected by the close values of measured K_c' and theoretical K in Table 1. For instance, at 433 K, K_c' is 7.1×10^{-6}, and theoretical equilibrium constant K is 8.5×10^{-6}.
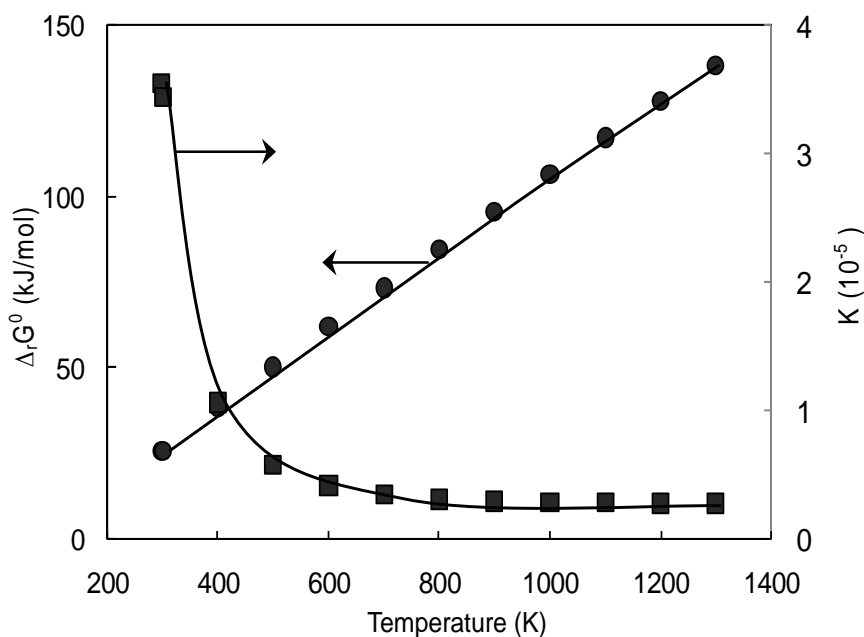
Figure 6 Dependence of $\Delta_r G^0$ (kJ/mol) (▲) and equilibrium constant K (■) on the reaction temperature of DMC direct synthesis from gaseous methanol and CO_2.
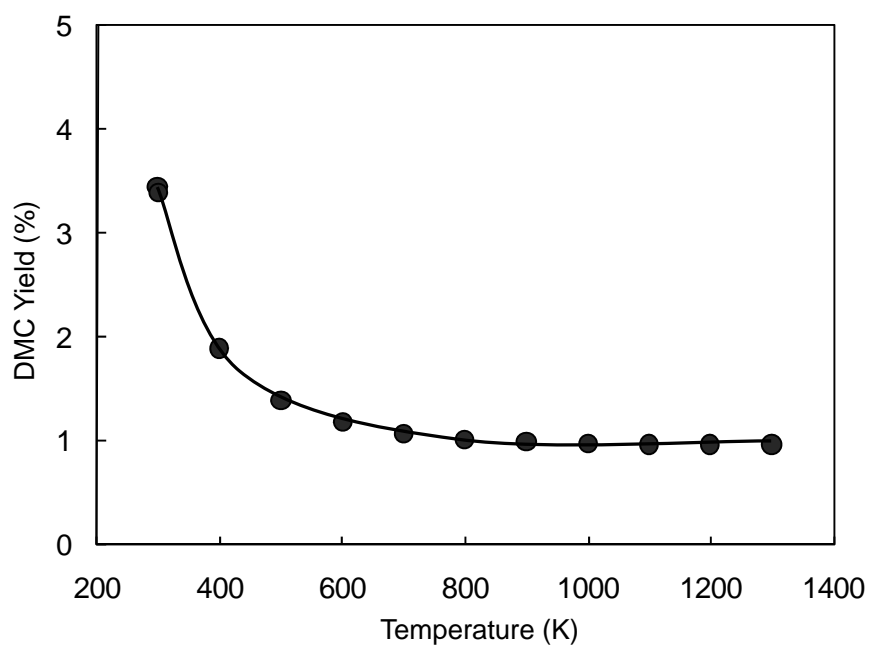
Figure 7 Dependence of DMC yield (CO_2 basis) from methanol and CO_2 on the reaction temperature. Total pressure: 100 bar (P_{CO2}: P_{CH3OH} = 1: 2).
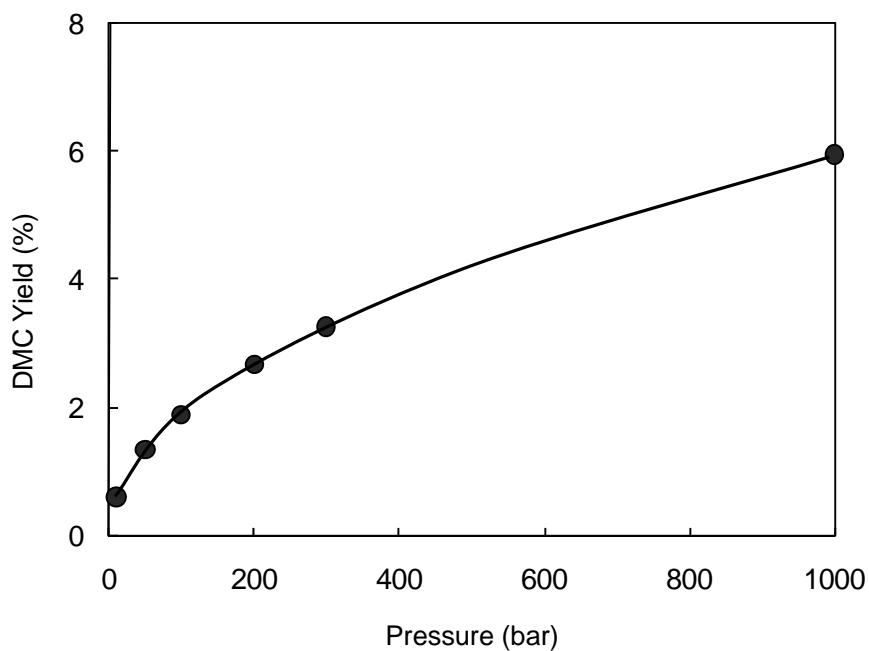
Figure 8 Dependence of DMC yield (CO_2 basis) at 400 K from methanol and CO_2 on the total pressure (P_{CO2} : P_{CH3OH} = 1 : 2).

Assuming the total pressure to be 100 bar, the effect of reaction temperature on the maximum predicted DMC yields are plotted in Figure 7. The DMC yield decreases with increasing the reaction temperature. Even at lower temperatures, e.g., 300 K, the DMC yield at equilibrium is estimated to be no higher than 4% assuming all reactants and products remain in the same phase. Accordingly, it seems difficult to improve the DMC yield to an applicable value by altering reaction temperature.

System pressure would only indirectly affect the reaction outcome, because a reaction occurring in liquid phase is hardly influenced by pressure change. Figure 8 shows the theoretical dependence of DMC yield on the total pressure of the system (filled only with two components, i.e. CO_2 and methanol) when reaction temperature is maintained at 400 K. Increasing system pressure is clearly beneficial for higher DMC yields due to higher partial pressures of the reactants, but it is still difficult to obtain a value higher than 6 % due to the low equilibrium constant (K ~ 1×10^{-5}). As shown in Figure 8, a yield of ~ 6 % can only be obtained when performing the reaction at 400 K and a total pressure as high as 1000 bar.

It is important to address the different trends of DMC yield with increasing CO_2 pressures shown by Figure 4 and Figure 8. For the title reaction in gas phase, when the ratio of partial pressures of CO_2 and methanol is *X*, Equation 11 determines the equilibrium constant (assuming that P_{CO2} and P_{CH3OH} remain almost unchanged before and after reaction):

$$K_p{}' = \frac{(P_{H2O}/P^o)*(P_{DMC}/P^o)}{(P_{CO2}/P^o)*(X \cdot P_{CO2}/P^o)^2} \tag{11}$$

The DMC yield in a gas phase reaction can be also defined as P_{DMC}/P_{CO2}, with $P_{DMC} \ll P_{CO2}$ under normal conditions due to the very low equilibrium constants. It is straightforward to derive Equation 12 from Equation 11 and to define the DMC yield as $P_{H2O} = P_{DMC}$:

$$\text{Yield}_{\text{DMC}}(\text{mol}\%) = X \cdot \left(\frac{K_p ' P_{CO2}}{P^o}\right)^{1/2} \qquad (12)$$

Equation 9 gives a good prediction of what Figure 4 shows for liquid phase reaction. In fact, the formed DMC amount always increases with increasing CO_2 pressure or CO_2 concentration in liquid, which again indicates that there is no intrinsic difference whether the reaction is conducted in gas phase or liquid phase.

To summarize, there are at least three types of equilibria established in the present reaction system: (a) equilibrium of CO_2 dissolution in methanol; (b) reaction equilibrium of DMC direct synthesis; (c) equilibrium of H_2O adsorption onto or inside the pores of zeolite 3A, if used. It has been shown that the strategy of increasing the reaction temperature and system pressure seems not to be an economically feasible way to improve DMC yield. With the liquid phase concentration (or partial pressure for a gas phase reaction) of CO_2 and methanol maintained, the only appropriate approach to enhance DMC yield would be to remove water from the reaction mixture and to do this by decoupling the reaction zone and the water adsorption (Table 2 and Figure 3).

2.5. Conclusions

From thermodynamic calculation and experimental results, it has been clearly demonstrated that DMC formation via reaction of CO_2 and methanol is highly equilibrium-limited and at very low tendency. Thermodynamics tell us that higher reaction temperatures lead to more positive values of Gibbs free energy changes and accordingly lower equilibrium constants of this reaction. It is therefore recommended that this reaction be done in a reasonably low temperature, though still not sufficient to gain much improvement in the DMC yield. Alternatively, an economic and facile strategy is established to be removing water to shift the chemical equilibrium to favor the formation of desired DMC. Zeolite 3A serves the purpose as such dehydrating agent and has been proved to gain a large increase in water adsorption efficiency,

without appreciable co-adsorption of methanol, at temperatures around or even below the freezing point of water. With this approach and under optimized reaction conditions, the DMC yield can be enhanced to above 17 %, a value that requires extremely high pressure to be achieved if no water removal is performed, and its concentration in liquid mixture can be improved for successive operations.

Notes and References

[1] D. Delledonne, F. Rivetti, U. Romano, Appl. Catal., A 221 (2001) 241-251.

[2] Y. Ono, Catal. Today 35 (1997) 15–25.

[3] Y. Ono, T. Baba, Catal. Today 38 (1997) 321–337

[4] P. Jessop, T. Ikariya, R. Noyori, Chem. Rev. 99 (1999) 475–494.

[5] S. Neil Isaaca, B. O. Sullivan, C. Verhaelen, Tetrahedron 55 (1999) 11949–11956.

[6] M. A. Pacheco, C. L. Marshall, Energy Fuels 11(1997) 2-29.

[7] H.-J. Buysch, H. Krimm, S. Bohm, (1982), US Patent 4335051.

[8] Y. Ono, Appl. Catal., A 155 (1997) 133–166.

[9] S. Uchiumi, K. Ataka, T. Matsuzaki, J. Organomet. Chem. 576 (1999) 279–289.

[10] I. J. Drake, K. L. Fujdala, A. T. Bell, T. D. Tilley, J. Catal. 230 (2005) 14–27.

[11] D. Delledonne, F. Rivetti, U. Romano, J. Org. Chem. 448 (1995) C15-C19

[12] Y. Sato, M. Kagotani, T.Yamamoto, Y. Souma, Appl. Catal., A 185 (1999) 219-226.

[13] K. Tomishige, T. Sakaihori, S. Sakai, K. Fujimot, Appl. Catal., A 181 (1999) 95-102.

[14] H. Cui, T. Wang, F. Wang, J. Supercrit. Fluids. 30 (2004) 63-69.

[15] A. Dibenedetto, M. Aresta, F. Nocito, C. Pastore, A. M. Venezia, E. Chirykalova, V. I. Kononenko, V.G. Shevchenko, I. A. Chupovaet, Catal. Today 115 (2006) 117-123.

[16] B. Yang, D. Wang, H. lin, J. Sun, X. Wang, Catal. Comm. 7 (2006) 472-477.

[17] M. Wang, N. Zhao, W. Wei, Y. Sun, Ind. Eng. Chem. Res. 44 (2005) 7596-7599.

[18] K. Tomishige, T. Sakaihori, Y. Ikeda, K. Fujimoto, Catal. Lett. 58(1999) 225-229.

[19] K. Tomishige, Y. Ikeda, T. Sakaihori, K. Fujimoto, J. Catal. 192 (2000) 355-362.

[20] J. Choi, T. Sakakura, T. Sako, J. Am. Chem. Soc. 121 (1999) 3793-3794.

[21] K. Tomishige, Y. Furusawa, Y. Ikeda, M. Asadullah, K. Fujimoto, Catal. Lett. 76 (2001) 71-74.

[22] C. J. Jiang, Y. Guo, C. G. Wang, C. Hu, Y. Wu, E. Wang, Appl. Catal., A 256 (2003)

203-212.

[23] X.-L. Wu, M. Xiao, Y.-Z. Meng, Y.-X. Lu, J. Mol. Catal. A 238 (2005) 158-162.

[24] X.L. Wu, Y.Z. Meng, M. Xiao, Y.X. Lu, J. Mol. Catal. A 249 (2006) 93-97.

[25] Y. Zhang, Ian J. Dranke, D. N. Briggs, A. T. Bell, J. Catal. 244 (2006) 219-229.

[26] K. Tomishige, K. Kunimori, Appl. Catal., A 237 (2002) 103-109.

[27] M. Aresta, A. Dibenedetto, E. Fracchiolla, P. Giannoccaro, C. Pastore, I. Pápai, G. Schbert, J. Org. Chem. 70 (2005) 6177-6186.

[28] Z. Hou, B. Han, Z. Liu, T. Jiang, G. Yang, Green Chem. 4 (2002) 467-471.

[29] J. Choi, L. He, H. Yasuda, T. Sakakura, Green Chem. 4 (2002) 230-234.

[30] T. Zhao, Y. Han, and Y. Sun, Nat Gas Chem. Ind. (Chin.) 23 (1998) 52-55.

[31] Y. Ikeda, Y. Furusawa, K. Tomishige, K. Fujimoto, ACS Symp. Ser. 809 (2002) 71

[32] G.K. Chuah, S. Jaenicke, B.K. Pong, J. Catal. 175 (1998) 80-92.

[33] W. Li, H. Huang, H. Li, W. Zhang, H. Liu, Langmuir 24 (2009) 8358-8366.

[34] Since the catalyst, ZrO_2, stays with the liquid mixture and only a small percentage of methanol is vaporized, there would be a negligible extent of gas phase catalytic reaction in our reactor. Accordingly, a set of thermodynamic parameters for compounds in the liquid state should have been used for estimation of theoretical equilibrium constants. However, the first calculation was conducted for the same reaction in gas phase due to the lack of parameters for some compounds in liquid phase. It will be shown in later sections that the two equilibrium constants match well and this is ascribed to similar vaporization enthalpies between the reactants and products.

[35] Physical chemistry, 15TH P.W. Atkins Oxford University Press. 1994.

[36] M.A. Pacheco, C.L. Marshall, Energy Fuels. 11 (1997) 2-29.

Chapter 3

Adsorption and diffusion of water and methanol in LTA and FAU zeolites and their uses as drying agents for dimethyl carbonate synthesis

Abstract

Isothermal adsorption and diffusion kinetics of water and methanol in LTA and FAU (13X) zeolites at different temperatures were studied in this paper. Adsorption and diffusion experiments were carried out by direct measurements of mass transport (DMMT) approach in liquid mixtures where the solvents were chosen to be oversized compared to the pore openings of LTA zeolites so that co-adsorption of solvents can be prohibited. Whenever it is so, the adsorption of water and methanol both followed the Langmuir isotherm patterns. Relevant diffusion coefficients were calculated, which disclosed not only a higher diffusivity of water than methanol but also a lower activation barrier of water diffusion in selected zeolites. Diffusion kinetics studies were

conducted with single-component (water or methanol in isobutanol) and two-components (water and methanol co-dissolved in isobutanol) systems, which both confirmed that 3A zeolite, among all zeolites tested in this study, has the highest activation energy for methanol diffusion and the largest difference between water and methanol diffusivities at 248 K. All zeolites play a role of shifting reaction equilibrium in dimethyl carbonate (DMC) synthesis by removing the coproduced water, while effective exclusion of methanol proves essential for the most prominent enhancement of DMC yield brought by 3A zeolite at 248K.

Key words: Adsorption; Diffusion; Water; Methanol; LTA zeolite; Dimethyl carbonate.

.

3.1. Introduction

Zeolites are porous materials consisting of aluminum and silicon tetrahedra connected via oxygen atom bridges with the negative charge on tetra-coordinated Al atoms compensated by different cations. They have excellent adsorption and molecular sieving properties, making them good candidates for catalysis, adsorption, selective membrane separation and ion-exchange agents [1, 2]. The size of the channels and cages in different zeolites covers a wide range, and accordingly, the type of molecules that can penetrate and get absorbed varies widely for different types of zeolites. Among them, small-pore zeolites have gained especially increasing interest in application fields such as selective gas adsorption/separation and membrane technology because of their high selectivity of adsorption and transportation for small size molecules.

Linde Type A (LTA, zeolite A) is a typical small-pore zeolite which has been widely used and studied since it was synthesized and reported [3, 4]. Currently, it has the biggest production scale among all small-pore zeolites, which is not only used as the additives for detergent, but also for adsorption and membranes [5-8]. In addition, all LTA zeolites can be used as dehydration agents for separation processes [11-13] and water scavengers for shifting chemical equilibriums [14-17]. Normally, zeolite A is synthesized in the Na-form, which has a chemical formula of $Na_{12}Al_{12}Si_{12}O_{48}$. Its structure is better described as space group Fm3c (a =24.6 Å) with eight formula units of the composition given above. Common designations are also 4A for the Na-LTA zeolite which has a pore opening of 4.1 Ångstroms. When Na cations are partly exchanged by Ca^{2+}, the pore opening size increase to 5 Ångstroms after which the 5A zeolite is named, which can accommodate molecules smaller than 5 Ångstroms. And 3A zeolite is named for the K-form of zeolite, when Na cations are partly exchanged by K^+ [9, 10].

All LTA zeolites share the same topological structure and the only difference lies in their compensating cations. However, they showed big differences when used as adsorption agents, especially for water in low alcohols. Many scientists realized this fact and did a lot of work to evaluate the effect of different cations on the adsorption performances of LTA zeolites [18-20], but no convincing and universal explanation was

given. J. Weitkamp et al. interpreted in a quite straightforward way that zeolites can only absorb molecules whose kinetic diameter or minimum cross sectional diameter is smaller than the pore openings of zeolites [1]. This is in most cases reasonable and true, but a notable exception must be mentioned here that 3A zeolites do absorb large amounts of methanol at certain conditions, whose kinetic diameter is 3.6 Ångstroms, being already larger than the acknowledged pore opening dimension of 3A zeolite. A detailed elucidation of diffusivities on the K-Na partition and temperature dependence in LTA zeolite will constitute the core of a forthcoming paper to understand such phenomena.

Some experimental studies have been carried out on adsorption of water and alcohols in 4A zeolite, and most of them revealed that Langmuir isotherm model fit their data adequately [6, 21-23]. However, due to the complexity of such experiments, only limited data are available, and research effort on 3A and 5A zeolites is still lacking. Because of the apparent lack of relevant adsorption kinetic measurements, many scientists performed a lot of simulations for modeling the adsorption and diffusion behaviors of different molecules in LTA zeolites [24-27]. Such work provides a useful insight into diffusion/adsorption behaviour of appropriately sized molecules within zeolite systems. But the efficiency of the computational implementation has not yet allowed productive simulations of most zeolite-adsorbate systems. Also, it is not surprising that discrepancies still exist between the experimental and simulation results, or results from different simulation studies.

In the present work, adsorption and diffusion behaviours were studied by the Direct Measurements of Mass Transport (DMMT) approach. Although many scientists prefer to apply Nuclear magnetic resonance (NMR) and infrared absorption (IR) to study the sorption kinetics of zeolites [28,29], DMMT represents a useful method for sorption kinetic studies when the diffusion rates are suitable and zeolite crystallizes are in the range of 1-10 μm [30]. According to what Barrer emphasized thirty years ago, "it must also be borne in mind that it is these directly measured sorption kinetics which are technically important because they determine the rates in practical applications".

The adsorption isotherms and adsorption kinetics of water and methanol, respectively, in LTA and FAU (13X) zeolites were studied. All experiments were carried out in liquid mixtures of which the solvents were deliberately chosen so that their kinetic diameters are bigger than 5 Ångstroms, the pore opening size of 5A zeolite, to preclude the co-adsorption of the solvents in inner pores of all LTA zeolites. A large pore zeolite 13X with a pore opening size of approximately 7.3 Å was selected as a reference. Diffusion kinetics were measured under analogous conditions for selected zeolites at different temperatures, and relevant diffusion coefficients and activation energies were calculated, following the method used by Barrer [30] and using the equilibrium adsorbed amount of water and methanol in each zeolites determined by adsorption isotherm measurements. Described at the end of this chapter, LTA and FAU (13X) zeolites were used as water scavengers in the direct DMC synthesis from CO_2 and methanol [31-34]. For such an equilibrium-limited reaction disclosed by other scientists and previous work [35, 36], removal of products, in this case water, is the only effective way to the enhancement of DMC yields. The comparison of diffusion coefficients of water and methanol in LTA and FAU (13X) zeolites at different temperatures can well explain the fact that 3A zeolite is the most effective in removing the water produced from DMC direct synthesis at 248 K.

3.2. Experimental

3.2.1. *Water and methanol adsorption isotherms*

3A, 4A, 5A and 13X zeolites (Sigma-Aldrich, UOP, beads 2.0 mm) were selected for adsorption isotherm measurements. Before use, all of these zeolites (30 g) were calcined in a tube furnace in an air flow of 100 ml/min at 723 K for 4 hours to get rid of adsorbed water and then were sealed to prevent further water adsorption from atmosphere.

For water adsorption isotherm experiments, isobutanol (Sigma-Aldrich, >99.9%) was used as solvent and a series of water/isobutanol solutions with certain concentrations from 0.1 to 5.0 wt % were prepared. Firstly, 5.0 g of each water/isobutanol mixture was charged into a glass tube and put into a jacket bottle filled with 50/50 v/v mixture of ethylene glycol and water. A water batch or a refrigerator (FBC 740) was used to keep the temperature for adsorption isotherm measurements at 298 or 248 K, respectively.

When the temperature was steady, 1.0 g of pre-sealed zeolite was put in to each of the glass tubes. The adsorption process lasted 48 hours when all adsorptions reached their equilibria. Then the samples were taken and analyzed by Karl-Fisher water analyzer (SCHOTT TA10 plus). From the residual water concentrations in liquid mixtures, adsorbed water amount by zeolites can be calculated.

For methanol (Sigma-Aldrich, >99.9%) adsorption isotherm measurements, 3-methyl pentane (3MP, Sigma-Aldrich, 99%) was used as solvent and a series of methanol/3MP solution with different concentrations from 1×10^3 to 5×10^4 ppm were prepared. Firstly, 5 g of each methanol/3MP mixtures was charged into a glass tube and put into the jacket bottle for adsorption isotherm measurements at 298 K. When the temperature reached setting point and remained constant, 1.0 g of pre-sealed zeolite was put in to each of the glass tubes. The adsorption process lasted 48 hours and then the samples were taken and analyzed by a Gas Chromatograph (FISONS GC8160) equipped with a RTX-5AM column. From the residual methanol concentrations in liquid mixtures, adsorbed amount of methanol by zeolites can be calculated.

3.2.2. *Water and methanol diffusion kinetics*

Diffusion kinetics of both water and methanol were separately measured for all LTA and 13X zeolites which were pretreated at 723 K for 4 hours to eliminate adsorbed water. The zeolites size distributions were analyzed with LASER scattering particle size distribution analyzer (Coulter LS230). All zeolites were ground to fine powder and treated in an ultrasonic bath for half an hour before the particle size distribution measurement.

For water and methanol diffusion kinetics measurements, isobutanol solutions containing 5×10^4 ppm (5 wt %) of water or methanol were prepared. Firstly, 25.0 g of methanol/isobutanol or water/isobutanol mixtures was charged into a glass conical beaker and put into the jacket bottle used for adsorption isotherm measurements which was filled with the mixture of ethylene glycol and water. When the temperature reached setting points (298, 273 or 248 K) and remained constant for a while, 5.0 g of pre-sealed zeolite was put in to the glass conical beaker. Samples were taken at intervals and

analyzed by a gas chromatograph or Karl-Fisher water analyzer. Based on the remaining water or methanol concentrations in liquid mixtures, the amounts of adsorbed water or methanol by zeolites were calculated.

3.2.3. *Co-adsorption of water and methanol over zeolites*

An isobutanol solution containing 5×10^4 ppm (5 wt %) of water and 5 wt % (5 wt %) of methanol was used for studying the co-adsorption kinetics of water and methanol in 3A and 4A zeolites. Firstly, 25.0 g of prepared solution was charged into a glass conical beaker and put into a jacket bottle used before. Temperature was set at 298 or 248 K. When the steady set temperature was attained, 5.0 g of zeolite was put in to the conical beaker. Samples were taken at intervals and analyzed by a gas chromatograph and Karl-Fisher water analyzer both for methanol and water. From the residual water and methanol concentrations in liquid mixtures, adsorbed water and methanol amounts by zeolites can be calculated.

3.2.4. *Direct DMC synthesis with water removal*

ZrO_2, which was prepared by calcining hydrous zirconia in an air flow of 100 ml/min at 673 K for 4 hours in a tube furnace, was selected as catalyst for DMC synthesis from methanol and CO_2. The synthetic procedures of hydrous zirconia were reported in the preceding chapter [36] and can also be found in related literature [37, 38].

Direct DMC synthesis was carried out in an optimized setup with a 70 ml autoclave shown in Figure 1 of chapter 2. The standard reaction procedure is as follows: 39.6 g of methanol and 2.0 g of catalyst were put into the autoclave. 3A, 4A, 5A and 13X zeolites used for adsorption experiments were also chosen as water scavengers for DMC direct synthesis. 18.0 g of the zeolites, whenever used, was filled in the drying agent container (segment 9 in Figure 1, chapter 2), and the temperature of water trap was maintained by circulation of the liquid from a refrigerator through the trap jacket tube. And then the reactor was purged with N_2 at 10 bar for 4 times. After that, liquid CO_2 (10 g, 227 mmol, Westfalen AG, 99.995%) was introduced into the autoclave at a flow rate of 10 ml/min using a syringe pump (Teledyne ISCO. Model500). When the autoclave was heated to

433 K, the circulation was started and zero time point was taken. The reactor was kept at set temperature and magnetically stirred during reaction. When the reaction mixture contains methanol, produced water and DMC is pumped out from the autoclave, it passes through a sintered metal filter to get rid of powder catalyst. Before going into a HPLC pump (GILSON 302), the reaction mixture is cooled down to room temperature in a cooler. In the dehydrating agent container, whose temperature is adjusted by a cooling bath, the produced water will be selectively absorbed by molecular sieves with a weight of 18.0 g, fully packed in the container. After water adsorption, the reaction mixture is driven back into the autoclave. During the reaction, samples can be taken and analyzed by GC at progressive extents of reaction. DMC yields are calculated based on initially fed amount of CO_2 according to Equation 1 (N_{DMC}: produced DMC in mmol, N^0_{CO2}: initial CO_2 amount in mmol). Whenever necessary, H_2O concentrations can be measured by a Karl-Fisher water analyzer.

$$Yield_{DMC}(mol\%) = \frac{N_{DMC}}{N^0_{CO2}} \times 100\%$$

(1)

3.3. Results

3.3.1 *Water and methanol adsorption isotherms*

In order to know the differences of water and methanol adsorption capacities in different zeolites, especially LTA type zeolites, adsorption isotherms for water and methanol were measured. Methanol and water are quite similar in sizes (methanol: 3.6 Å; water: 2.6 Å), polarities and many chemical properties, which renders it difficult to separate these two molecules. The solvents selected for water and methanol are isobutanol and 3-methyl pentane, whose kinetic diameter are 5.3 and 5.9 Å, respectively [39]. Though they are still smaller than the pore size (ca. 7.3 Å) of 13X zeolite, both are bigger than those of LTA zeolites, thereby precluding the possibility of the solvents occupying adsorption sites in LTA zeolites.

Figure 1 shows water adsorption isotherms in LTA and 13X zeolites at 248 and 298 K with isobutanol as the solvent. From the water concentration remaining in the liquid mixture, adsorbed water amount by zeolites was calculated and plotted against

corresponding residual water concentration. Preliminary experiments suggested that 48 hours of adsorption was typically necessary and also sufficient for the establishment of equilibrium.
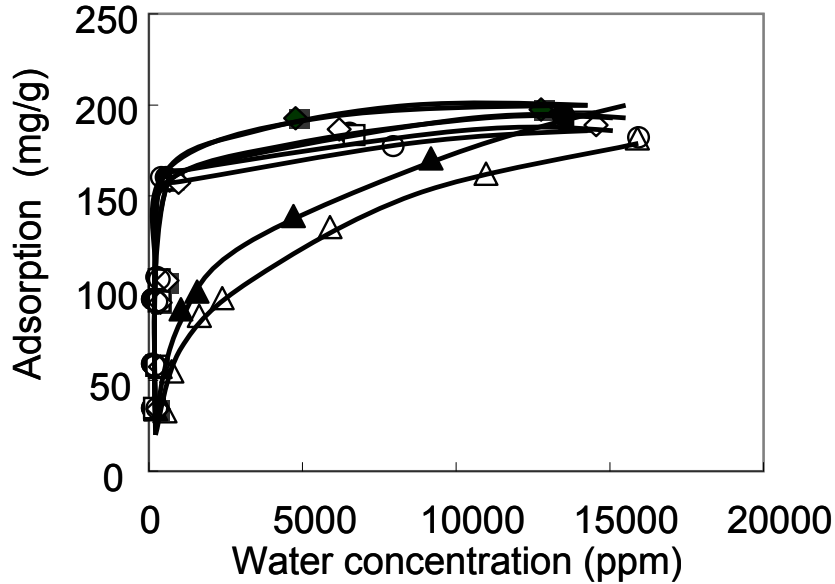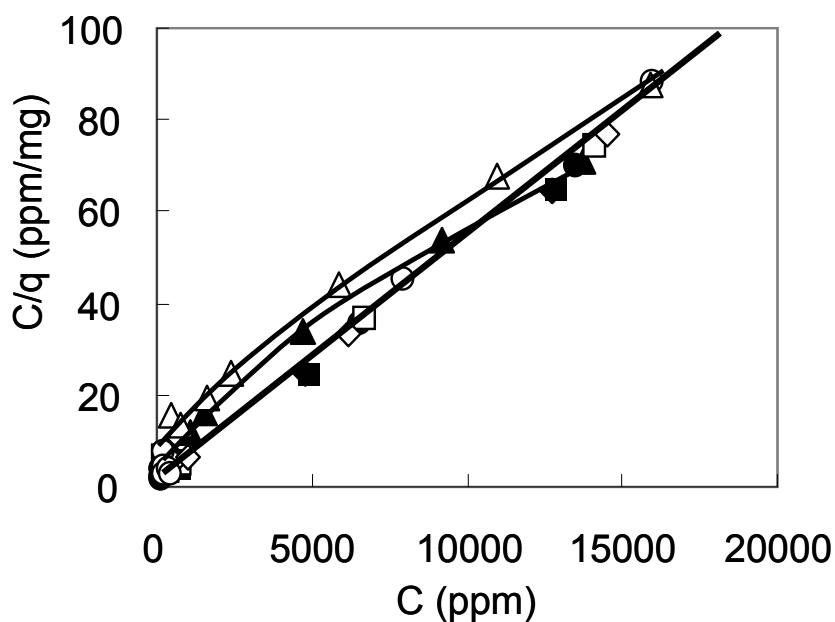

Figure 1 Water adsorption isotherm results in (▲) 13X 248K, (Δ) 13X 298K; (●) 5A 248K, (○) 5A 298K; (◆) 4A 248K, (◊) 4A 298K; (■) 3A 248K (□) 3A 248K. Adsorption conditions: T= 298 K, 248K, zeolites 1.0 g, water/ isobutanol 5.0 g, initial water concentrations in the mixture: 1000-50000 ppm. Adsorption time: 48 hours.

Equation 2 shows the Langmuir adsorption which is normally used for single component and gas phase adsorption. (θ: adsorption coverage, q: adsorption amount, q_m: maximum adsorption amount, K_L: Langmuir adsorption constant, p, partial pressure of adsorbate) When the solvents were carefully chosen so that their co-adsorption can be neglected, this model can also be used for one component in the solution for liquid adsorption isotherms (concentration term displaces pressure term). A simple transformation of equation 2 leads to equation 3 [40, 41].

$$\theta = \frac{q}{q_m} = \frac{K_L p}{1 + K_L p} \tag{2}$$

$$\frac{C}{q} = \frac{1}{q_m} C + \frac{1}{K_L q_m} \tag{3}$$

Figure 2 Langmuir adsorption simulations of water adsorption isotherms (▲) 13X 248K, (Δ) 13X 298K; (●) 5A 248K, (○) 5A 298K; (◆) 4A 248K, (◊) 4A 298K; (■) 3A 248K (□) 3A 248K. LTA zeolites: y = 0.005 X + 2.7483, q_m =200 mg/g, K_L=1.46×10^{-3}.

Figure 2 shows the simulated results of water adsorption isotherm in LTA and 13X zeolites at 248 and 298 K when C/q is plotted against C, the concentration of water remaining in liquid phase when equilibrium is reached. From the simulations it can be seen that the water adsorption of LTA group zeolite: 3A, 4A and 5A, follows the Langmuir adsorption pattern when water is dissolved in isobutanol. But 13X does not, which is due to the competitive adsorption of solvent in its inner pores.
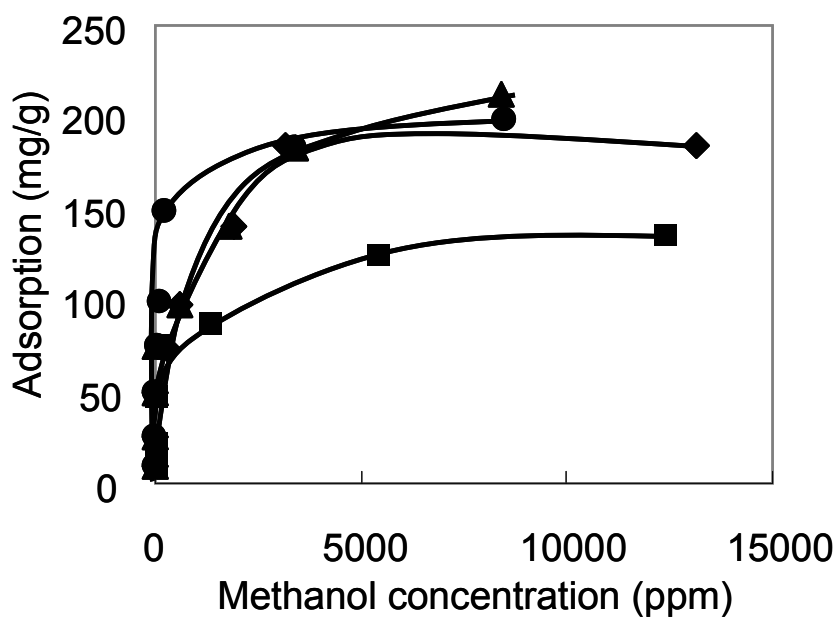
Figure 3 Methanol adsorption isotherms at 298K in (■) 3A, (◆) 4A, (●) 5A and (▲) 13X. Conditions: T= 298 K, zeolites 1.0 g, methanol/ 3-methyl pentane 5.0 g, initial methanol concentrations in the mixture: 1000-50000 ppm. Adsorption time: 48 hours
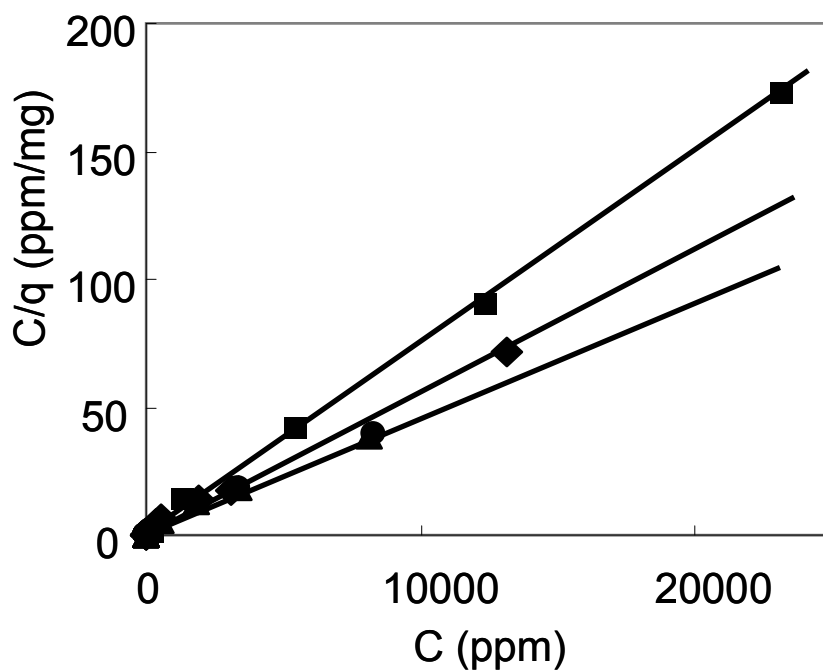

Figure 4 Langmuir adsorption simulations of methanol adsorption isotherms. (■) 3A, q_m =133 mg/g, K_L =6.1×10^{-3}; (◆) 4A, q_m =185 mg/g, K_L=4.3×10^{-3}; (●) 5A q_m =208 mg/g K_L=1.1×10^{-3} and (▲) 13X. qm =208 mg/g, K_L =3.9×10^{-3}.

Methanol adsorption isotherms and the adaptability of Langmuir adsorption model when 3-methylpentane was used as solvent are shown in Figures 3 and 4, respectively. From the results it is clearly seen, again, that all adsorption isotherms obey Langmuir formalism, even for 13X whose pores 3MP can enter, whereas the molecules kinetic diameter of 3MP (5.9 Å) is smaller than the pore opening size. Unlike the case of water-isobutanol pair, methanol is much more polar than 3MP, and is therefore likely to be much more preferentially absorbed over adsorption sites of 13X. Accordingly, the competitive adsorption of 3MP can be neglected in 13X, and the adsorption of methanol in 13X fits the Langmuir isotherm as experimentally shown. Anyhow, the selection of solvent does not influence the adsorption pattern of the solute, especially when the molecular size of the solvent is bigger than the opening pores of the adsorbate, just like isobutanol and 3MP to LTA zeolites.

It is observed that a simple Langmuir adsorption model interprets almost all adsorption data, except for water adsorptions in 13X where isobutanol co-adsorption interferes. Ideally, Langmuir adsorption requires that all adsorption sites homogeneously natured (having the same potential energy for the adsorbate) and distributed over the sorbents and all interactions between absorbed molecules can be neglected. Though the adsorptions of water and methanol over LTA zeolites are not compacted exactly in one layer, when all inner pores of zeolites can be filled with a constant amount of sorbate molecules, whose interactions can be neglected when have no obvious influence, such an adsorption can also be fitted to Langmuir isotherm adsorption. According to Equation 3, the maximum amount of adsorbed water (q_m) over 1.0 g of zeolite can be calculated from the slope of regression line, which shows essentially the same value (ca. 200 mg/g-zeolite) for all LTA group zeolites. Interestingly, such a value hardly changed when temperature varied from 248 to 298 K. This reflects the fact that all LTA zeolites have the same and constant inner volumes for water, which can be viewed as on layer adsorption over certain area. It is worth mentioning that other classical adsorption models, such as Freundlich and Temkin isotherms, are also tested for their adaptabilities, but they all fail to fit the adsorption data satisfactorily.

3.3.2. *Diffusion kinetics of water and methanol*
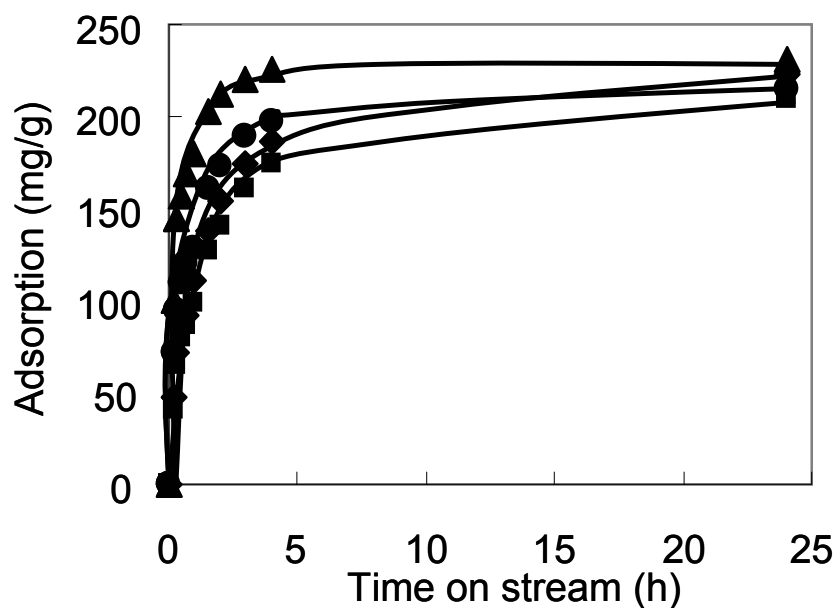
Figure 5a Water adsorption kinetic experimental results at 298 K.
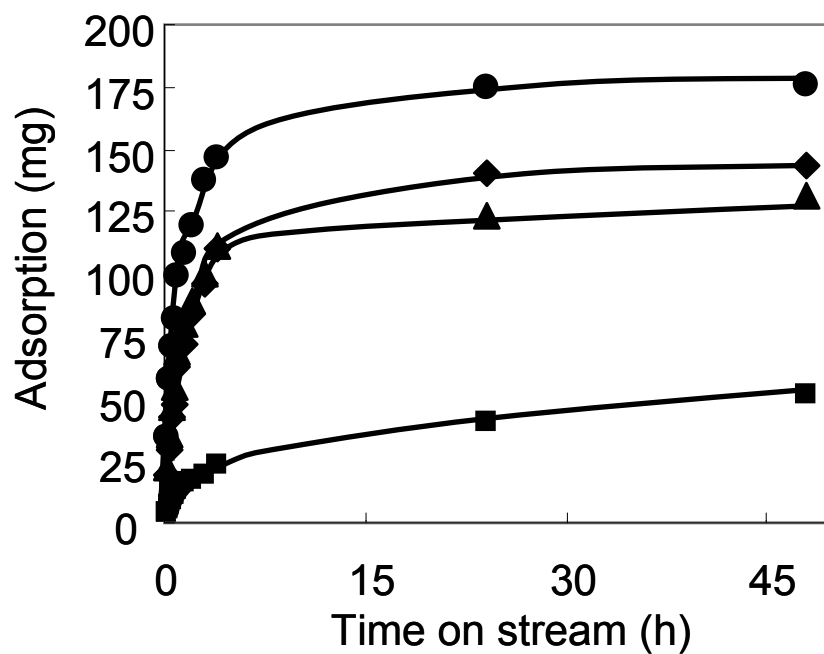
Figure 5b Methanol adsorption kinetic experimental results at 298 K

Adsorption conditions: zeolites 5.0 g, water (or methanol) / isobutanol in (■) 3A, (◆) 4A, (●) 5A and (▲) 13X.

Measurements of diffusion kinetics for water and methanol in LTA and 13X zeolites were both conducted with isobutanol as solvent at different temperatures. The results obtained at 298 K are shown in Figure 5 (a) and (b), while the whole sets of data at 248, 273 and 298 K are shown in Table 1 and 2.

Under the conditions used in the present study, the adsorptions of water or methanol in zeolites are processes governed by the diffusion from the bulk phase to their inner pores. To be more specific, the intracrystalline diffusion has the lowest diffusion coefficient among all diffusion patterns and is at least 2 or 3 orders of magnitude smaller than other diffusion coefficients such as surface diffusion, Knudsen diffusion and bulk diffusion [41]. Intracrystalline diffusion always plays the key step for and offers the main resistance in total diffusion, as the adsorption of water or methanol in LTA zeolites whose adsorption vacancies mostly locate inside the crystals. The solvent for water and methanol we used is isobutanol, which is bigger than the pore opening of LTA zeolites and can not go into the inner pores [1]. Then the diffusion kinetics can be simplified to a single diffusant or tracer diffusion with a constant diffusion coefficient D (D_T), and the method (Equation 4) used by Barrer [30] can be revised into a pattern of equation 5 for cubic LTA zeolites, regarding q_0 as zero when adsorption starts. At the beginning of adsorption when uptake or coverage is not so high and water or methanol concentration changes not so much and imposes little impact on diffusion coefficients, diffusion coefficients can be calculated from the slope of trend line when plotting $-\ln$ (1-E) versus time t. And then the diffusion coefficient can be calculated according to Equation 3 based on the averaged particle size of used zeolite.

$$\ln\left(\frac{q_m - q_t}{q_m - q_0}\right) = \ln\frac{512}{\pi^6} - \frac{D\pi^2 t}{4}\left(\frac{1}{a^2} + \frac{1}{b^2} + \frac{1}{c^2}\right) \tag{4}$$

$$-\ln(1 - E) = kt + s \tag{5}$$

$$k = \frac{D\pi^2}{4}\left(\frac{3}{a^2}\right) \quad \text{(When a=b=c)} \tag{6}$$

(Where the symbols bear the meanings as follows. q_m: the maximum adsorption amount; q_t: adsorption amount at time t; q_0: adsorption amount at time 0; D: diffusion coefficient; t: adsorption time; a, b, c: edges of rectangular parallelepipeds, with 2a, 2b and 2c in length; $E=q_t/q_m$; k: slope; s: intercept)

Table 1 Diffusion kinetics measurements of water in zeolites

| Time | Adsorption amounts-zeolites-temperature (mg H_2O/g zeolite) | | | | | | | | | | | |
| | 3A | | | 4A | | | 5A | | | 13X | | |
(hour)	248 K	273 K	298 K	248 K	273 K	298 K	248 K	273 K	298 K	248 K	273 K	298 K
0.17	0.36	-	40.16	0.82	-	46.66	2.79	-	71.15	9.68		100.59
0.33	0.63	9.14	65.37	1.87	2.23	72.25	5.27	21.75	95.16	12.76	52.06	144.67
0.50	5.02	-	80.28	2.32	-	86.91	4.93	-	109.54	15.95	-	156.25
0.67	7.26	22.68	86.56	1.81	30.54	91.42	17.01	41.30	119.83	16.65	72.06	168.26
1.00	10.50	39.43	99.19	4.23	45.33	110.42	17.59	62.20	128.20	23.67	95.02	180.40
1.50	15.01	54.46	127.57	11.06	59.61	137.26	20.53	79.77	161.00	34.20	103.52	202.30
2.00	23.39	62.29	140.48	28.89	68.25	153.53	32.11	90.46	172.36	43.96	118.85	212.05
3.00	43.69	85.68	160.40	44.09	97.34	174.27	59.14	108.06	189.75	67.09	145.30	220.34
4.00	49.46	106.37	173.98	51.54	107.41	185.82	66.66	125.70	197.28	78.26	166.60	225.97
24.00	136.56	194.14	209.35	140.70	200.48	222.34	151.41	206.24	214.76	162.77	224.76	230.83

Table 2 Diffusion kinetics measurements of methanol in zeolites

| Time | Adsorption amounts-zeolites-temperature (mg CH_3OH/g zeolite) | | | | | | | | | | | |
| | 3A | | | 4A | | | 5A | | | 13X | | |
(hour)	248K	273K	298K	248K	273K	298K	248K	273K	298K	248K	273K	298K
0.17	0.01	-	3.59	0.45	-	19.69	2.17	-	34.45	5.84	-	22.48
0.33	0.11	0.44	7.46	1.67	1.62	29.50	3.76	2.17	57.32	6.91	13.84	35.64
0.50	0.58	-	9.00	1.31	-	42.05	4.11	-	70.56	8.15	-	46.00
0.67	1.06	1.05	11.54	1.49	3.69	47.24	2.95	14.65	81.97	9.08	18.16	54.13
1.00	2.07	2.24	12.89	2.22	4.12	63.05	3.31	20.02	99.42	11.96	24.75	68.55
1.50	2.25	2.04	16.44	2.87	3.73	71.55	2.91	26.48	108.17	17.71	31.63	79.42
2.00	1.32	2.52	16.90	3.70	8.78	84.28	4.97	31.71	119.22	19.27	33.09	89.10
3.00	1.62	3.12	19.41	6.61	12.81	96.41	6.87	40.62	137.29	22.86	37.29	100.37
4.00	1.44	3.79	22.88	7.47	16.70	110.37	8.35	53.21	146.59	25.33	42.55	111.47
24.00	2.68	11.56	40.51	19.13	58.45	139.97	27.81	96.37	174.61	49.40	125.20	123.12
48.00	4.90	-	51.95	33.77	-	143.43	49.23	-	176.08	65.67	-	130.96
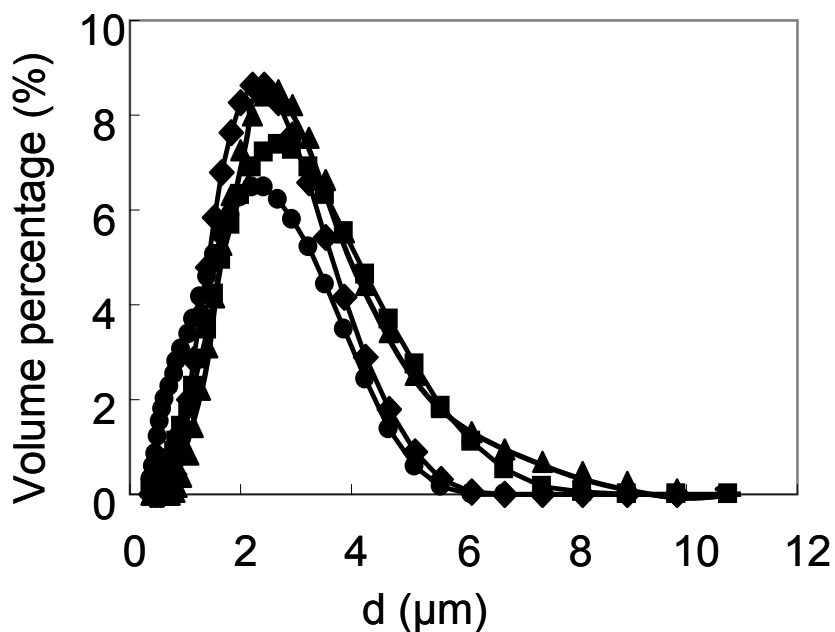
Fig. 6 Particle size distribution of zeolites (d=2a). Averaged particle size (d),
(■) 3A: 2.47 µm; (◆) 4A: 2.30 µm; (●) 5A: 1.82 µm; (▲) 13X: 2.76 µm.
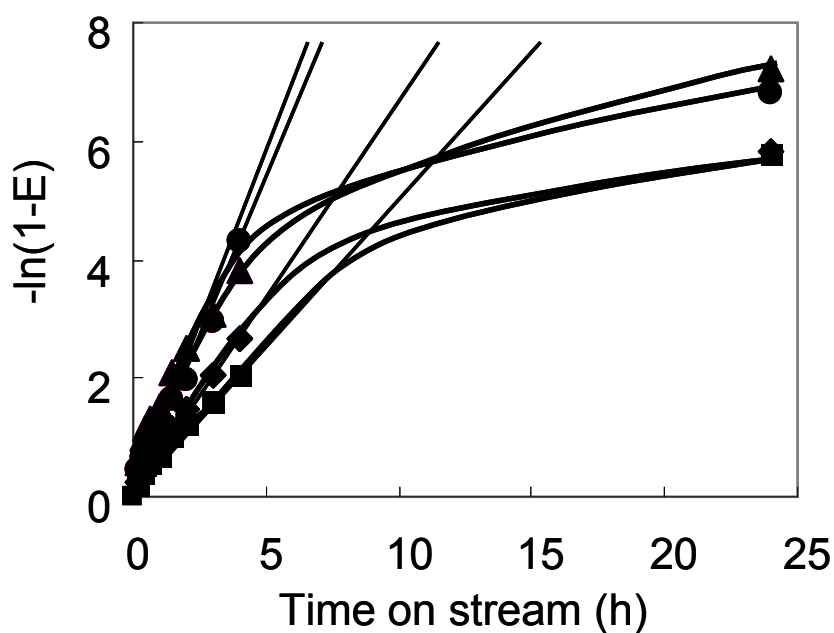
Figure 7 Simulations of water adsorption kinetic experimental results at 298K (■)
3A: y = 0.5096x + 0.1735; (◆) 4A: y = 0.6103x + 0.2198; (●) 5A: y = 0.8697x + 0.3037;
(▲) 13X: y = 0.8086x + 0.7054.

The particle size distribution was determined by LASER scattering particle size distribution analyzer, the results of which are shown in available in Figure 6. From the

averaged particle sizes we can get the edges' values need for calculations of diffusion coefficients.
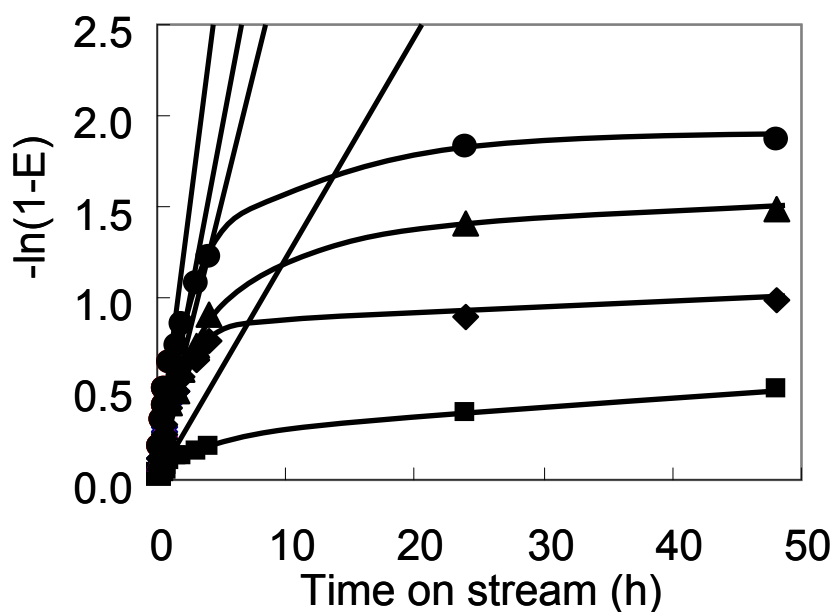
Figure 8 simulations of methanol adsorption kinetic experimental results at 298K. (■) 3A: y = 0.1215x + 0.0108; (◆) 4A: y = 0.2864x + 0.0919; (●) 5A: y = 0.374x + 0.0576; (▲) 13X: y = 0.5485x + 0.1212.

Table 3 Water adsorption kinetic results in zeolites

Zeolites	Ea (kJ mol^{-1})	Water diffusion coefficients (10^{-14} cm^{2}s^{-1})		
		248 K	273 K	298 K
3A	29.18	2.37	9.35	25.3
4A	30.61	2.95	13.2	35.3
5A	25.59	3.46	9.21	27.1
13X	23.00	8.95	26.3	57.9

Table 4 Methanol adsorption kinetic results in zeolites

| Zeolites	Ea (kJ mol^{-1})	Methanol diffusion coefficients (10^{-14} cm^{2}s^{-1})		
		248 K	273 K	298 K
3A	91.57	0.03*	0.12	6.98
4A	62.61	0.25*	0.89	14.3
5A	53.54	0.22	2.19	17.1
13X	29.11	2.44	5.62	26.8

* Values are not included for the activation energy calculations [42]

Two examples of simulation which used Equation 5 for adsorption kinetics of water and methanol at 298 K are shown in Figure 7 and Figure 8. Detailed results are listed in Table 3 and 4.

Intracrystalline diffusion within porous crystals normally obeys the Arrhenius Equation 7. Diffusion coefficients of a certain zeolite at different temperatures were obtained from simulations of diffusion data according to Equation 5 and 6. If lnD is plotted against 1/RT values at different temperatures (equation 8), the activation energy for diffusion processes can be calculated from the slope of the trend line, which are also listed in Table 3 and 4. Figure 9 (a, b) give examples how the values were plotted for water diffusions in different zeolites. (D: diffusion coefficient, R: ideal gas constant, D_0: pre-exponential constant, T: temperature in Kelvins, Ea: activation energy for diffusion in kJ mol^{-1})

$$D = D_0 \exp\left(-\frac{Ea}{RT}\right) \qquad (7)$$

$$\ln D = -\frac{Ea}{RT} + \ln D_0 \qquad (8)$$
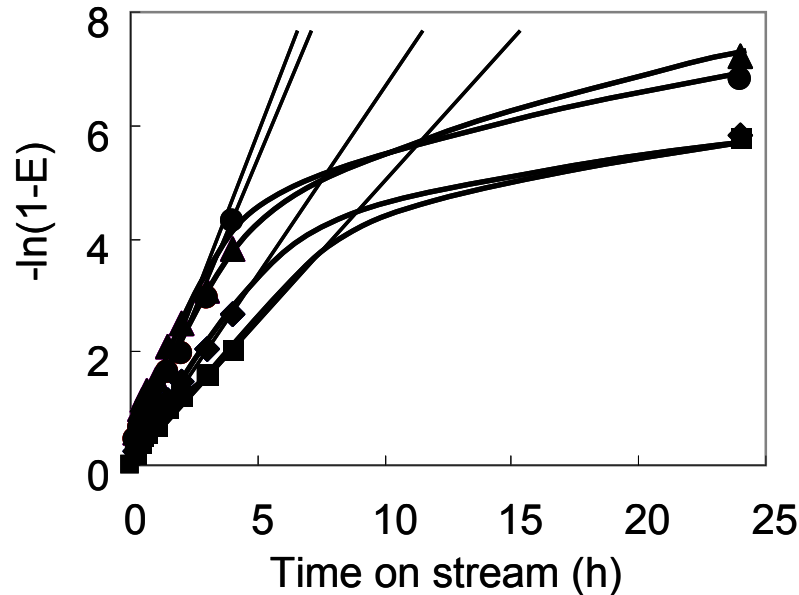
Figure 9a Simulations of water adsorption kinetic experimental results at 298K, (■) 3A: y = 0.5096x + 0.1735; (◆) 4A: y = 0.6103x + 0.2198; (●) 5A: y = 0.8697x + 0.3037; (▲) 13X: y = 0.8086x + 0.7054.
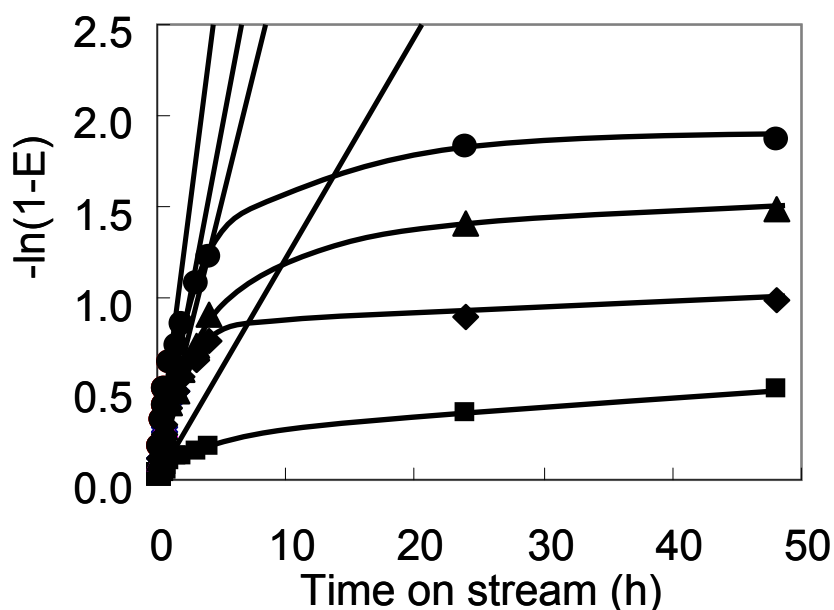
Figure 9 b simulations of methanol adsorption kinetic experimental results at 298K, (■) 3A: y = 0.1215x + 0.0108; (◆) 4A: y = 0.2864x + 0.0919; (●) 5A: y = 0.374x + 0.0576; (▲) 13X: y = 0.5485x + 0.1212.

From the results listed in Table 3 and 4, we can see that diffusion coefficients of water and methanol both decrease with increasing temperature, the trend is more dramatic in the case of methanol. Methanol has a diffusion coefficient of 6.98×10^{-14} cm^2s^{-1} at 298 K, more than two orders of magnitude at 248 K of 0.03×10^{-14} cm^2s^{-1}; for water, such value drops only from 25.3×10^{-14} to 2.37×10^{-14}, a factor about 10. This gives the indication that temperatures influence the diffusion of methanol more significantly.

Methanol diffusion has an activation energy of ca. 91 kJ mol^{-1} in 3A zeolite while water diffusion has a number of only 29 kJ mol^{-1}. There is a fact lies behind: the diffuse rate ratio of water to methanol at 298K in 3A is 3.6, and increase to about 80 at 248K; but for 4A zeolite, the ratio increase from 2.5 to 12 only. And there are only relatively small differences between the diffusion coefficients of water and methanol are observed in other investigated zeolites with larger pore openings. One may predict from the foregoing analysis that 3A is more effective at 248 K than other zeolites when used as dehydrating agent for the mixture of water and methanol, in view of the differences of diffusion coefficients. However, direct tests are needed to verify this.
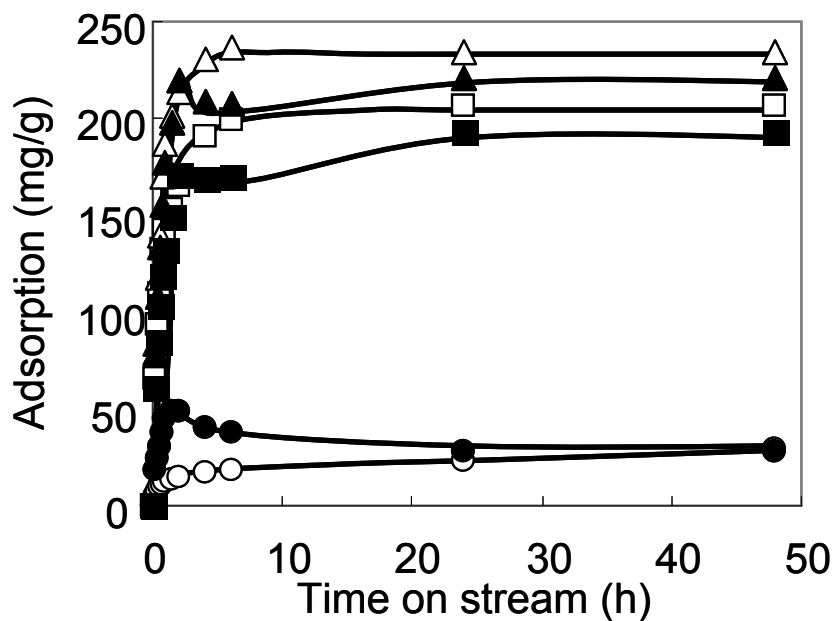
(a)
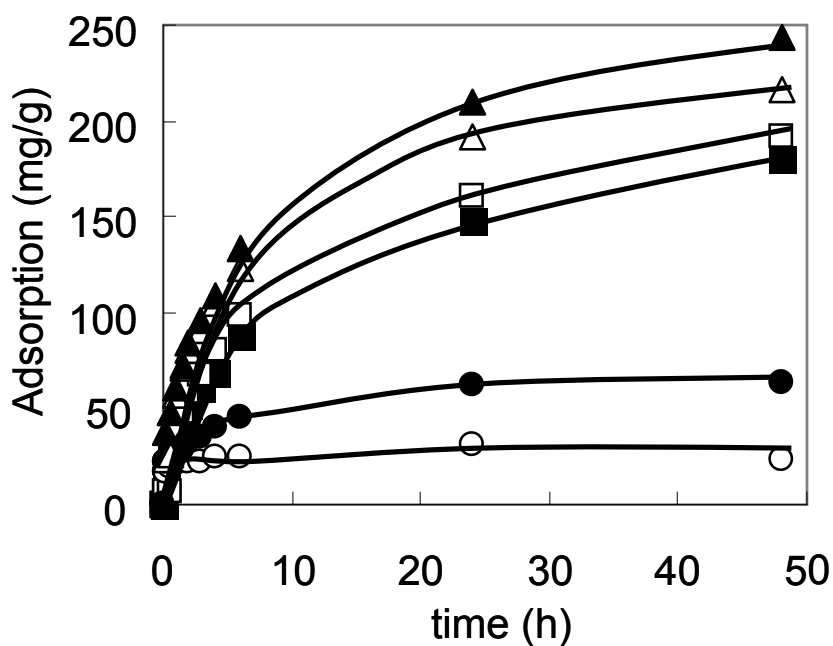
(b)

Figure 10 Co-adsorption of water and methanol at 298K (a) and 248 K (b), in 3A and 4A zeolites. (▲) 4A total; (Δ) 3A total; (■) 4A water; (□) 3A water; (●) 4A methanol; (○) 3A methanol. Adsorption conditions: zeolites 5.0 g, water + methanol/isobutanol 25.0 g, initial concentration: water 5×10^4 ppm, methanol 5×10^4 ppm in the mixture.

3.3.3. *Co-adsorption of water and methanol over zeolites*

The results of water and methanol co-adsorption in 3A and 4A zeolites at 298 and 248 K when isobutanol was used as solvent are shown in Figure 10 (a and b). It can be seen that the adsorption of water are much stronger than that of methanol when the same primary concentrations of water and methanol in isobutanol were used.

If the influence of concentration to diffusion coefficients was ignored, the estimations of diffusivities can be made to the Co-adsorption of water and methanol in 3A and 4A zeolites. It was known from the section 3.2 that water has a diffusion coefficient of 25.3×10^{-14} cm^2s^{-1} and methanol has a number of 6.98×10^{-14} cm^2s^{-1} in 3A zeolite at 298 K. these numbers are 35.3×10^{-14} and 14.3×10^{-14} cm^2s^{-1} respectively in 4A zeolite. This clearly indicates that both water and methanol diffuse at the same magnitude level in these two zeolites at 298 K. Adsorbed water and methanol in 4A zeolite at 298 K both increased very fast in quantity at the beginning because there were enough vacancies in zeolites when the diffusion kinetics plays a key role. But adsorbed amount of methanol started to decrease from the second hour on and that of water continued to increase. The only explanation would be that the adsorption of water is stronger than methanol, and therefore water molecules begin to snatch the adsorption sites once occupied by methanol when adsorption equilibrium is starting its determine role. Then this gives a clue that both the adsorption equilibria and diffusion kinetics influenced the uptakes of water and methanol in 4A zeolite across the time. An analogous phenomenon was noticed by other researchers when they studied the simultaneous uptake of n-heptane and benzene in X zeolite [43].

Such an uptake replacement of methanol by water was not found in 3A zeolite because the diffusion rate of methanol in it is not as fast as in 4A zeolite, comparing the difference of water's diffusions. That is also why we did not find such replacements in the experiment results at 248 K shown in Figure 10 b, even for 4A zeolite. We had known that both of water and methanol's diffusion rates in zeolite decrease a lot when temperature decrease, and methanol's decreasing is more significant comparing with water's. And then the adsorption equilibria need not change the uptake values of water

and methanol determined by diffusion kinetics influenced in those two kinds of zeolites at 248 K.

3.3.4. *Direct DMC synthesis with water removal*

In chapter 2, It was disclosed that DMC direct synthesis from methanol and CO_2 is a thermodynamically infeasible reaction, and the DMC yield is limited by the reaction equilibrium and can not be higher than 2 % (CO_2 based) at 433 K when no dehydrating agent was used to remove produced water. DMC yield-time profiles over ZrO_2 at 433 K with 3A zeolite as dehydrating agent at different temperatures are shown in Figure 11. Lowering the working temperature of dehydrating agent favored the production of dimethyl carbonate because of enhanced efficiency of 3A zeolite for water removal. When 3A zeolite was used at 248 K, DMC yield can be enhanced to 5.7% after 24 hours of reaction. Figure 12 shows the DMC yield-time profiles over ZrO_2 at 433 K when different zeolites were used as drying agent at 248 K. All zeolites help to enhance DMC yields compared to the case without using drying agent. 3A zeolite works by far the best among all zeolites applied in this study.
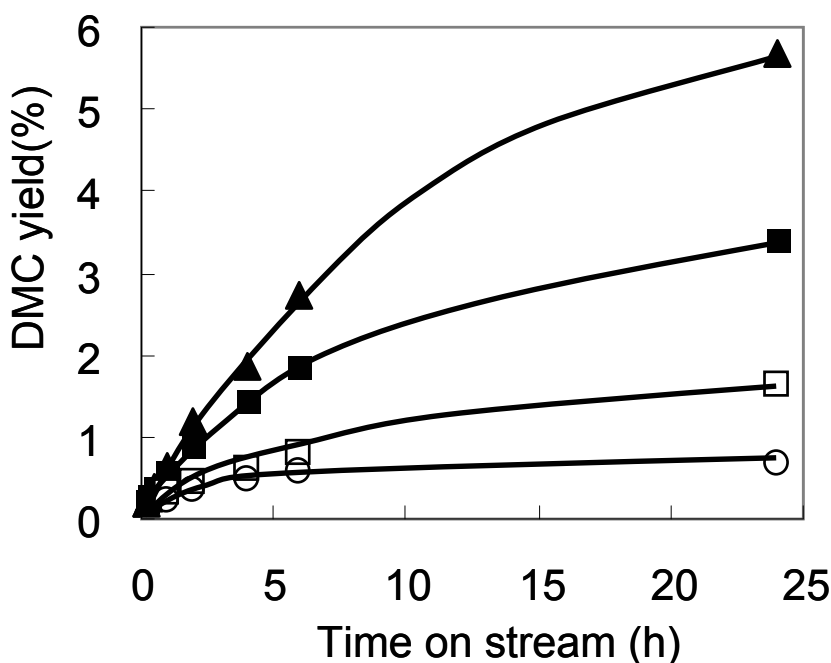
Figure 11 DMC yields when 3A zeolite was used as water removal agent at (□) 298K, (■) 273K, (▲) 248K and (○) no dehydrating agent. Reactor conditions: T = 433 K, total pressure =42 bar, ZrO_2 2.0 g, liquid CO_2 10 g, methanol 39.6 g, zeolite 18.0 g, liquid mixture circulation rate 2.0 ml/min.
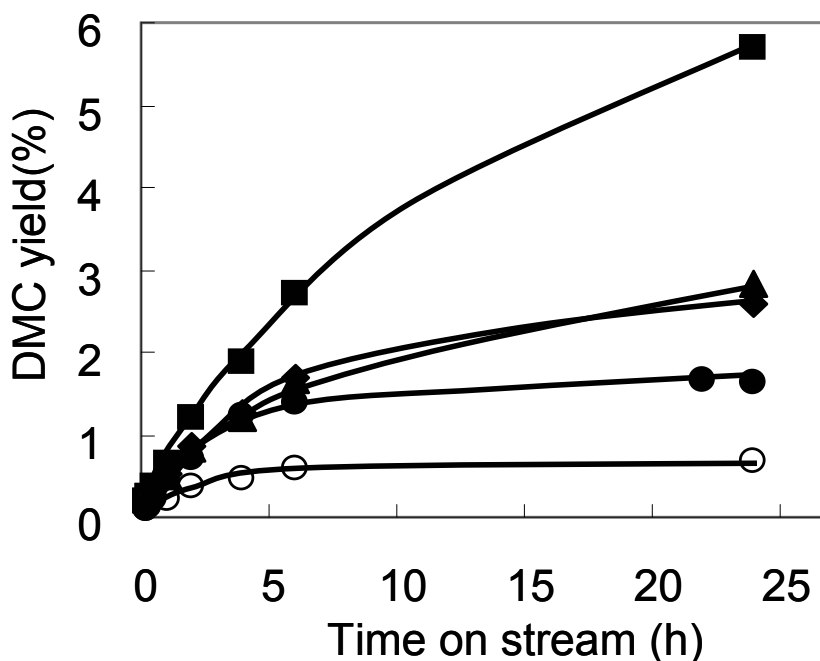
Figure 12 Enhanced DMC yields when using (■) 3A, (◆) 4A, (●) 5A , (▲)13X and (○) no   as dehydrating agent at 248 K. Reaction conditions: T = 433 K, ZrO_2 2.0 g, CO_2 10 g, methanol 39.6 g, zeolites 18.0 g, total pressure =42 bar, liquid mixture circulation rate 2.0 ml/min.

3.4. Discussion

It has been disclosed by the isotherm experiments, diffusion kinetics and co-adsorptions of water and methanol over tested zeolites that the dehydration properties of several zeolites differ much. However, cautions must be exercised when connection is to be built between the those experimental results and the fact that only 3A zeolite can effectively remove the produced water at 248 K from the reaction mixture of DMC direct synthesis from methanol and CO_2. From the results shown in Tables 3 and 4, it can be seen that the activation energies of water diffusion in tested zeolite vary from 20 to 30 kJ mol^{-1}, and is less sensitive to methanol. The reason comes from that the kinetic diameter of water molecule is much smaller than that of methanol, which is intensively hindered by zeolites' pore openings.

3A zeolite absorbed less amount of methanol compared with other tested zeolites from the isotherm experimental results showed in Figure 2 and 3. But it is obviously not enough to explain why 3A zeolite works better as a dehydrating agent for DMC

synthesis, because other zeolites can also absorb the same amount of water. The reason why 3A adsorbed less amount of methanol than other zeolites can be due either to the time was not enough or the methanol molecules can not go into the sodalite cages of it.

One should bear in mind that there is very small amount of water which varies from several hundreds to several thousands ppm and mostly is methanol in the reaction mixture of DMC direct synthesis, even when the reactions reached their equilibria. The request is much more critical removing the produced water from such a mixture with so low a water concentration. It was known that equilibrium favor water's adsorption than methanol's adsorption. However, things needed to be taken care of the kinetics of the adsorptions. The ratio of diffusion coefficients water to methanol at 248 K in 3A zeolite is 80, much bigger than at higher temperatures or in other zeolites. 4A has such a diffusion coefficient ratio of only 12 at 248 K, and may also absorb water from the mixture of water and methanol (Figures 10 a, b). However, it is not enough to remove the trace concentration of water efficiently form a mixture full with methanol. From the comparing of the diffusion coefficients, diffusion activation energies and results of Co-adsorption of water and methanol, it is sufficient to explain by diffusion kinetics why there is only 3A zeolite and at lower temperatures can remove the produced water from the DMC reaction mixture more efficiently.

It needs to be pointed out here that there are also factors that may influence the accuracy of calculations from diffusion kinetics. One is the measurement of average particle sizes, which were used for diffusion coefficient calculations. One can hardly get the identically sized zeolites and the average dimension value will influence the accuracy inevitably. Furthermore, it is still doubtable whether the methanol adsorption in 3A at 248 K is due to the contribution from inner cages, and it is hardly possible to exclude the possibility that the adsorption also occurs over the outer surface of the zeolite. This will not influence the accuracy so much when the total adsorption amount is big enough, but when the total adsorption amount is very small, it will bring in large uncertainties for calculation. That is why the methanol diffusion coefficients of 3A and 4A zeolite at 248 K are not included for activation energy calculations. The reason why the diffusion rate of methanol in 3A zeolite drops so dramatically needs further studies.

3.5. Conclusions

It has been demonstrated in this paper that adsorption of either water or methanol in LTA and FAU zeolites follow Langmuir isotherms as long as competitive adsorption does not exist. The diffusions of methanol are more severely influenced by temperature than those of water in LTA zeolites, indicating higher activation barriers for methanol intracrystalline diffusion in LTA zeolites. Such barriers mount up in a descending order of pore openings for methanol diffusion, i.e. 13X, 5A, 4A and then 3A zeolite. They vary only to a limited extent for water diffusions. The highest ratio of diffusion coefficients of water to methanol appears on 3A zeolites at 248 K. It is correlated with the fact that 3A zeolite, when working at 248 K, is the most effective in removing the produced water from the reaction mixture in DMC direct synthesis from methanol and CO_2.

Acknowledgments

Notes and References

[1] D. W. Breck, Zeolite molecular sieves, Structure Chemistry and Use. New York, John Wiley, 1974.

[2] J. Weitkamp, L. Puppe, Catalysis and Zeolites fundamentals and applications, Springer, 1999.

[3] D. W. Breck, W. G. Eversole, R. M. Milton. J. Am. Chem. Soc. **1956**, 78, 5963–5972.

[4] R. M. Milton. (1959) US Pat 4534947.

[5] V. P. Lakeev, Razrabotka Gazovykh Mestorozhdenii, Transport Gaza, **1974**, 1, Pt2, 120-136.

[6] K.-I. Okamoto, H. Kita, K. Horii, K. T. Kondo, Ind. Eng. Chem. Res. **2001**, 40, 163-175.

[7] T. C. Bowen, R. D. Noble, J. L. Falconer, J. Membr. Sci. **2004**, 245, 1–33.

[8] Y. Li, W. Yang, J. Membr. Sci. **2008**, 316, 3–17.

[9] R.X. Fischer, W.H. Baur. Microporous and other Framework Materials with Zeolite-Type Structures, Springer, 2006.

[10] R. M Barrer, Zeolites and Clay minerals as sorbents and Molecular Sieves, Frs. Chemistry Department, Imperial College, London. 1978.

[11] Salem M. Ben-Shebi, Chem. Eng. J. **1999**, 74, 197-204.

[12] Kokai Tokkyo Koho, (1982) JP 57101757

[13] X. Liu, H. Yao, Gaoxiao Huaxue Gongcheng Xuebao, **1992**, 6(2), 153-159.

[14] D. E. Chasan, L. L. Pytlewski, R. O. Hutchins, N, M, Karayannis and C. Owens, Inorg. Nucl. Chem. Lett. **1975**, 11(1), 41-45.

[15] M. Goyal, R. Nagahata, J. Sugiyama, M. Asai, M. Ueda, K. Takeuchi, Polymer, **1999**, 40, 3237–3241.

[16] Q. Wang and R. Huang, Tetra. Lett. **2000**, 41, 3153–3155.

[17] C. E. Outlaw, C. F. Fillers, B. T. Smith, K. H. Maness, D. J. Olsen, WO 2000029366.

[18] I. E. Neimark, M. A. Piontkovskaya, A. I. Lukash, R. S. Tyutyunnik, Otd. Khim. Nauk. **1962**, 49-58.

[19] R. Maachi, M. J. Boinon, J. M. Vergnaud, Journal de Chimie Physique et de Physico-Chimie Biologique **1978**, 75(1), 116-120.

[20] N. Tessa, B. Tyburce, G. Joly, Journal de Chimie Physique et de Physico-Chimie Biologique, **1991**, 88(5), 603-613.

[21] T. Shigetomi, T. Nitta, T. Katayama, J. Chem. Eng. Jpn. **1982**, 15(4), 249-254.

[22] C. Akosman, M. Kalender, Fresenius Environ. Bull. **2007**, 16(5), 500-507.

[23] K. F. Loughlin, Adsorption, **2009**, 15(4), 337-353.

[24] Gábor Rutkai, Éva Csányi, Tamás Kristóf, Microporous Mesoporous Mater. **2008**, 114, 455–464.

[25] Éva Csányi, Tamás Kristóf, and György Lendvay, J. Phys. Chem. C **2009**, 113, 12225–12235.

[26] J. Y. Wu, Q. L. Liu, Y. Xiong, A. M.Zhu, Y. Chen, J. Phys. Chem. B **2009**, 113, 4267–4274.

[27] J. Kuhn, J. M. Castillo-Sanchez, J. Gascon, S. Calero, D. Dubbeldam, T. J. H. Vlugt, F. Kapteijn, J. Gross, J. Phys. Chem. C **2009**, 113, 14290–14301.

[28] K. Cho, H. S. Cho, L. de Menorval, R. Ryoo, Chem. Mater. **2009**, 21(23), 5664-5673.

[29] C. A Koh, J. A.Zollweg, K. E. Gubbins, Stud. Surf. Sci. Catal. **1994**, 87(Characterization of Porous Solids III), 61-70.

[30] R. M. Barrer, Zeolites and Clay minerals as sorbents and Molecular Sieves, Frs. Chemistry Department, Imperial College, London, 1978, P273-275, 318.

[31] K. Tomishige, T. Sakaihori, Y. Ikeda, K. Fujimoto, Catal. Lett. **1999**, 58, 225-229

[32] J. Choi, T. Sakakura, T. Sako, J. Am. Chem. Soc. **1999**, 121, 3793-3794.

[33] J. Choi, L. He, H. Yasuda, T. Sakakura, Green Chem. **2002**, 4, 230-234.

[34] Y. Zhang, Ian J. Dranke, D. N. Briggs, A. T. Bell, J. Catal. **2006**, 244, 219-229.

[35] T. Zhao, Y. Han, and Y. Sun, Nat Gas Chem. Ind. (Chin) **1998,** 23, 52-55.

[36] Chapter 2.

[37] G.K. Chuah, S. Jaenicke, B.K. Pong, J. Catal. **1998**, 175, 80-92.

[38] W. Li, H. Huang, H. Li, W. Zhang, H. Liu, Langmuir **2009**, 24, 8358-8366.

[39] Robert C. Reid, John M. Prausnitz, Thomas K, The Properties of Gases and Liquids, Sherwood, Mcgraw-Hill book company, third edition, 1977, P24, 679.

[40] Physical chemistry, 15TH P.W.Athins Oxford University Press. 1994.

[41] Chemical process of adsorption and separation, Zhen Hua Ye, Beijing, Sinopec press, 1992.12, P 48, 81.

[42] There are two reasons why these two numbers are not included for activation energy calculation: (i) At 248K, both of 3A zeolite and 4A zeolites' methanol adsorptions are very weak. Compared to total adsorption, the adsorption over outer surface can not be neglected like 5A and 13X or adsorptions of water. The use of these two numbers may increase the inaccuracy of activation energies' calculations. (ii) The diffusion coefficient D is determined over a range of temperatures, when the diffusion mechanism does not change. Owing to the similarity of 3A zeolite and 4A zeolites' pore opening sizes and methanol kinetic diameter, from our experiment results, we think that the pore openings of these two zeolites seem to have been closed or partially closed

for methanol at 248K, at least for 3A zeolite. In another word, the diffusion mechanism has changed and the diffusion coefficient D does not suit for energy calculations.

[43] J. Kärger, M.Bulow and Schirmer, Zeit. Phys. Chem., Leipzig 1975.

Chapter 4

Extensive potassium exchanged LTA zeolites for yield enhancement of dimethyl carbonate

(Influence of potassium concentration on the dimension restricting effect of the zeolite pore openings)

Abstract

Highly potassium exchanged (up to 91%) LTA zeolite was used as the in situ dehydrating agent for dimethyl carbonate (DMC) direct synthesis from methanol and CO_2. Based on the diffusion kinetics of water and methanol, the impact of exchanged potassium concentrations on the diffusion properties and adsorption capacities of LTA zeolites were elucidated. It is proposed that the size of the free pore opening in LTA zeolite is determined by the distribution of Na^+ and K^+ cations in its three types of location sites, which is also influenced by temperatures. The long-standing misconception that the pore openings of LTA zeolites are rigid features is thereby challenged. The temperature and

exchanged potassium levels affect the local Na^+/K^+ partition in the 8-member ring window tuning its critical dimension for small molecules to permeate. Experiments were carried out by the direct measurements of mass transport (DMMT) approach in liquid mixtures, where the isobutanol was used as the solvent considering the pore openings of LTA zeolites so that co-adsorption of solvent can be excluded.

Key words: Diffusion kinetics; Water; Methanol; potassium ion exchange; LTA zeolites; Dimethyl carbonate.

4.1. Introduction

First synthesized and reported in 1950s [1, 2], Linde Type A (LTA, zeolite A) zeolites have attracted interest from a wide variety of fields such as detergent additives, selective adsorption/separation and membrane technology, etc [3, 4]. The whole LTA family has currently the largest production volume among all small-pore zeolites. An important application for LTA zeolites, and their membrane counterparts, has been established as dehydration agents for separation processes (e.g., traces of water in organic solvents) and shifting reaction equilibria [5-14].

Normally, LTA zeolite is first synthesized in the Na-form, which has a chemical formula of $Na_{12}Al_{12}Si_{12}O_{48}$ for one unit cell, or better described as space group Fm3c (a = 24.6 Å) with eight formula units of the composition given above [15]. When partly exchanging Na^+ by K^+ or Ca^{2+} to controlled extents, 3A or 5A zeolites can be respectively produced from the original full-Na-form LTA zeolite (known as 4A) [16]. Thereby, all LTA zeolites share the same topological structure and the only difference lies in their charge-compensating cations, the bulkiness of which determines the pore opening sizes. Common designations of 3A, 4A and 5A indicate the approximate opening sizes of their eight membered ring windows.

Due to their diverse pore opening dimensions, different adsorption capacities are to be expected when probe molecules are appropriately chosen [17-19]. Taking advantage of this feature, it has been successfully shown that substantial yield enhancement can be achieved by using commercial LTA zeolites to remove traces of water produced in direct dimethylcarbonate (DMC) synthesis, a highly equilibrium-limited reaction [20]. As a dehydrating agent, 3A zeolite works more efficiently than 4A zeolite in removing the produced water from the reaction mixture. Explanations were given by comparatively showing the diffusion rate differences of water and methanol in 3A zeolite at different temperatures derived from diffusion kinetics measurement [21]. However, the mechanism has not been elucidated how exchanged K^+ cations influence the diffusion properties of water and methanol in 3A zeolite.

Some has been published on evaluating the effect of cations on the adsorption

performances of LTA zeolite [12, 22-24]. However, due to the complexity of such experiments, only limited data are available, and research effort adsorption and diffusions of methanol and water on 3A and 5A zeolites is still lacking. It is often interpreted in a quite straightforward way that only molecules whose kinetic diameter or minimum cross sectional diameter is smaller than the pore openings of zeolites can enter the inner cages of zeolites and adsorb. This, in most cases, proves reasonable, but notably 3A zeolites adsorb large amounts of methanol at room temperature [21], whose kinetic diameter is 3.6 Å, being already larger than the estimated pore opening diameter of 3A zeolite.

In order to address this, a series of potassium exchanged LTA zeolites with increasing exchange levels were prepared in the present work, with emphasis placed on elucidating (i) how diffusivities of water and methanol in LTA zeolites change with temperatures and potassium exchange levels and (ii) how the K^+-Na^+ partition in the local structure of 8-ring pores is influenced by temperature and exchanged potassium level. All K^+, Na^+-containing LTA zeolites were used in direct DMC synthesis to explore their potential as water scavengers in enhancing DMC yields by the shifting chemical equilibra. Since it was previously shown that additional energy input is required for cooling 3A zeolites to lower temperatures (so that water in trace amount can be selectively removed without appreciably co-adsorbing methanol that is in large excess) [20], it is attractive, if such water separation could be achieved at elevated temperatures. As described in a previous chapter, adsorption and diffusion behaviours of water and methanol were studied by the Direct Measurements of Mass Transport (DMMT) approach, which represents a useful method for sorption kinetic studies when the diffusivities rates and zeolite crystallite sizes lie in appropriate ranges [16].

4.2. Experimental

4.2.1 *Potassium ion exchange and elemental determination of LTA zeolites*

Commercially available 3A and 4A zeolites (Sigma-Aldrich, UOP, beads 2.0 mm) were selected as dehydrating agents for direct DMC synthesis [20] and the parent materials for potassium ion exchange. Potassium ion exchange was carried out by charging 50 g of 3A or 4A zeolites into a glass conical beaker with 200 cm^{-3} of 1.0 M KNO$_3$ aqueous solution. The ion exchange lasted for one week at room temperature, and every day, a fresh portion

of KNO_3 solution was used for exchange. After ion exchange, the zeolites were washed with deionized water for 5 times, kept at room temperature for 24 h and then dried at 378 K for another 24 h.

The elemental analyses of K, Na, Si and Al were performed by atomic absorption spectrophotometer (AAS UNICAM SOLAR 939). All zeolites were calcined at 723 K for 4 h to eliminate adsorbed water before use. For the sake of brevity, all potassium exchanged LTA zeolites are denoted as KA-XX according to their molar percentage of potassium out of total cations. 4A is named as KA-0, 3A as KA-40, and the other two are named as KA-82 and KA-91.

All zeolites were ground to fine powder and treated in an ultrasonic bath for half an hour before particle size distribution measurements performed with a laser scattering particle size distribution analyzer (Coulter LS230).

4.2.2 *Direct DMC synthesis combined with water removal*

ZrO_2, which was used as catalyst material for DMC synthesis from methanol and CO_2, was prepared by calcining hydrous zirconia in an air flow of 100 cm^{-3} min^{-1} at 673 K for 4 h in a tube furnace. The synthetic procedures of hydrous zirconia were reported in chapter 2 and 3 and can also be found in refs. [25, 26].

Direct DMC synthesis was carried out in a 70 cm^{-3} autoclave equipped with a 100 cm^{-3} gas chamber and the reaction mixture is recirculated between the autoclave and zeolite trap operated at low temperatures [20]. The standard reaction procedure is as follows: 39.6 g of methanol (Aldrich, 99.9%) and 2.0 g of ZrO_2 were first put into the autoclave. The dehydrating agent container, whose temperature (typically 248 K) was adjusted by circulation of the coolant through a jacket tube, fully packed with 18.0 g of zeolite. Then the reactor was purged with N_2 at 10 bar for 4 times. When the autoclave was heated to 433 K, liquefied CO_2 (10.0 g Westfalen AG, 99.995%) was fed into the system at a flow rate of 10 cm^{-3} min^{-1} using a syringe pump (Teledyne ISCO. Model 500), and zero residence time was then taken. The reactor was kept at the set temperature and the liquid phase was stirred by a magnetically driven stirrer during reaction. The liquid mixture containing methanol, produced water and DMC was pumped from the autoclave, passed

through a sintered metal filter to retain the catalyst in the reactor. Before going entering the HPLC pump head, the mixture was cooled to ambient temperature and then passed through the container with the dehydrating agent. Then, the liquid was pumped back into the autoclave. During the reaction, samples were taken at different residence times and analyzed by a gas chromatography (FISONS GC8160) equipped with a RTX-5AM column. DMC yields are calculated based on initially fed amount of CO_2 according to Equation 1 (N_{DMC} = produced DMC in mmol, N^0_{CO2} = initial CO_2 amount in mmol).

$$Yield_{DMC}(mol\%) = \frac{N_{DMC}}{N^0_{CO2}} \times 100\% \qquad (1)$$

As a special case, KA-91 was also used as insitu dehydrating agent at higher temperatures (393 and 433 K) for DMC synthesis. Specified, 18.0 g of dried KA-91 zeolite, 39.6 g of methanol and 2.0 g of ZrO_2 were loaded into the autoclave. Then the reactor was purged with N_2 at 10 bar for 4 times. When the autoclave was heated to desired temperatures, liquid CO_2 (10 g) was introduced into the autoclave at a flow rate of 10 cm^{-3} min^{-1} using the syringe pump. No liquid phase recirculation was needed in this case.

4.2.3 *Water and methanol diffusion kinetics*

4.2.3.1 *Low temperature (248-298 K)*

Diffusion kinetics of both water and methanol at low temperatures (248-298 K) were measured for KA-0 (4A), KA-40 (3A), KA-82 and KA-91 zeolites, which had been pretreated at 723 K for 4 h to eliminate adsorbed water before the measurement.

For low temperature diffusion kinetic measurements reported here, isobutanol (Sigma-Aldrich, > 99.9%) solutions containing 5.0×10^4 ppm of water or methanol were used. 25.0 g of methanol/isobutanol or water/isobutanol mixture was charged into a glass conical beaker and put into the jacket bottle which was filled with the mixture of ethylene glycol and water (50:50, v/v). A water bath or a refrigerator was used to maintain a constant temperature for adsorption measurements. When the temperature reached set values and remained constant for a while, 5.0 g of pre-sealed zeolite was put into the glass conical beaker. Samples were taken at intervals and analyzed by a gas chromatography or Karl-

Fischer water analyzer (SCHOTT TA10 plus). Based on the remaining water or methanol concentrations in the liquid mixtures, the amounts of water or methanol adsorbed by the zeolite were calculated.

4.2.3.1 *High temperature (393-458 K)*

Diffusion kinetics at higher temperatures (393-458 K) was measured in a 70 cm^{-3} autoclave, and isobutanol was again used as solvents for water and methanol. 5.0 g of pretreated selected zeolite was loaded into the autoclave. Subsequently, the reactor was purged with N_2 at 10 bar for 4 times. When the autoclave reached set temperatures, magnetic stirring was started and 25.0 g of methanol/isobutanol or water/isobutanol mixture containing 5×10^4 ppm of water or methanol was introduced into the autoclave at a flow rate of 20 cm^{-3} min^{-1} using the syringe pump. This flow rate was selected to minimize the error of initial time counting. During the adsorption process, samples were taken at intervals and analyzed by the GC or Karl-Fischer water analyzer. Based on the remaining water or methanol concentrations in liquid mixtures, the amounts of water or methanol adsorbed by the zeolites were calculated.

4.3. Results

4.3.1 *Elemental analyses and particle size determination of LTA zeolites*

Based on the results from AAS elemental analysis, chemical formulas for all K^+-exchanged LTA zeolites are given in Table 1. Also listed in this table are the average crystal sizes, which are very similar for all 3A- and 4A-derived zeolites studied in this work. The molar concentration of K^+ is calculated on the basis of all K^+ and Na^+ cations.

Table 1 Elemental analysis results and average crystal sizes of LTA zeolites.

| Zeolites	Parent materials	Composition formula	K^+ (mol %)	Average crystal sizes (µm)
KA-0	(4A)*	$Na_{11.68}Al_{11.68}Si_{12.32}O_{48}$	0	2.3
KA-40	(3A)*	$K_{4.65}Na_{6.88}Al_{11.53}Si_{12.47}O_{48}$	40.3	2.4
KA-82	4A	$K_{9.64}Na_{2.06}Al_{11.70}Si_{12.30}O_{48}$	82.4	2.3
KA-91	3A	$K_{10.41}Na_{0.93}Al_{11.34}Si_{12.66}O_{48}$	91.1	2.4

* used as received

4.3.2 *Direct DMC synthesis from methanol and CO$_2$ with drying agents*
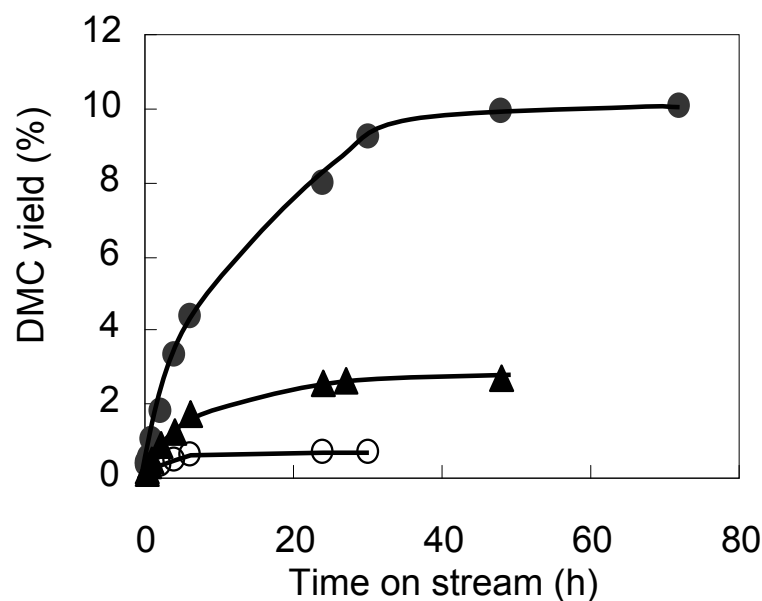
Figure 1 DMC yield versus residence time using (●) KA-40 (3A) and (▲) KA-0 (4A) and as water scavenger at 248 K, (○) no water scavenger. Reaction conditions: temperature 433 K, ZrO$_2$ 2.0 g, CO$_2$ 10 g, methanol 39.6 g, zeolites when used 18.0 g, liquid phase mixture circulation rate 2.0 ml min^{-1}.

It has been previously demonstrated [20, 27] from both, thermodynamic calculations and experimental results that direct DMC formation via CO$_2$ and methanol is strongly equilibrium-limited. The reaction can be significant shifted towards DMC production, if water scavengers are used to remove the formed water. It has been reported that KA-40 (3A) zeolite is the best drying agent at temperature of 248 K and it had been shown that water could be efficiently removed to under these conditions. As shown in Figure 1, DMC yield reached 10 % after 72 h, when it was used as the water scavenger. However, KA-0 (4A) having the same structure, but not containing potassium, did only moderately enhance of water removal. It hardly improved the yields compared with the situation in the absence of a dehydrating agent. Similarly, KA-40 was ineffective when it was used as in situ water scavenger at 393K (Figure 2). Since we anticipated that pore openings of LTA zeolites could be further tuned by exchanging potassium to higher extents, more extensive K$^+$-exchanged LTA zeolites were prepared and evaluated.

When working at 248 K, the DMC yield was not improved by using KA-91 compared to using KA-40. However, when it was used as drying agent in situ, i.e., in the autoclave

together with the reactants and catalyst at 433 K, the DMC yield increased to a maximum of 6.5 wt. % after 50 h (Figure 2). At 393 K, 12 wt. % DMC could be reached. The longer time needed for reaching a plateau is attributed to the lower reaction rate and diffusion rate for the uptake of water at a lower temperature.
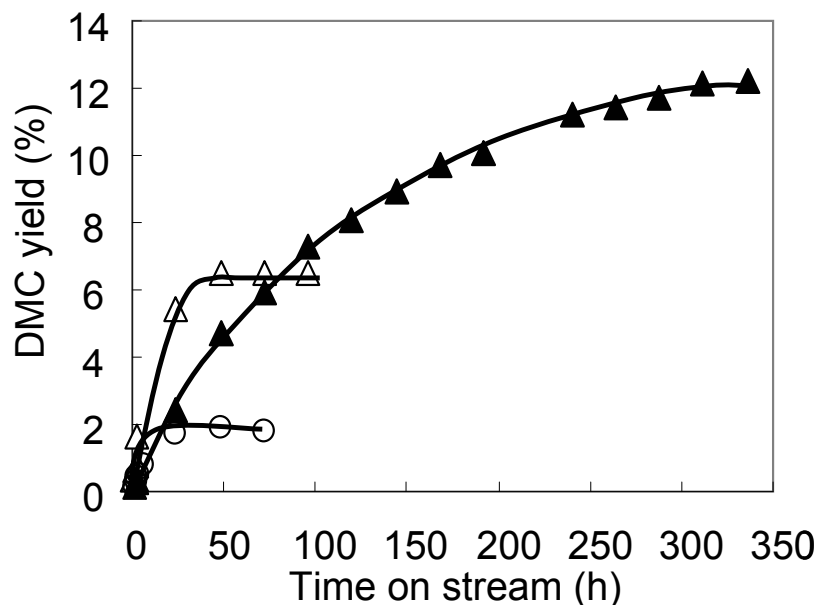
Figure 2 DMC yield versus residence time using KA-91 and KA-40 as in situ water scavenger Reaction conditions: temperature ($\triangle$) KA-91, 433 K; ($\blacktriangle$) KA-91, 393K; ($\bigcirc$) KA-40, 393K; ZrO_2 2.0 g, CO_2 10 g, methanol 39.6 g, zeolite 18.0 g.

4.3.3 *Diffusion kinetics of water and methanol*

Measurements of diffusion kinetics for water and methanol were conducted with isobutanol as solvent. As the kinetic diameter of isobutanol is 5.3 Å [28] and is so much larger than that of the pore opening so that it does not interfere with the adsorption of water or methanol [2]. Under the conditions used, the adsorption of water and methanol is governed by the diffusion from the bulk liquid phase to the inner pores, whereby the intracrystalline diffusion is the rate determining step [29].

Then, the diffusion kinetics can be simplified to the diffusion of single diffusant with a constant diffusion coefficient D, and the method used by Barrer [16] can be revised into a pattern of Equation 2 for cubic LTA zeolites, regarding q_0 as zero at the start of the adsorption process. According to Equation 4, at the beginning of adsorption when the uptake or the coverage is not high and water or methanol concentrations changes not so much and impose little impact on diffusion rates, the diffusion coefficient (D) can be

calculated by applying the average particle size and the slope (k) of trend line, when plotting –ln (1-E) versus time t (Equation 3).

$$\ln\left(\frac{q_m - q_t}{q_m - q_0}\right) = \ln\frac{512}{\pi^6} - \frac{D\pi^2 t}{4}\left(\frac{1}{a^2} + \frac{1}{b^2} + \frac{1}{c^2}\right) \tag{2}$$

$$-\ln(1 - E) = kt + s \tag{3}$$

$$k = \frac{D\pi^2}{4}\left(\frac{3}{a^2}\right) \quad \text{(If a = b = c)} \tag{4}$$

[The symbols in these equations denote the maximum amount adsorbed (q_m), the adsorbed amount at time t (q_t), the adsorbed amount at time 0 (q_0), the diffusion coefficient (D), adsorption time (t), the edges of rectangular parallelepipeds (a, b, c) with 2a, 2b and 2c in length, E = q_t/q_m, and the slope (k) and the intercept (s)].

Intracrystalline diffusion within porous crystals obeys the Arrhenius law (Equation 5). If ln D is plotted against 1/RT at different temperatures (Equation 6), the activation energy for intracrystalline diffusion processes can be calculated from the slope of the trend line. (D: diffusion coefficients, R: ideal gas constant, D_0: pre-exponential factor, T: temperature in Kelvin, Ea: activation energy for diffusion in kJ mol^{-1})

$$D = D_0 \exp\left(-\frac{Ea}{RT}\right) \tag{5}$$

$$\ln D = -\frac{Ea}{RT} + \ln D_0 \tag{6}$$

4.3.3.1 *Low temperature (248-298 K) diffusion kinetics*

The whole sets of data of diffusion kinetics of water and methanol at 248, 273 and 298 K are listed in Table 2 and 3. Two examples of water and methanol at 298 K are shown in Figure 3 (a) and (b), calculated diffusion coefficients and activation energy derived from these data are listed in Tables 4 and 5.

Table 2 Diffusion kinetics measurements of water in zeolites

Adsorption amounts-zeolites-temperature (mg H_2O/g zeolite)

| Time	KA-0			KA-40			KA-82			KA-91		
(hour)	248 K	248 K	248 K	248 K	248 K	298 K	248 K	273 K	298 K	248 K	273 K	298 K
0.17	0.36	2.79	2.79	2.79	0.36	46.66	0	-	12.51	0	-	4.69
0.33	0.63	5.27	5.27	5.27	0.63	72.25	0.61	9.79	20.78	0	0	10.34
0.50	5.02	4.93	4.93	4.93	5.02	86.91	0	-	29.07	0	-	13.59
0.67	7.26	17.01	17.01	17.01	7.26	91.42	0.30	6.95	31.92	0	0	8.39
1.00	10.50	17.59	17.59	17.59	10.50	110.42	0	8.59	36.25	0	0	16.68
1.50	15.01	20.53	20.53	20.53	15.01	137.26	0	19.93	51.69	0	4.46	16.54
2.00	23.39	32.11	32.11	32.11	23.39	153.53	1.68	23.76	59.25	1.35	7.97	20.72
3.00	43.69	59.14	59.14	59.14	43.69	174.27	7.60	32.30	69.28	-	9.11	20.18
4.00	49.46	66.66	66.66	66.66	49.46	185.82	8.97	41.13	72.68	-	11.72	20.86
24.00	136.56	151.41	151.41	151.41	136.56	222.34	43.11	68.69	107.92	14.30	21.49	22.30

Table 3 Diffusion kinetics measurements of methanol in zeolites

Adsorption amounts-zeolites-temperature (mg CH_3OH/g zeolite)

Time	KA-0			KA-40			KA-82			KA-91		
(hour)	248K	273K	298K	248K	273K	298K	248K	273K	298K	248K	273K	298K
0.17	0.45	-	19.69	0.01	-	3.59	0.33	-	0.44	0.58	-	1.88
0.33	1.67	1.62	29.50	0.11	0.44	7.46	1.37	-	4.36	1.94	-	2.63
0.50	1.31	-	42.05	0.58	-	9.00	1.74	-	3.03	0.25	-	5.78
0.67	1.49	3.69	47.24	1.06	1.05	11.54	1.74	-	4.05	0.75	-	6.78
1.00	2.22	4.12	63.05	2.07	2.24	12.89	0.40	-	3.80	1.78	-	5.66
1.50	2.87	3.73	71.55	2.25	2.04	16.44	1.15	-	5.22	0.33	-	3.87
2.00	3.70	8.78	84.28	1.32	2.52	16.90	0.77	-	3.77	0.82	-	3.26
3.00	6.61	12.81	96.41	1.62	3.12	19.41	1.01	-	5.29	0.05	-	4.98
4.00	7.47	16.70	110.37	1.44	3.79	22.88	2.07	-	5.13	1.36	-	4.22
24.00	19.13	58.45	139.97	2.68	11.56	40.51	2.10	-	6.15	2.20	-	4.07
48.00	33.77	-	143.43	4.90	-	51.95	3.07	-	6.34	2.35	-	4.77
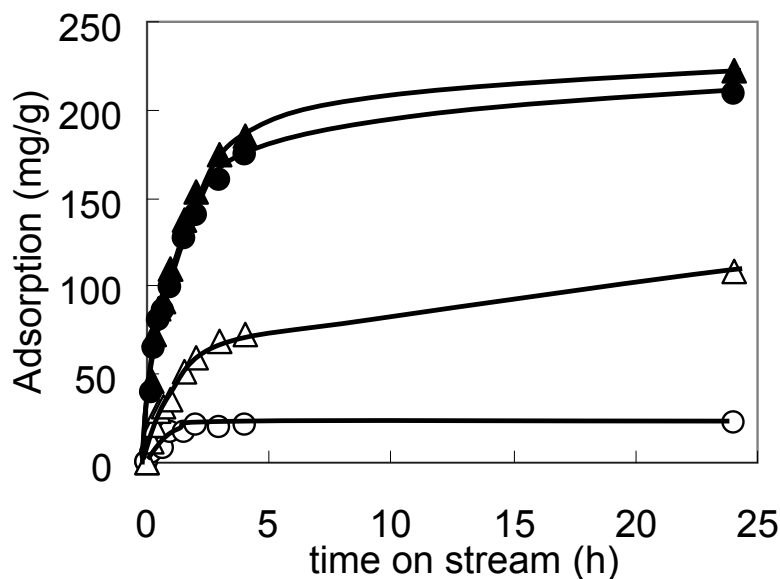
Figure 3a Water adsorption kinetics at 298 K.

(▲) KA-0 (4A), (△) KA-82, (●) KA-40, (○) KA-91
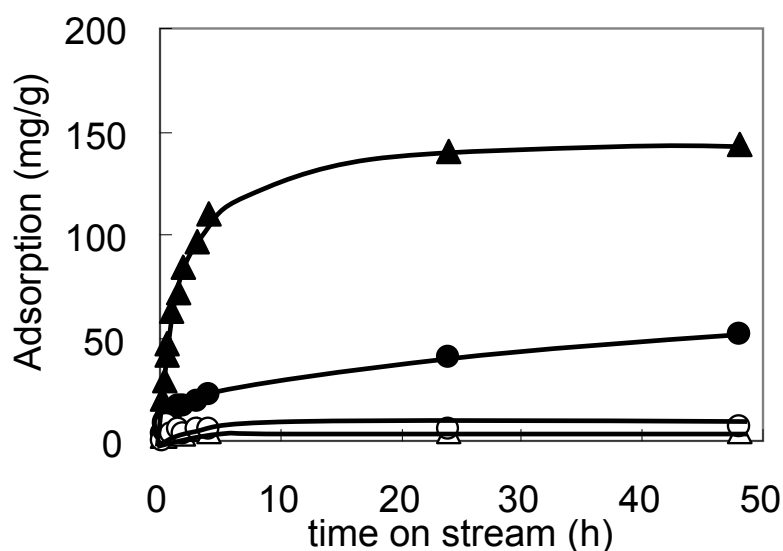
Figure 3b Methanol adsorption kinetics at 298 K.

(▲) KA-0 (4A), (△) KA-82, (●) KA-40, (○) KA-91. Adsorption conditions: zeolites 5.0 g, water (or methanol) / isobutanol 25.0 g, initial water (methanol) concentration in the mixture: 50000 ppm. Temperature: 298K.

Table 4 Activation energies and diffusion coefficients of water in LTA zeolites

Zeolites	Ea (kJ mol^{-1})	Water diffusion coefficients (10^{-14} cm^2 s^{-1})		
		248 K	273 K	298 K
KA-0	30.6	2.95	13.2	35.3
KA-40	29.2	2.37	9.35	25.3
KA-82	32.6	0.57	2.90	7.99
KA-91	n.a.	n.a.	n.a.	n.a.

**Table 5** Activation energies and diffusion coefficients of methanol in LTA zeolites

Zeolites	Ea (kJ mol^{-1})	Methanol diffusion coefficients (10^{-14} cm^2 s^{-1})		
		248 K	273 K	298 K
KA-0	62.6	0.25	0.89	14.3
KA-40	91.6	0.03	0.12	6.98
KA-82	n.a.	n.a.	n.a.	n.a.
KA-91	n.a.	n.a.	n.a.	n.a.

As shown in Figure 3 (a), the diffusion rates (initial slopes) of water in the KA materials decrease with increasing exchanged potassium concentrations. Water diffuses the fastest in KA-0 and the slowest in KA-91. Moreover, the adsorbed water in KA-91 at 298 K increased to only about 20 mg/g zeolite after the first two hours and did not further increase anymore. Note that diffusion coefficient and activation energy are not calculated for KA-91 because of the low uptake and the corresponding low accuracy.

It is speculated that the 20 mg of water per gram of zeolite were mainly adsorbed on the external surfaces of LTA zeolites and that the pore openings of KA-91 are hardly penetrable for water at 298 K. Note that even fully potassium exchanged zeolite A should be able to accommodate 24 molecules of water in one unit cell, only slight less than that for KA-0 (27molecules per unit cell) [1]. Similarly, methanol adsorption over KA-82 and KA-91 at 298 K occurred to very minor extent as seen in Figure 3 (b).

The results compiled in Tables 4 and 5 show that all diffusion coefficients of water and methanol increase with increasing temperatures suggesting that a better differentiation for the uptake in KA-82 and KA-91 can be reached at higher temperatures.
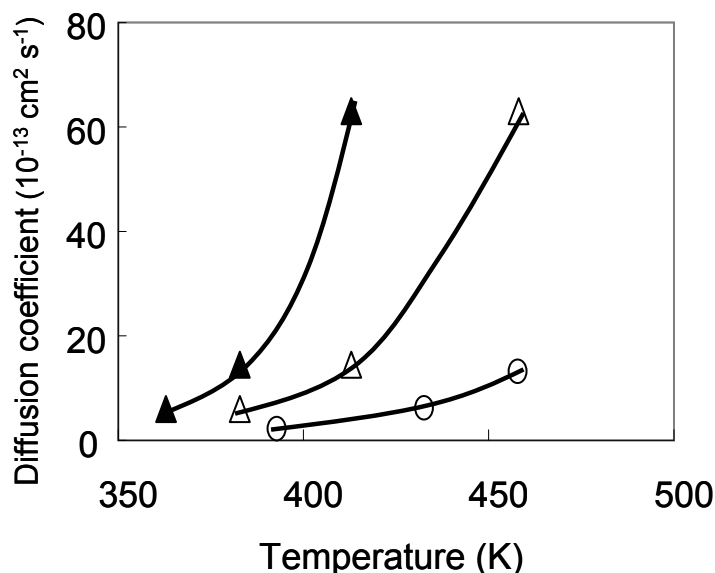
4.3.3.2 *High temperature diffusion kinetics*
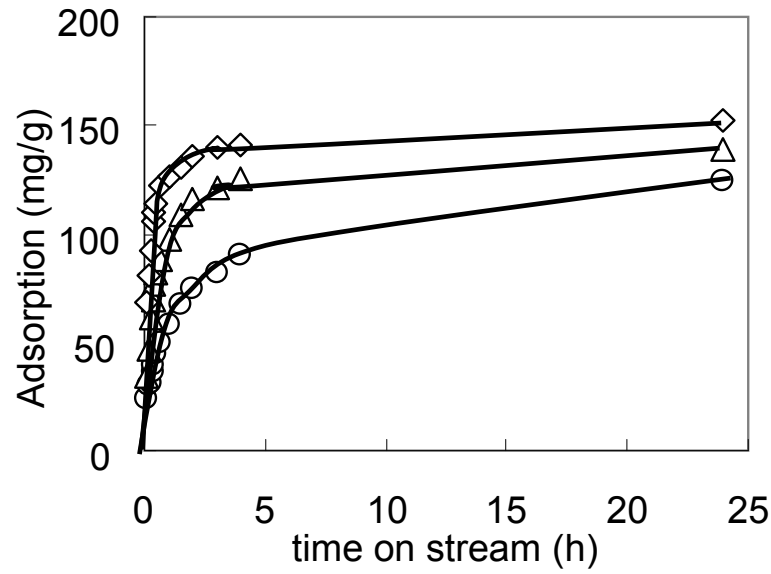
Figure 4 Water adsorption kinetics in KA-91 zeolite at (○) 393 K, (△) 433 K, (◇) 458 K. Adsorption conditions: 70 ml autoclave, zeolites 5.0 g, water/isobutanol 25.0 g, initial water concentration in the mixture: 5×10^4 ppm.
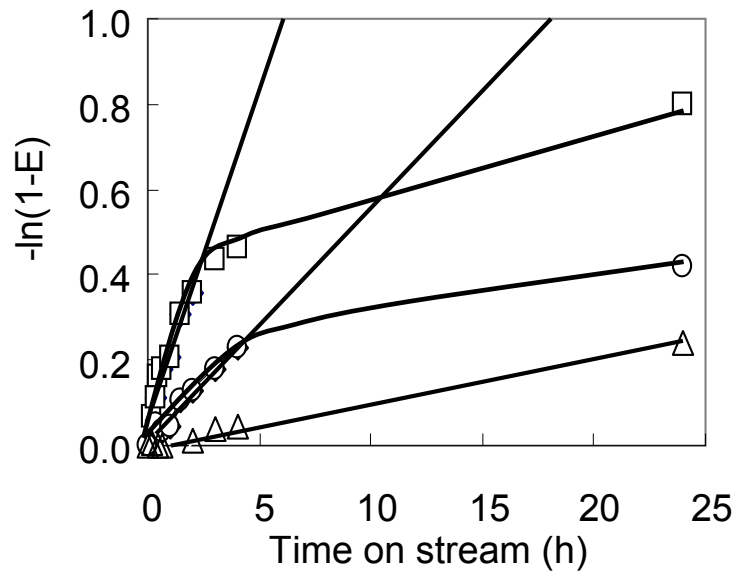
Figure 5 Simulation for the calculation of diffusion coefficients of water in KA-82 at (△) 248K: y = 0.0106x - 0.011, (○) 273K: y = 0.0547x + 0.0082, (□) 298K: y = 0.1543x + 0.0622.
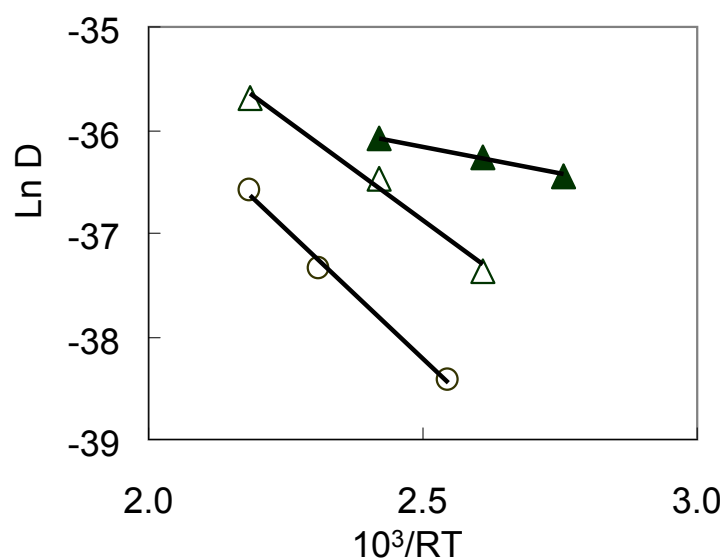
Figure 6 Water diffusion coefficients D at high temperatures in (▲) KA-0 (4A), (△) KA-82, (○) KA-91. Adsorption conditions: 70 ml autoclave, zeolites 5.0 g, water/isobutanol 25.0 g, initial water concentration in the mixture: 5×10^4 ppm.

Figure 4 shows the diffusion kinetics of water from 393 K to 458 K in KA-91 zeolite as an example. Water exhibits much faster diffusion rates at higher temperatures and can absorb more water than that at lower temperatures. Figure 5 gives an example how the trend lines of water diffusion kinetics in KA-82 are simulated according Equation 3 to get needed slope values, which are essential for further calculations according Equation 4. Calculated water diffusion coefficients in KA-0, KA-82 and KA-91 zeolites at high temperatures are shown in Figure 6.

Figure 7 gives an example how the trend lines are simulated for water intracrystalline diffusion activation energies at higher temperatures in the range from 393 K to 458 K in LTA zeolites based on Equations 5, 6. Calculated activation energy values for KA-0 (8.81kJ mol^{-1}4A), KA-82 (32.2 kJ mol^{-1}) and KA-91 (42.0 kJ mol^{-1}) are also given.

Discuss in terms of overall, the diffusion coefficients increase in a sequence of KA-91, KA-82 and KA-0, in parallel to the decreasing concentration of potassium. The intracrystalline diffusion activation energies of water in the investigated zeolites compiled in Figure 7 increase with the potassium contents, this suggests that higher potassium content in LTA is related to the higher constraints of the diffusions. The diffusion

activation energies of water in KA-82 at different temperatures are almost the same (248-298K, 32.6kJ mol^{-1}; 393-458K, 32.2kJ mol^{-1}). However, the diffusion activation energy of water in KA-0 in the ranges from 363K to 413K is only 8.81 kJ mol^{-1} and much lower than 30.61 kJ mol^{-1} in the ranges from 248K to 298K. When the temperatures were sufficiently high, the intracrystalline diffusion rates become very fast. Under these conditions the intracrystalline diffusions are not the key step any more. Thus for, the value for the diffusion may be related to Knutson diffusion or Bulk diffusion through materials pores at high temperatures.


Figure 7 Activation energies simulation for intracrystalline diffusion of water estimated from diffusion coefficients at different temperatures for (▲) KA-0 (4A), 8.81kJ mol^{-1}; (Δ) KA-82, 32.2 kJ mol^{-1}; (○) KA-91, 42.0 kJ mol^{-1}.

Figure 8 shows the uptakes of methanol at higher temperatures in KA-0, KA-82 and KA-91 zeolites. The potassium concentrations also influence the diffusion rates of methanol in tested LTA zeolites being the fastest for KA-0 decreasing via KA-82 to KA-91. Note as with water we assume that the 25 mg per gram adsorbed Methanol may occur on the outer surface of the zeolite particle.

The diffusion rates of methanol in KA-91 at elevated temperatures are too small to be calculated. However, a roughly understanding was got by comparing methanol diffusion coefficients at high temperatures in KA-0 and KA-82, which are shown in Figure 8.
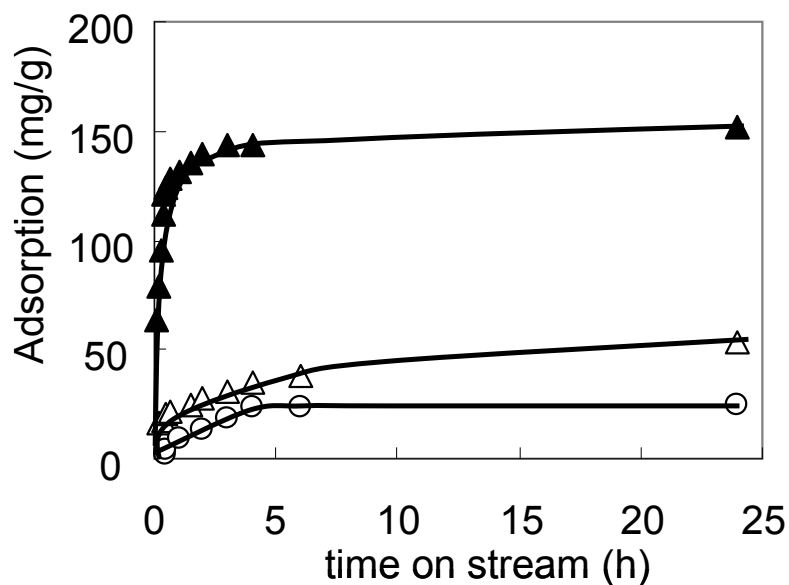
Figure 8 Methanol adsorption kinetics for (▲) KA-0, 413K; (Δ) KA-82, 458K; (○) KA-91, 458K. Adsorption conditions: 70 ml autoclave, zeolite 5.0 g, methanol/ isobutanol 25.0 g, initial methanol concentration in the liquid mixture: 5×10^4 ppm.
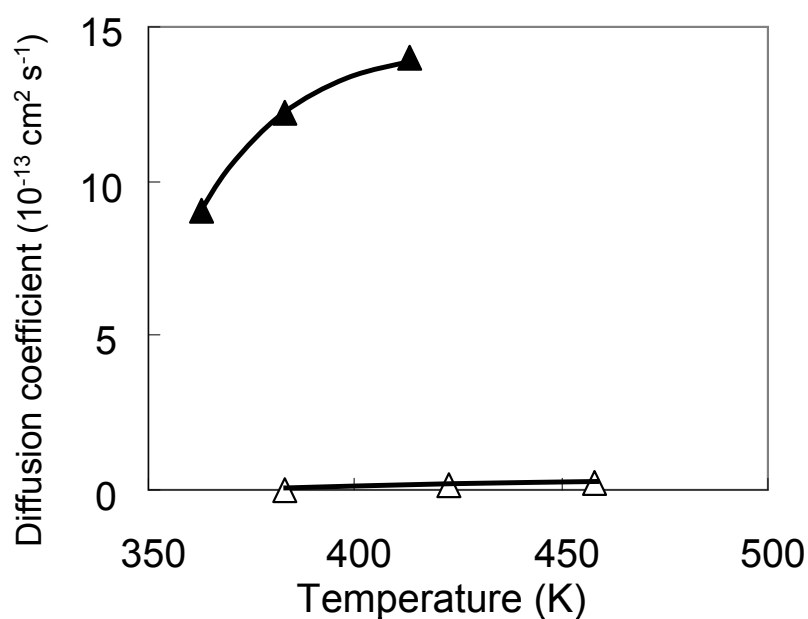

Figure 9 Methanol diffusion coefficients at high temperatures in (▲) KA-0, (Δ) KA-82.

The increasing potassium content hindered the diffusion of methanol in LTA zeolites. Though the calculated diffusion coefficients of methanol in KA-82 increase with temperature increasing also, they are over two orders of magnitude smaller than the value with KA-0 at the same temperature.

4. 4. Discussion

The results presented above show that the exchanged potassium of LTA zeolites hinders the diffusions of both water and methanol. For the most extensively potassium exchanged KA-91, the hindrance is most pronounced. Between 248 and 298K the uptake of both of these two molecules is essentially suppressed. Only at elevated temperatures water can be adsorbed, while methanol is still excluded. Thus, KA-91 can only be used as dehydrating agent at higher reaction temperatures. However, in another also highly potassium exchanged KA-82, methanol can overcome the diffusion hindrance and come into its inner cages at higher temperatures. Then the mechanism that how exchanged potassium cations restrict the pore opening of LTA zeolites need to be more detailed elucidated.
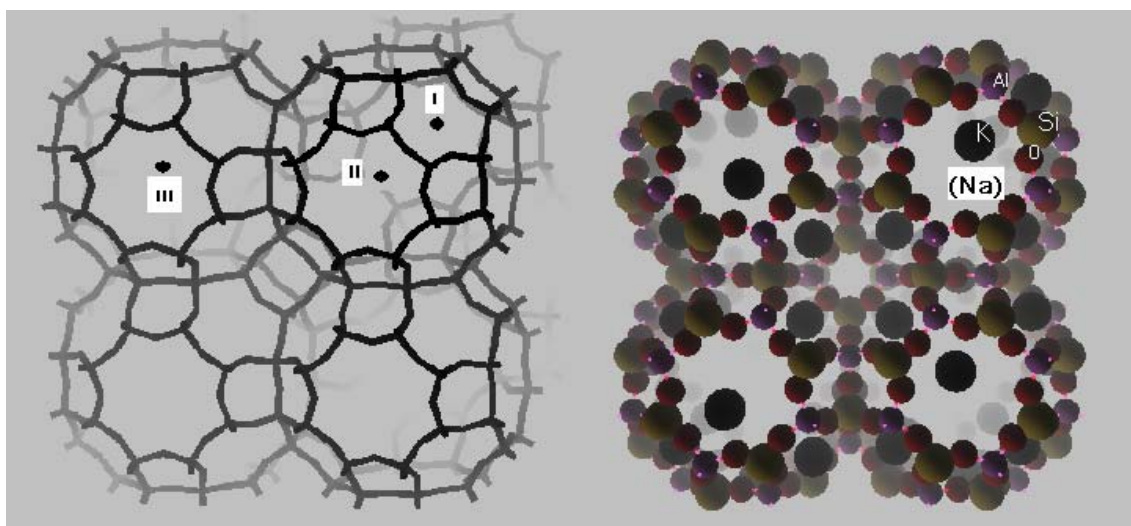
Figure 10 Stereo view of LTA unit cell with cations placed statistically in three kinds of sites (left), and site II which located in the 8-rings (right).

The locations of cations in LTA need to be discussed in detail. Figure 10 shows a graphical representation of the LTA unit cell with statistical cation location sites in it. For hydrated sodium type or fully K^+ exchanged A, the statistical location sites of cations are almost identical and are shown in the left picture of Figure 10. Among these 12 sodium cations in one unit cell ($Na_{12}Al_{12}Si_{12}O_{48}$), eight are displaced by 0.2Å into the α-cage from the center of six-membered rings (sites I). Three Na^+ locate in the plane of 8-membered rings 1.2 Å from the center (site II). The twelfth Na^+ is located in the center of the α-cage and coordinated with water molecules (site III). For fully K^+ exchanged A, the statistical location sites are almost the same and the differences are related to minor variations of the

distances from site I to the center of six-membered rings, and from site II, which is occupied by K^+ cation near the center of the eight-membered rings [30, 31].

The small differences of the sittings in hydrated Na^+ and K^+ exchanged zeolite A stem from differences in their ionic radii (for Na^+ it is 0.95Å while it is 1.33Å for K^+). This leads also to the differences of the free openings, when different cations occupy the site II in the 8-membered ring, the pore openings. Because all cations tend to occupy positions with minimum free energies, in partially K^+ exchanged LTA zeolites, the minimum steric hindrance of the larger cations determines the occupations of K^+ in different sites. Site II is occupied first followed by site III and at last to site I [32]. On the other hand, the free energies or the energy requirements levels of those three sites for exchanged K^+ cations are in the order of E2< E3 <E1 which represent Site II, Site III and Site I respectively.

In KA-40 (zeolite 3A) 4.65 K^+ cations and 6.88 Na^+ cations exist on average in each unit cell. Following the above argument three K^+ will be located in site II, one in site III and only 0.65 in Site I. Thus, three Sites II at the pore openings of KA-40 are all occupied by K^+ cations (right picture in Figure 10) and molecules with kinetic diameters larger than 3Å should be excluded [1]. At room temperature KA-40, however, adsorbs a significant concentration of methanol whose kinetic diameter is 3.6 Å. Only at a much lower temperature of 248 K, the adsorption of methanol in KA-40 is quantitatively hindered [20, 21].

KA-82 has 9.64 K^+ and 2.06 Na^+ cations in one unit cell and all pore openings should be occupied by K^+ cations. However, it is able to absorb methanol above 458 K, but not at room temperature. KA-91 with 10.41 K^+ and only 0.91 Na^+ cations in one unit, in contrast, does not absorb methanol at any temperature tested. At 298K, even water molecules with kinetic diameter of 2.6 Å cannot access the pores. This indicates that the K^+ and Na^+ cations change positions reversibly as a function of temperature and that with KA-40 the pore openings must be occupied with Na^+ cations at 298 K. This shows that with increasing level of exchange K^+, an increasing diffusion hindrance is generated by the more complete location of the K^+ cations in the size determining Sites II.

There are strong grounds that the locations of Na^+ and K^+ cations in partially potassium exchanged LTA zeolite are exchangeable. Though free energy levels of those three sites

for K^+ cations are in the order of E2 < E3 < E1, and K^+ cations preferentially locate in sites with lower free energy. It is also possible that K^+ cations snatch the sites of free higher energy and once occupied by Na^+ cations when the temperature is high and K^+ cations have enough active energy. Under such circumstance, Na^+ cations have to locate in the vacated sites once occupied by K^+ cations. For example, one Na^+ cation will locate in Site II when One K^+ cation jumps from it to Site I. Then the space restricting to this 8-ring will be undermined and molecules with bigger diameters such as methanol may pass through this pore opening and go into the α-cage of such a unit cell.

This is what had happened to zeolite KA-40 and also the reason why such a zeolite can absorb methanol at room temperature. However, such transitions of location sites are restricted at low temperatures, when K^+ cations have no enough active energy to snatch the location sites of Na^+ cations. That is why KA-40 can not absorb methanol at 248K. The statistical distribution of Na^+ (K^+) in site II / site I of LTA zeolite can be made in complete analogy with Boltzmann distribution principle [33] (Equation 7).

$$\frac{N_{II}}{N_I} = \frac{e^{-\varepsilon_{II}/kT}}{e^{-\varepsilon_I/kT}} = \exp(-\frac{\Delta\varepsilon}{kT}) \qquad (7)$$

(Where the symbols bear the meanings as follows. N_{II} / N_I: the distribution ratio of Na^+ in site II and site I, ε_{II}: free energy when Na^+ locate in site II, ε_I: free energy when Na^+ locate in site I, $\Delta\varepsilon$: energy difference between ε_{II} and ε_I, k: Boltzmann constant, T: temperature in K.)

Inner cages of partially potassium exchanged LTA zeolites can adsorb methanol only when Na^+ cations locate in Sites II, which are near the center of 8-rings and restrict their free openings. Zeolite KA-82 has 9.64 K^+ and 2.06 Na^+ cations in one unit cell. Higher temperature is essential to make sure a big enough ratio of N_{II}/N_I and enough Na^+ cations locate in its pore openings. That is why that zeolite KA-82 can only adsorb methanol at elevated temperatures. KA-40 can adsorb methanol at 298K because there are 4.65 K^+ cations and 6.88 Na^+ cations in one unit cell and room temperature is enough for a sufficient ratio of N_{II}/N_I. However, Things are totally different for KA-91 zeolite, which has only 0.91 Na^+ cations in one unit cell averagely. Even at very high temperatures that all Na^+ cations located in the pore openings, the α-cages cannot connect to each other to

form accessible and successive free inner spaces for methanol because there is less than one Na^+ cation for each unit cell averagely. Methanol molecules may come into the α-cages that have one Na^+ cation in their pore openings in the outer surface of zeolite crystals, but they cannot go deeper of the α-cages inside the zeolite.

The temperature influenced the distribution of Na^+ and K^+ cations, the distribution of Na^+ and K^+ cations influences the shape restricting of the pore openings, who determine the diffusions possibilities of different molecules by size. It is the potassium concentration of LTA zeolites determines how much the shape restricting effect relies on the temperature variations. This is the mechanism how the potassium concentration of LTA zeolites influenced the diffusions of water and methanol in them.

4.5. Conclusions

It has been demonstrated in this chapter that exchanged potassium concentration of LTA zeolites influence the diffusion rates of water and methanol in them. High potassium concentration will hinder the diffusions of both water and methanol and decelerate their diffusion rates in LTA zeolites. The zeolites' shape restricting of the pore openings, which governs the adsorption possibilities of molecules with different size, is determined by the distributions of Na^+ and K^+ cations in the location Sites II of LTA zeolites. High potassium concentration favors that more K^+ cations occupy the Sites II in the pore openings, and makes shape restricting more severe. Temperatures also influence the distributions of Na^+ and K^+ cations. For a LTA zeolite with certain exchanged potassium degree, elevated temperature favors more Na^+ cations locate in Sites II and undermine the shape restricting of LTA zeolites. That is the reason why KA-40 can selectively adsorb water at 248K and KA-91 can even at elevated temperatures (in the range from 393 K to 458 K). The KA-91, one highly potassium exchanged LTA zeolite, was successfully used as the in situ dehydrating agent at reaction temperatures for DMC direct synthesis from methanol and CO_2, which can be regard as a direct factual proof for conclusions above.

References

[1] D. W. Breck, Zeolite molecular sieves, Structure Chemistry and Use. New York, John Wiley, 1974, P89.

[2] J. Weitkamp, L. Puppe, Catalysis and Zeolites fundamentals and applications, Springer, 1999, P327-333.

[3] D. W. Breck, W. G. Eversole, R. M. Milton. J. Am. Chem. Soc. **1956**, 78, 5963–5972.

[4] R. M. Milton. (**1959**) US Pat 4534947.

[5] Salem M. Ben-Shebi, Chem. Eng. J. **1999**, 74, 197-204.

[6] Kokai Tokkyo Koho, (**1982**) JP 57101757.

[7] X. Liu, H. Yao, Gaoxiao Huaxue Gongcheng Xuebao, **1992**, 6(2), 153-159.

[8] M. Goyal, R. Nagahata, J. Sugiyama, M. Asai, M. Ueda, K. Takeuchi, Polymer, **1999**, 40, 3237–3241

[9] Q. Wang and R. Huang, Tetra. Lett. **2000**, 41, 3153–3155.

[10] C. E. Outlaw, C. F. Fillers, B. T. Smith, K. H. Maness, D. J. Olsen, WO 2000029366.

[11] K. Okamoto, H. Kita, M. Kondo, N. Miyake, Y. Matsuo, (1996) U.S. Patent.5554286.

[12] K. Okamoto, H. Kita, K. Horii, K. T. Kondo, Ind. Eng. Chem. Res. **2001**, 40, 163-175.

[13] K.D. Kreuer, J. Membr. Sci. **2001**, 185, 29-35.

[14] Y. Li, W. Yang, J. Membr. Sci. **2008**, 316, 3–17.

[15] R.X. Fischer, W.H. Baur. Microporous and other Framework Materials with Zeolite-Type Structures, Springer, **2006**, 15-18.

[16] R. M. Barrer, Zeolites and Clay minerals as sorbents and Molecular Sieves, Frs. Chemistry Department, Imperial College, London, **1978**, P93, 273-275, 315.

[17] I. E. Neimark, M. A. Piontkovskaya, A. I. Lukash, R. S. Tyutyunnik, Otd. Khim. Nauk. **1962**, 49-58.

[18] R. Maachi, M. J. Boinon, J. M. Vergnaud, Journal de Chimie Physique et de Physico-Chimie Biologique **1978**, 75(1), 116-120.

[19] N. Tessa, B. Tyburce, G. Joly, Journal de Chimie Physique et de Physico-Chimie Biologique, **1991**, 88(5), 603-613.

[20] Chapter 2.

[21] Chapter 3.

[22] T. Shigetomi, T. Nitta, T. Katayama, J. Chem. Eng. Jpn. **1982**, 15(4), 249-254.

[23] C. Akosman, M. Kalender, Fresenius Environ. Bull. **2007**, 16(5), 500-507.

[24] K. F. Loughlin, Adsorption, **2009**, 15(4), 337-353.

[25] G.K. Chuah, S. Jaenicke, B.K. Pong, J. Catal. **1998**, 175, 80-92

[26] W. Li, H. Huang, H. Li, W. Zhang, H. Liu, Langmuir **2009**, 24, 8358-8366.

[27] T. Zhao, Y. Han, and Y. Sun, Nat Gas Chem. Ind. (Chin.) **1998**, 23, 52-55.

[28] R. C. Reid, J. M. Prausnitz, T. K. Sherwood, The Properties of Gases and Liquids, Mcgraw-Hill Book Company, third edition, **1977**, P24, 679.

[29] Z. H. Ye, Chemical process of adsorption and separation, Beijing, Sinopec press, **1992**.12, P 48, 81.

[30] R. Y. Yanagida, A. A. Amaro, K. Seff, J. Phys. Chem. **1973**, 77(6), 805-809.

[31] P. C. W. Leung, K. B. Kunz, K. Seff, J. Phys. Chem. **1975**, l79 (20), 2157-2162.

[32] J. M. Adams, D. A. Haselden, J. Solid State Chem.**1983**, 47, 123-131.

[33] Physical chemistry, 15TH P.W.Athins Oxford University Press. **1994**.

Chapter 5

Potassium exchanged LTA zeolite membrane for methanol dehydration

Abstract

A novel method for preparing potassium exchanged LTA zeolite membrane is disclosed. The membrane can be used for the separation of water from methanol and other circumstances (e.g., direct methanol fuel cells) where the permeation of methanol has to be reduced or even blocked. This preparation method is composed of two steps. The first is the synthesis of compact sodium type zeolite LTA membrane over certain substrates. In the second step, the sodium content in the synthesized membrane is then ion-exchanged with potassium to a desired level. The advantages are that the membrane is highly selectively permeable for water compared to methanol, and at mild operative conditions. Moreover, the membrane is also a possible candidate for the membrane of direct methanol fuel cells, which need to decrease the methanol crossover from anode to cathode.

Key words: LTA zeolite membrane, Potassium exchange, methanol dehydration.

5.1. Introduction

The methanol production capacities throughout the world have increased from 18.5 $\times 10^6$ tons/year in 1985 to 26.8 $\times 10^6$ tons/year in 1995, and are expected to reach 50.5 $\times 10^6$ tons/year by the year of 2010 [1-3]. Methanol has already established itself as a leading chemical feedstock. It is one of the three basic primary chemicals, after ammonia and ethylene. About 70% of the present methanol production is used as a feedstock for chemical syntheses like the synthesis of formaldehyde, methyl tertiary butyl ether (MTBE), acetic acid, methyl methacrylate and dimethyl terephthalate. In addition, methanol is used as antifreeze, inhibitor and solvent. Moreover, methanol can be catalytically converted into olefins (MTO technology), the demand of which is extremely high especially for the production of polyolefins. Methanol can also be converted into gasoline (MTG process). With oil reserves diminishing, it may play a significant role as a synthetic fuel for the future.

Presently, the majority of methanol is made from natural gas, but also some methanol is made from coals. Both are converted into synthesis gas, via catalytic steam reforming in the case of natural gas, and through gasification in the case of coals. Further steps of the methanol plant are usually based on the ICI technology, including three steps of syngas compression, methanol synthesis and distillation of crude methanol. Crude methanol leaving the reactor contains water and other impurities, which are generally separated in several stages. First, all components boil at lower temperature, and impurities with low boiling points are removed in the light end from the distillation column. Second, heavier impurities are removed in a second distillation column. At last, pure methanol is distilled overhead in one or more distillation columns to remove excess water. Purifications and distillations are essential for methanol production though they are highly energy-demanding. In modern methanol production processes, energy relationships have been integrated among different sections in various ways to minimize the overall energy input per unit

of purified product methanol [4-11]. However, the inevitable energy loss during distillations is still as high as 800-900 MJ per ton of methanol [12].

Vapor permeation (VP) and pervaporation (PV) of membranes have gained widespread acceptance in the chemical industry as an effective process for separation of some mixtures that are difficult to separate by distillation, extraction or sorption [13-16]. Membranes used for VP and PV are operated continuously without regeneration, and they are modular-designed, which are flexible. These advantages make membrane processes or hybrid processes involving membranes economically attractive to many industrial applications. It has been applied to the dehydration of organic liquids (ethanol, i-propanol or ethylene glycol etc.) [15-16].

Practical applications of polymeric membranes have been carried out for dehydration of alcohols. However, no successful application has been reported for the separation of methanol and water [17]. Inorganic membranes are generally superior to polymeric membranes in terms of thermal, mechanical, and chemical stability, and zeolite membranes have received the most attention among inorganic membranes [18-25]. Researchers have noticed that zeolite NaA membranes are nearly ideally suited for removing residual water in organics because they are highly hydrophilic and their pore opening diameters (0.41 nm) are smaller than most organic molecules but larger than water. However, the molecular sizes, polarities and chemical properties of water and methanol are similar. More critically, the kinetic diameter of methanol is only 0.36 nm, smaller than the pore openings of zeolite NaA, allowing it to pass through the membranes, hindering the separation efficiency of methanol and water. Some scientists reported some dehydration membranes for methanol, but with very low separation factors [26], or very thick membrane with higher separation factors but very small fluxes [27, 28].

Direct (oxidation) methanol fuel cells (DMFCs) have drawn a great deal of interest in recent years for several applications due to their lower weight and volume compared to indirect fuel cells. However, current membranes used for DMFCs have

high methanol permeability and large methanol crossover from anode to cathode, which spoils the cell performance [29, 30]. Though many scientists have done a lot of work to improve the membrane performance used for DMFCs [31-33], it is still imperative to develop a membrane which can not be permeated by methanol and has other corresponding characteristics.

In this chapter, in order to prevent the methanol permeation through the membrane, a new method for membrane synthesis was developed. The synthesized membrane via such a method allows the permeation of water while remarkably reduces the crossover of methanol. A successful synthesis comprises two main rationally designed steps. The first step is the synthesis of dense zeolite membrane. The second one is the ion exchanging of sodium with potassium. The main advantage of the K^+ ion exchanging is that the structure of zeolite membrane is not damaged if the ion exchanging is kept at a certain level. The pore openings of zeolite LTA can be modified to a desired size by controlling the degree of potassium-exchange such that water can permeate the membrane while methanol can not.

5.2. Experimental

5.2.1. *Preparation of KA wafer*

Commercially available zeolite 3A (Sigma-Aldrich, UOP, beads 2.0 mm, $K_{4.65}Na_{6.88}Al_{11.53}Si_{12.47}O_{48}$) was selected as parent material for potassium ion exchange. The processes are as follows: 50 g of zeolite 3A was charged into a glass conical beaker with 200 ml 1.0 M KNO_3 aqueous solution which was used for ion exchange. The ion exchange lasted for one week at room temperature, and every day, a fresh portion of KNO_3 solution was used for exchange. After ion exchange, the zeolite was washed with deionized water for 5 times and then kept at room temperature for 24 hours and then dried at 378 K for another 24 hours. The dried zeolite has a chemical formula of $K_{10.41}Na_{0.93}Al_{11.43}Si_{12.66}O_{48}$ as determined by elemental analysis and was named as zeolite KA.

KA zeolite was ground to fine powder and sieved (<50 µm) for pressed wafer making. 0.75 g of KA fine powder was used for each wafer and the pressing strength is kept at 17.6 kN cm^2 for 10 seconds. By this means pressed wafers have a diameter of 19 mm and a thickness of 2 mm the wafers which were used as the membrane substrate. The pressed KA wafers were calcined in a muffle oven at a heating rate of 1.0 K/min and kept at 873 K for 4 hours

5.2.2. *LTA Zeolite membrane synthesis over KA wafer*

Zeolite LTA membrane over KA wafers was synthesized via a hydrothermal approach and the process is described as follows: (A) the aluminate solution was prepared by dissolving 196.7 g of sodium hydroxide and 20.0 g of sodium aluminate (53% Al_2O_3, 43 %Na_2O) in 893.5 g of deionized water. After dissolving the solids in water and stirring for 2 hours, the transparent solution was sealed and kept at room temperature overnight. (B) the silicate solution was prepared by mixing 208.5 g of sodium hydroxide, 78.2 g of silica sol (40% SiO_2) and 871 g of deionized water. After dissolving and stirring for 2 hours, the solution was also sealed and kept at room temperature overnight.

The synthesis mixture was prepared by pouring the aluminate solution into the prepared silicate solution under vigorous stirring. And the stirring lasted for 2 hours to make sure that the synthesis mixture was homogenous. The molar ratio (SiO_2: Al_2O_3: Na_2O: H_2O) of the resultant clear solution is 5:1:50:1010.

The KA wafers obtained before were placed vertically in 100 ml Teflon autoclaves, into which 80 ml of the synthesis mixture obtained was added. All the autoclaves were put in an air oven which was kept at 358 K. The hydrothermal synthesis lasted for 1.5 hours and autoclaves were taken out of the oven by cooling down to room temperature automatically. In order to get denser membrane without defects, the hydrothermal synthesis was repeated for one more time.

After hydrothermal synthesis, the membrane was rinsed and then immersed in deionized water for 1 day. Meanwhile, the alkalified water was exchanged for several times. The treated membrane was then dried in air at room temperature overnight and then collected for further treatments, characterizations or tests.

5.2.3. *Ion exchanges of synthesized membranes*

The synthesized Na-LTA zeolite membranes were treated with pre-prepared sodium nitrate and potassium nitrate mixtures for ion exchange. Membranes with different cations and certain different K/Na ratio were obtained from the process as follows.

Na-LTA zeolite membrane: one prepared membrane was charged into a glass conical beaker with 50 ml 1.0 M $NaNO_3$ aqueous solution which was used for ion exchange. The ion exchange lasted for one week at room temperature, and every day, a fresh portion of $NaNO_3$ solution was used for ion exchange. After ion exchange, the membrane was rinsed and immersed into deionized water for 24 hours to remove excessive $NaNO_3$, and a Na-LTA (100%, according to elemental analysis) membrane was thereby prepared.

Potassium exchanged LTA zeolite membrane: the membranes with different K/Na ratios were prepared as stated in Na-LTA zeolite with the only difference that the solutions used for ion exchange are mixtures of $NaNO_3$ and KNO_3 with a total concentration of 1.0 M and varying molar ratio of 7:93 resulted in a membrane with a K/Na ratio of 90:10 which was named as K90 membrane.
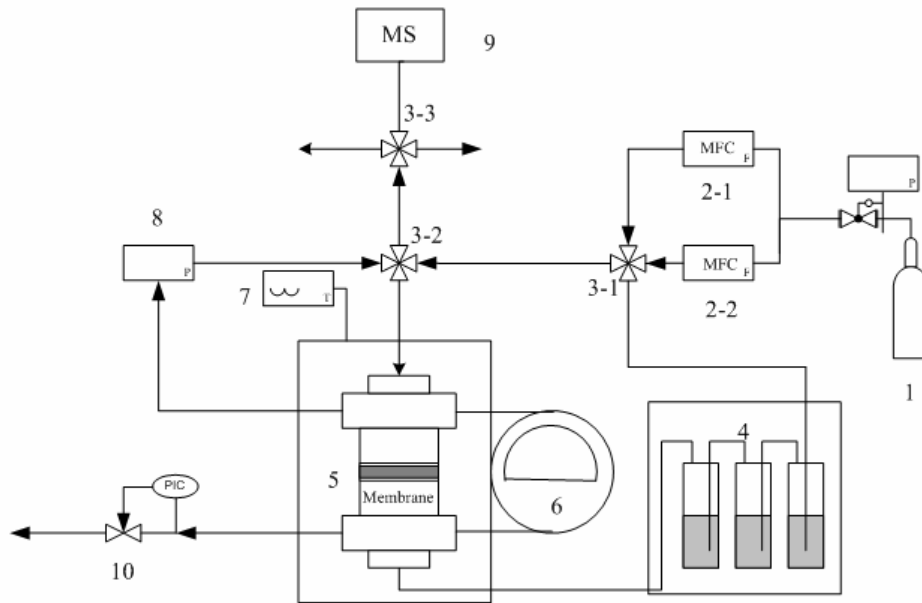
5.2.4. *Vapor Permeation experiments*

The apparatus used for vapor permeation to separate the mixture of water and alcohols is illustrated in Figure 1.

Nitrogen was used as the carrier gas and kept at a flow rate of 50 ml/min for both mass flow controllers (MFC 2-1 and 2-2). The feed gas was introduced to three

serially-arranged bubblers, which were filled with a mixture of water and ethanol or methanol and kept at 293 K in a temperature controlled water bath. The saturated vapor mixture went into the vapor permeation cell equipped with KA wafer or synthesized membranes, which were sealed with two FKM o-rings. The vapor permeation cell was heated by a heater equipped with a temperature controller. The permeate-containing carrier gas was analyzed by Mass Spectrometer (MS, PFEIFFER VACUUM). From the concentrations of the permeated water and alcohols contained in the carrier gas, the separation factors can be calculated according Equation 1. (α is separation factor, Y_W/Y_o is the weight ratio of water to alcohol in the permeate, X_W/X_o is the weight ratio of water to alcohol in the permeate)

$$\alpha = \frac{(Y_W / Y_O)}{(X_W / X_O)}$$

(1)

**Figure 1** Schematic diagram of Membrane Vapor Permeation experimental unit

1: N_2 Gas bottle; 2: Mass flow controllers; 3: Four-way valves; 4: Bubble bottles and water bath; 5 Membrane vapor permeation cell; 6 Differential pressure gauge; 7: Temperature controller; 8: pressure gauge; 9: MS; 10: Relief valve.

5.3. Results and discussions

5.3.1. *Prepared KA wafer and synthesized LTA zeolite membrane*

A typical SEM picture of as-prepared KA wafer is shown in Figure 2. A lot of macrospores can be seen in the pressed KA wafer.

From the XRD patterns (Figure 3) of synthesized A zeolite membrane over KA wafer, no impurities were found. The SEM picture of prepared membrane over KA wafer are shown in Figure 4 a, b, which is tight and no obvious defect with a thickness around 5 μm .
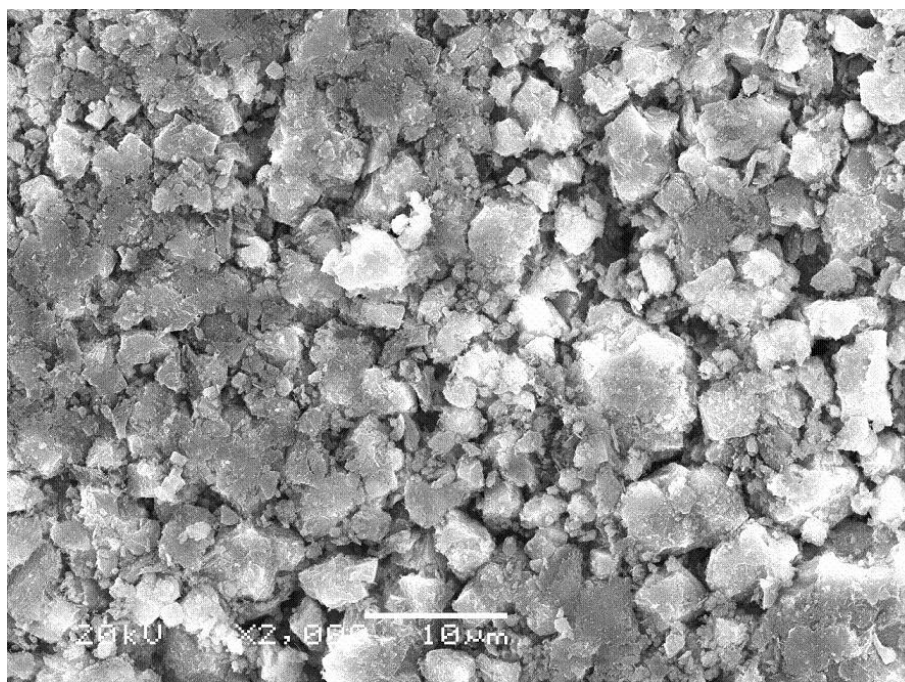
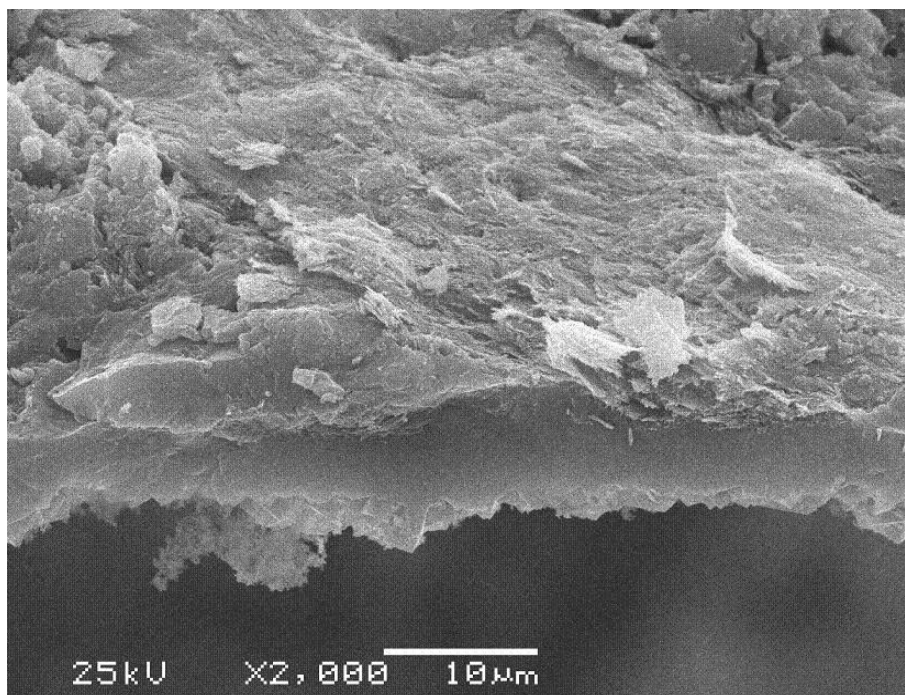**Figure 2** KA wafer before membrane synthesis (magnitude×2000)
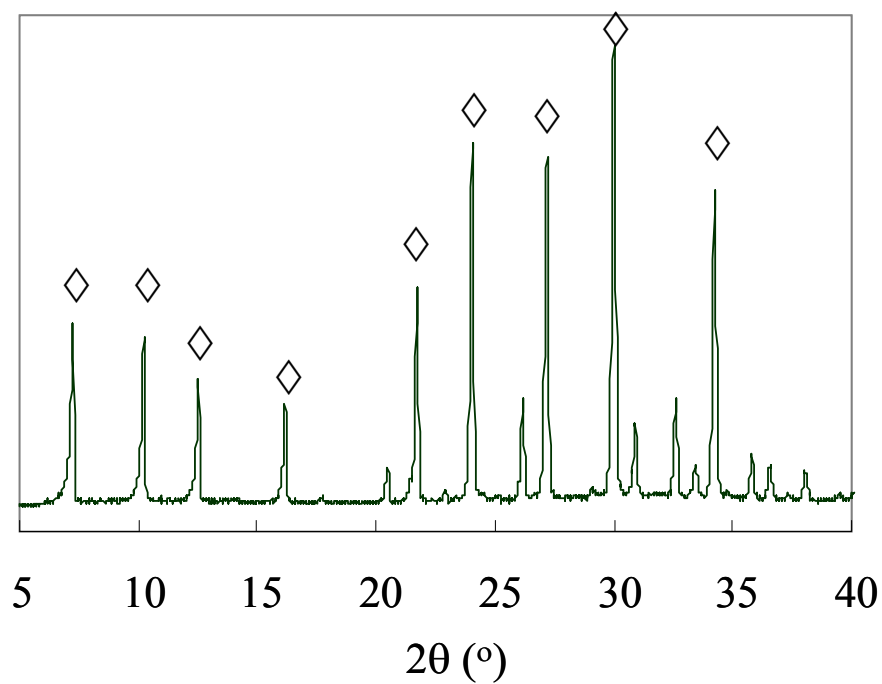
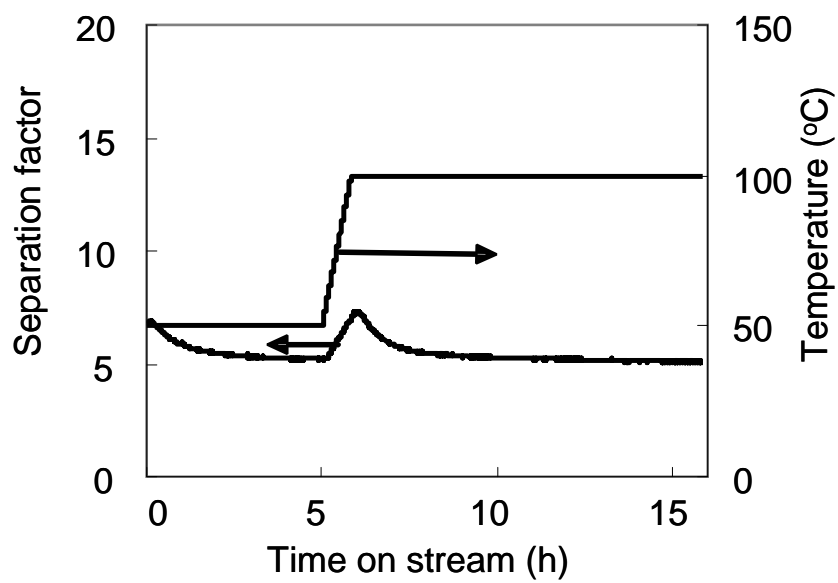**Figure 3** XRD pattern of synthesized LTA zeolite membrane (◊ LTA zeolite)
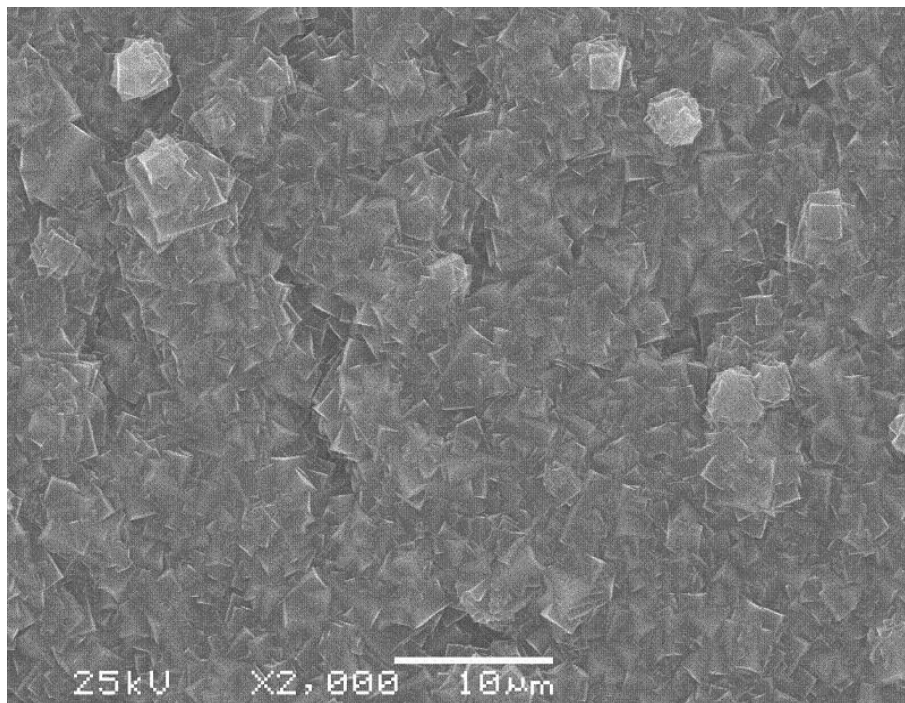
(a) Surface

(b) Side view

Figure 4 SEM images of zeolite LTA membrane on KA wafer

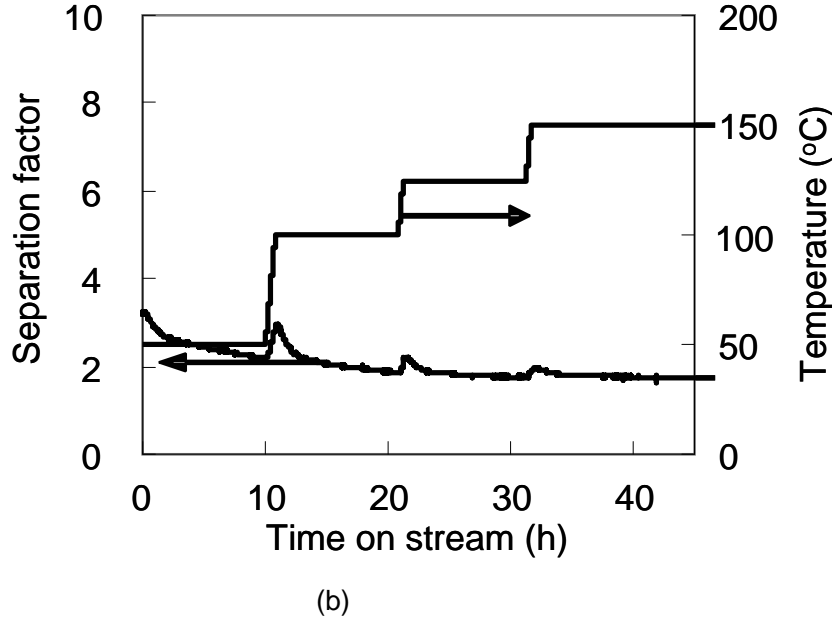(a) Surface and (b) side view (magnitude: ×2000)

5.3.2. *Vapor Permeation*

**5.3.2.1.** *Vapor Permeation of KA wafer*

(a)

(b)

Figure 5 Separation results of KA wafer (a). Water + ethanol; (b). Water + methanol.

The Vapor Permeation separation results of KA wafer without membrane are shown in Figure 5. KA wafer has very low separation factors both for ethanol and methanol against water; the separation factors are around 5 for ethanol/water mix and 2 for methanol/water mix. The separation effects come not only from Knudsen diffusion (calculated according Equation 2, ethanol/water: 1.60; methanol/water: 1.33), but also the shape selective effects. Water can pass through the pores of KA zeolite crystals but methanol and ethanol cannot at tested temperatures. The reason arises from the intrinsic structure of the pressed wafer, which has many macrospores inside as shown in Figure 2.

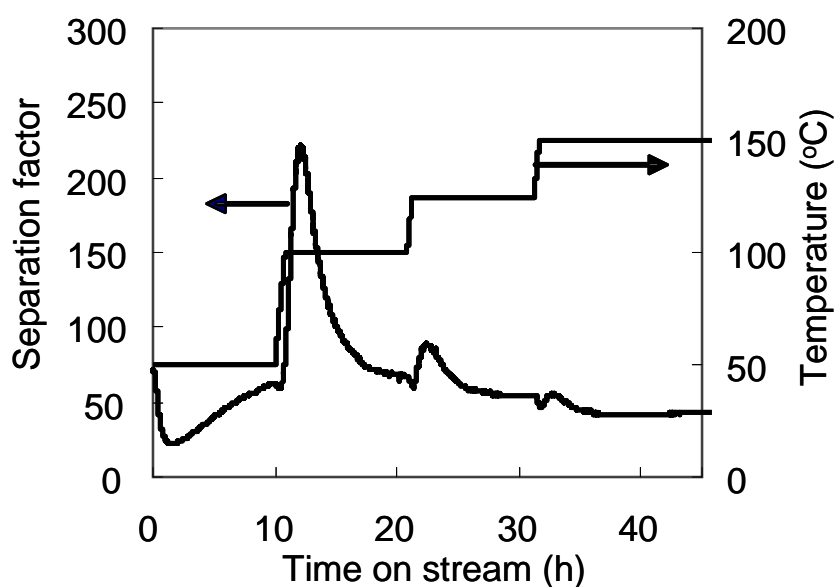$$D_K = \frac{2r_p}{3}\sqrt{\frac{8RT}{\pi M}}$$

(2)

(D_k: Knudson diffusion coefficients, r_p: averaged pore radius, R: ideal gas constant, T: temperature in Kelvin, M: molecular weight)

5.3.2.2. *Vapor Permeation of Na-LTA zeolite membrane*
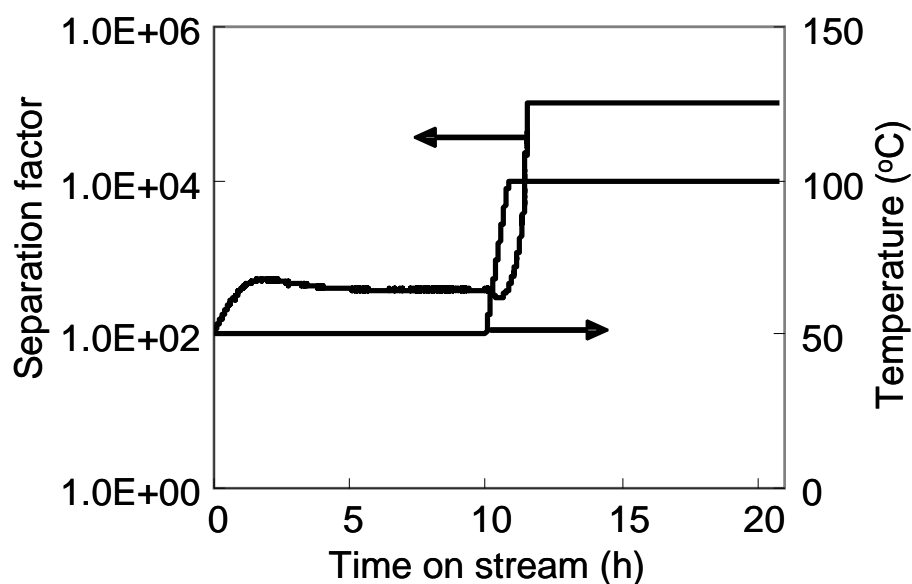
(b)

(b)

Figure 6 Separation results of zeolite Na-LTA zeolite membrane.

(a) Water + ethanol; (b) Water + methanol.

The separation results of zeolite Na-LTA zeolite membrane for water/ethanol and water/methanol are shown in Figure 6(a), (b). Na-LTA zeolite membrane has very high separation factors for ethanol dehydration but very low separation factors for methanol dehydration. The separation factors are over 10000 for ethanol dehydration and only 50 for methanol at 100 °C. A relatively high H_2O permeance of about 9.70×10^{-7} mol m^{-2} s^{-1} Pa^{-1} for ethanol/water mix has been obtained, but for methanol/water mix, H_2O permeance is much lower and is about 5.02×10^{-7} mol m^{-2}

$s^{-1} Pa^{-1}$.

It has been pointed out and elucidated in chapter 3 and chapter 4 that the hindrances of pore openings of the LTA zeolites to different molecules. The size of the pore openings of Na-LTA zeolite is 4.1 Å, which is smaller than the kinetic diameter of ethanol (4.6 Å), but is bigger than the kinetic diameters of Methanol (3.6 Å) and water (2.6 Å). Both methanol and water can pass through the pore openings of the Na-LTA zeolite membrane but ethanol cannot. That is the reason why Na-LTA zeolite membrane has so big separation factors（＞10000) for water/ethanol and only 50 for water/methanol.

5.3.2.3. *Vapor Permeation of K90 zeolite membrane*
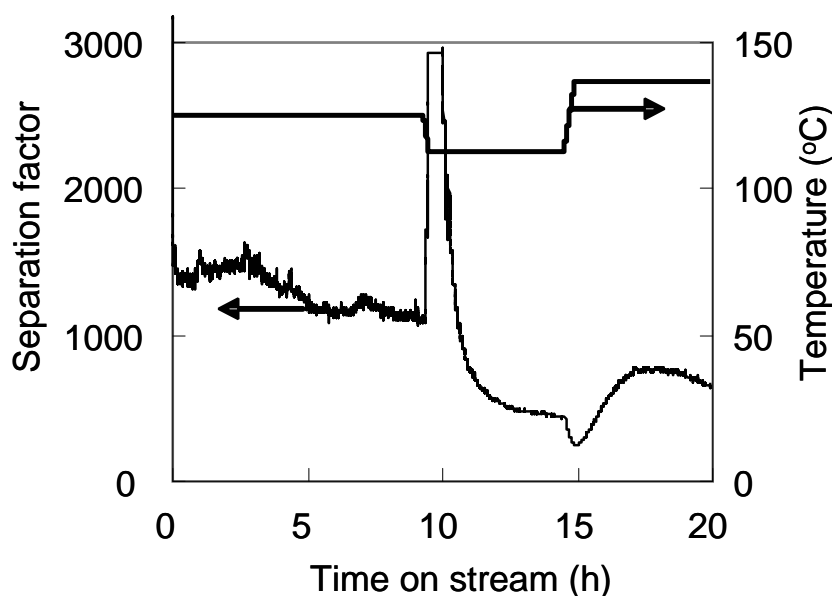
Figure 7 Vapor permeation experimental results of K90 zeolite membrane for water/ methanol separation.

The experimental results for water/ methanol separation using K90 membrane are shown in Figure 7. K90 membrane has separation factors over 1000 at 125 °C for water/ methanol, the H_2O permeance is about 4.16×10^{-7} mol m^{-2} s^{-1} Pa^{-1}.

It has also been elucidated in chapter 4 that increasing exchanged potassium of LTA zeolites decreases the diffusion rates of methanol in them. High potassium

concentration favors that more K^+ cations occupy the Sites II in the pore openings, and makes shape restricting more severe. When all the Sites II in pore openings of LTA zeolite are occupied by K^+ cations, methanol cannot pass the pore openings and cannot be absorbed in the inner cages of K-LTA zeolites. However, it has been verified that water can pass through the pore openings of highly potassium exchanged LTA zeolites and be absorbed. Water can pass through the pore openings of KA90 membrane but methanol cannot. That is the reason why K90 membrane has much bigger separation factors（＞1000) than Na-LTA zeolite membrane for methanol dehydration.

5.4. Conclusion

The highly potassium exchanged of LTA zeolite membrane was successfully produced and was used for water/methanol separation. It was verified that KA90 membrane has much bigger separation factors（＞1000) for water/methanol than NaA zeolite membrane and can be used for than methanol dehydration. On the other hand, the proposed and detailed elucidated mechanism that exchanged potassium can enhance the pore opening restriction of LTA zeolite was confirmed. When exchanged potassium concentration of LTA zeolite reach a certain level, all the location Sites in pore openings of LTA zeolite are occupied by K^+ cations, methanol can not pass the pore openings and cannot be absorbed in the inner cages of K-LTA zeolites.

References

[1] K. J. Ptasinski, C. Hamelinck, P. J. A. M. Kerkhof, Energy Convers. Manage. 43 (2002) 1445–1457

[2] G. Ertl, H. Knözinger, J. Weitkamp, Handbook of Heterogeneous Catalysis,

Weinheim, Sellchaft mbH, 1997, P1856-1876.

[3] P. Galindo Cifre, O. Badr, Energy Convers. Manage. 48(2) (2002) 519-527.

[4] R. H. Scott, (1977) USP 4013521.

[5] A. Pinto, (1977) USP. 4065483.

[6] A. Pinto, (1979) USP. 4419940.

[7] A. Pinto, (1980) USP. 4210495.

[8] Y. Saito, O. Hashimoto, (1988) USP. 4744869.

[9] C. Rescalli, R. Ricci, A. Scazzosi, F. Cianci, (1989) USP. 4874474.

[10] R. L. Kao, Sarabijit. S. Randhava, Surjit. S. Randhava, (1992) USP. 5079267.

[11] Methanol production, comparing the LP and LCM process, SenterNovem, Available

at://www.senternovem.nl/mmfiles/Project_experience_factsheet_MethanolUK_tcm24

-239416.pdf; November 2009.

[12] D. F. Othmer, (1983) USP 4405343.

[13] H.L. Fleming, Chem. Eng. Prog. (1992) 46-52.

[14] R.Y.M. Huang (Ed.), Pervaporation Membrane Separation Processes, Elsevier, Amsterdam, 1991.

[15] S.I. Semenova, H. Ohya, K. Soontarapa, Desalination 110 (1997) 251-286.

[16] X. Feng, R. Y. M. Huang, Ind. Eng. Chem. Res. 36 (1997) 1048-1066.

[17] Y. Morigami, M. Kondo, J. Abe, H. Kita, K. Okamoto, Sep. Purif. Tech. 25 (2001) 251–260

[18] J. Caro, M. Noack, P. Kölsch, R. Schäfer, Microporous Mesoporous Mater.38 (2000) 3-24.

[19] T. C. Bowen, R. D. Noble, J. L. Falconer, J. Membr. Sci. 245 (2004), 1–33

[20] Y. Li, W. Yang, J. Membr. Sci. 316 (2008), 3–17.

[21] J. Caro, M. Noack, Microporous Mesoporous Mater. 115 (2008) 215-233.

[22] M. E. Davis, Nature 417 (2002) 813-821.

[23] S. A. I. Barri, G. J. Bratton, T. d. Naylor, (1997) US 5605631.

[24] J. C. Jansen, F. Kapteijn, S. A. Strous, (2007) US 7214719, B2.

[25] A. S. T. Chiang, G. Shu, J. Liu, R. Selvin, (2007) US 7253130, B2.

[26] Q. Liu, R.D. Noble, John. L. Falconer, H. H. Funke, J. Membr. Sci. 117 (1996) 163-174.

[27] K. Okamoto, H. Kita, M. Kondo, N. Miyake, Y. Matsuo, U.S. Patent. (1996) 5554286.

[28] K. Okamoto, H. Kita, K. Horii, K. T. Kondo, Ind. Eng. Chem. Res. 40 (2001) 163-175.

[29] K.D. Kreuer, J. Membr. Sci. 185 (2001) 29-35.

[30] A. Heinzel, V. M. Barragan, J. Power Sources 84 (1999) 70-74.

[31] T. Yamaguchi, F. Miyata, S. Nakao, Adv. Mater. 15 (2003) 1198.

[32] K. Okamoto, Y. Yin, O. Yamada, Md. N. Islam, T. Honda, T. Mishima, Y. Suto, K. Tanaka, H. Kita, J. Membr. Sci. 258 (2005) 115–122.

[33] R. P. Hamlen, (1998) US 5849428.

Chapter 6

Summary

6.1. Summary

Direct synthesis of dimethyl carbonate (DMC) from CO_2 and methanol is a strongly equilibrium limited reaction. Both experimental results and thermodynamic calculations showed that the thermodynamic limitation leads to achievable DMC yield of only 1-2%, if the produced water is not removed from the system. In order to get water eliminated, solid dehydrating agents were used to shift the reaction towards a higher DMC yield. Therefore, a back-mixed reactor was combined with recycling the reactor educt through a fixed bed reactor containing the sorbent. By decoupling the reaction zone from the removal of water at lower temperature, the DMC yield (with ZrO_2 as catalyst) was increased to 17 % by using zeolite 3A zeolite as drying agent at 248 K.

The isothermal adsorption and diffusion kinetics of water and methanol in LTA and FAU (13X) zeolites were studied at different temperatures, using the direct measurements of mass transport (DMMT) method for establishing the diffusion kinetics. It has been demonstrated that adsorption of either water or methanol in LTA and FAU zeolites follow Langmuir isotherms as long as competitive adsorption does not exist.

The diffusion rates of methanol are more severely influenced by temperature than those of water in tested LTA zeolites, indicating higher activation barriers for methanol intracrystalline diffusion in LTA zeolites. Such barriers mount up in a descending order of pore openings for methanol diffusion, i.e. 13X, 5A, 4A and then 3A zeolite. They vary only to a limited extent for water diffusions. The highest ratio of the diffusion coefficients of water and methanol was found for 3A zeolites at 248 K. This was correlated with the experimental data indicating that 3A zeolite is the most effective material in a drying process operating at 248 K and consequently increases the DMC yield significantly.

All tested commercial LTA zeolites have the same topological structure and differ

only in the charge-compensating cations. It was therefore important to understand why 3A zeolite, which is a partially potassium exchanged LTA member, at 248 K, was effective in selectively absorbing the produced water. A series of LTA zeolites with higher in potassium exchange level were prepared for further studies, both to study the diffusion kinetics of water and methanol and to be applied as dehydrating agents for DMC direct synthesis.

It was found that sample KA-91 (91% potassium exchange) can be used as dehydrating agent for DMC direct synthesis at reaction temperatures. Based on the diffusion kinetics of water and methanol, the impact of exchanged potassium concentrations and temperatures on the diffusion properties and adsorption capacities of LTA zeolites were elucidated. It has been demonstrated that exchanged potassium concentration of LTA zeolites influence the diffusion rates of water and methanol in them. High potassium concentration will hinder the diffusions of both water and methanol and decelerate their diffusion rates in LTA zeolites.

It was shown that the restricting effects or the free pore opening sizes in LTA zeolites are determined by the distribution of Na^+ and K^+ cations in their three types of topological location sites. The exchange degree of potassium affects the local Na^+/K^+ partition in the 8-member ring window of LTA zeolite. For an LTA zeolite with certain potassium exchanged degree, the temperatures also dramatically influence its Na^+/K^+ partition in the pore openings. If all the possible location sites in the pore openings of LTA zeolite are occupied by K^+ cations, methanol cannot pass the pore openings, whereas water still can at certain temperatures. That is the reason why KA-40 can selectively adsorb water at 248 K and KA-91 can do so even at elevated temperatures (in the range from 393 K to 458 K).

It was clear that the direct DMC synthesis from CO_2 and methanol, from the beginning, the only possibility of improving the DMC yield was by the removal of in-situ formed water by highly selective materials. This was particularly challenging because the reaction mixtures contained mostly methanol which enhances the demand

of selectivity for water adsorption. Furthermore, the separation of water and methanol is in fact very difficult because their polarities, chemical properties and even molecular sizes of water and methanol (2.6 Å and 3.6 Å) are similar. In industrial practice, distillations have to be performed for methanol purification, which needs extremely long column and very high reflux ratios. It was well known that methanol distillation is one of the most difficult chemical processes known for its high energy consuming.

After gaining an understanding of the mechanism, by which the exchanged potassium and temperature determine the pore opening restriction effect of LTA zeolites. And KA-91, which can absorb water selectively, was successfully utilized as an in situ dehydrating agent for DMC direct synthesis. In this way, from concept to practice, an ideal material, i.e. highly potassium exchanged LTA zeolite membrane, for water/methanol separation has been developed. Enhanced separation factors ($>$ 1000) for water/methanol mixtures have been verified which shows that this material is well suited for industrial methanol dehydration/purification processes.

6.2. Zusammenfassung

Die Synthese von Dimethylcarbonat aus Kohlenstoffdioxid und Methanol ist eine stark gleichgewichtslimierte Reaktion. Sowohl experimentelle Daten als auch theoretische Rechnungen haben gezeigt, dass die maximale Ausbeute 1-2% beträgt, falls das entstehende Wasser nicht beseitigt wird. Daher werden feste Materialien verwendet um jenes Wasser aus der Reaktionsmischung zu entfernen und somit die Ausbeute zu steigern. Hierfür wurde ein vollständig durchmischter Reaktor mit einer Eduktrecycling-Schleife verbunden, in welcher ein Rohrreaktor eingebaut. Dieser Rohrreaktor ist mit Trocknungsmittel gefüllt. Dadurch ist es möglich, die Reaktion bei deutlich höheren Temperaturen durchzuführen als die Trocknung der Reaktionsmischung, was zu einer Erhöhung der Ausbeute auf 17% (ZrO_2 Katalysatoren) führt. Als Trocknungsmittel wurde Zeolith 3A bei 248 K verwendet.

Die isothermen Adsorption- und Diffusionskinetiken von Wasser und Methanol wurden für die Zeolithtypen LTA und FAU (13X) bei verschiedenen Temperaturen untersucht. Hierzu wurde das sogenannte „direct measurement of mass transport" (DMMT) verwendet um die Kinetik der Diffusion näher zu untersuchen. Weiterhin konnte gezeigt werden, dass die sowohl die Adsorption von Methanol als diejenige von Wasser durch den Langmuir Formalismus beschrieben werden kann, solange keine kompetitive Adsorption vorliegt.

Die Untersuchung der Diffusion zeigte, dass Methanol deutlich stärker durch die Veränderung der Temperatur beeinflusst wird als Wasser, was für eine stärkere Aktivierungsbarriere spricht. Derartige Barrieren konnten in absteigender Reihenfolge an Zeolithen mit für Methanol zugänglichen Poren beobachtet werden, daher wurde diese in der Reihe 13X, 5A, 4A und schließlich 3A stärker. Das größte Verhältnis der Diffusionskoeffizienten von Wasser und Methanol in den vorliegenden Studien wurde in Zeolith 3A bei 248 K gemessen. Dieses Ergebnis wurde mit den experimentellen Data der DMC Synthese korreliert, welche ebenfalls zeigte, dass Zeolith 3A eingesetzt bei 248 K das effektivste Trocknungsmittel ist und somit die DMC

Ausbeute erheblich steigern konnte.

Alle untersuchten Zeolithe haben die gleiche Topologie und unterscheiden sich ausschließlich in der Art der eingelagerten Kationen. Es ist daher von entscheidender Bedeutung zu verstehen, warum Zeolith 3A, welcher ein Mitglied der LTA Familie und teilweise kaliumgetauscht ist, die größte Effektivität und Selektivität für die Adsorption unter den untersuchten Materialien zeigt, wenn er bei 248 K eingesetzt wird. Für weitere Studien der Diffusionskinetik von Wasser und Methanol, als auch für den Einsatz in der DMC Synthese wurde eine Serie LTA Zeolithe mit einem höheren Kaliumgehalt hergestellt.

Damit konnte gezeigt werden, dass die Probe KA-91 (91% Kaliumgehalt) sogar bei Reaktionstemperaturen eingesetzt werden kann. Basierend auf den Diffusionskinetiken von Wasser und Methanol wurde die Abhängigkeit der Diffusionseigenschaften und der Adsorptionskapazität von Temperatur und Kaliumgehalt untersucht. Es wurde gefunden, dass das enthaltene Kalium die Diffusion von Wasser und Methanol im Porensystem des Zeolithen beeinflusst. Hierbei verlangsamt sich die Diffusion von Wasser als auch von Methanol mit steigendem Kaliumgehalt.

Er wurde weiterhin gezeigt, dass der restriktive Effekt beziehungsweise die Größe der Porenöffnung abhängig von der Verteilung der Natrium- und Kaliumkationen an den drei räumlich unterschiedlichen Bindungsstellen ist. Der Anteil an Kaliumionen im Gitter beeinflusst das Verhältnis Na^+/K^+ in den Öffnungen bestendend aus 8-gliedriegen Ringen des LTA Zeolithen. Sobald alle Bindungsstellen in jenen Porenöffnungen durch K^+ okkupiert sind, ist es für Methanol bei bestimmten Temperaturen unmöglich in das Porensystem des Zeolithen zu sorbieren, während dies für Wasser weiterhin möglich ist. Dies ist der Grund, warum KA-40 bei 248 K und KA-91 sogar bei erhöhten Temperaturen (393-458 K) Wasser sehr selektiv aus der Reaktionsmischung entfernen können.

Bereits zu Beginn des Projekts war augenscheinlich, dass eine Erhöhung der DMC Ausbeute in der Direktsynthese aus Wasser und Methanol nur über die selektive Eliminierung des in der Reaktion entstehenden Wasser aus dem Reaktionsgemisch zu realisieren sein würde. Dies war besonders anspruchsvoll, da die Reaktionsmischung beinahe ausschließlich aus Methanol besteht und somit die Anforderungen an die Selektivität besonders hoch waren. Dabei stellt sich die Trennung von Wasser und Methanol aufgrund der Ähnlichkeit der Substanzen bezogen auf die Polarität, das chemische Potenzial und sogar die Größe der Moleküle (2.6Å Wasser, 3.6Å Methanol) als besonders schwierig dar. Daher wird ein solches Gemisch großtechnisch durch Destillation getrennt. Dazu werden sehr große Kolonnen und hohe Flüsse benötigt. Die Destillation von Methanol zählt deshalb zu den aufwendigsten industriell angewandten, chemischen Prozessen und ist bekannt für einen hohen Energieverbrauch.

Durch die beschriebenen Studien wurde Mechanismus der Veränderung der Porengröße in LTA Zeolithen durch Austausch mit Kaliumionen als auch der Einfluss der Temperatur auf jene verstanden. Daraufhin konnte KA-91 erfolgreich als Trocknungsmittel in der DMC Reaktion eingesetzt werden. Weiterhin konnte aufgrund der gesammelten Erkenntnisse eine Membran zur Trennung von Wasser und Methanol entwickelt werden. Auch diese hat einen hohen Kaliumionengehalt. Trennfaktoren >1000 für Mischungen Wasser/Methanol konnten erhalten werden, was eindeutig die Anwendbarkeit für industrielle Trocknung von Methanol anzeigt.

Curriculum vitae

Herui Dou was born on February 24, 1975 in Shandong, P. R. China. After graduating from high school in 1994, he started his study in Department of Applied Chemistry in Dalian University of Technology, China and received his bachelor degree in 1998. He went on to study physical chemistry at Dalian Institute of Chemistry and Physics (DICP), Chinese Academy of Science, under the supervision of Professor Chenglin Sun. In 2001, he finished his thesis, entitled *Leaching control of Cu in copper-based catalysts for wastewater catalytic wet air oxidation,* and obtained his master degree. He was employed as a research assistant in Group 1501, DICP and was promoted to Assistant Professor in 2004. On March 2006, he joined Technical Chemistry II group, supervised by Professor J. A. Lercher at Technical University of Munich, Germany and started a research on dimethyl carbonate from CO_2.

List of Patent and Papers to be submitted

Potassium Exchanged Zeolite LTA Membrane for Methanol dehydration, Herui Dou, Xuebing li, Johannes A. Lercher; (Patent to be filed and one paper will follow).

Yield Improvement for Direct Synthesis of Dimethyl Carbonate from Methanol and CO_2, Herui Dou, Xuebing Li, Johannes A. Lercher; in preparation.

Direct Dimethyl Carbonate Synthesis from Methanol and CO_2: Strategies for Yield Improvement, Herui Dou, Hui Shi, Xuebing Li, and Johannes A. Lercher; in preparation.

Adsorption and diffusion of water and methanol in LTA and FAU zeolites and their uses as dehydrating agents for dimethyl carbonate synthesis, Herui Dou, Xuebing Li, Johannes A. Lercher; in preparation.

Influence of exchanged potassium contents on the dimension restricting effect of the pore openings in LTA zeolite, Herui Dou, Xuebing Li, Johannes A. Lercher, in preparation. .